POLITECNICO
MILANO 1863

SCUOLA DI INGEGNERIA INDUSTRIALE
E DELL'INFORMAZIONE

Core Neutronics for Space Reactors: Analysis of HALEU Configurations

Tesi di Laurea Magistrale in
Nuclear Engineering - Ingegneria Nucleare

Author: **Chiara Genoni**

Student ID: 943625
Advisor: Prof. Stefano Lorenzi
Co-advisors: Marco Enrico Ricotti
Academic Year: 2021-22

Abstract

One of the most critical technological gaps that need to be filled to support space exploration involving expedition to other planets concerns power generation systems capable of providing for several years a power source bigger than 1 kWe to planetary settlements. Among all the possible power supply systems, nuclear fission reactors represent the most attractive solution, thanks to their high specific power and the ability to produce energy regardless of their location or the external environment. This thesis work aims at analysing - from a neutronics perspective - different possible configurations for a space reactor employing High-Assay Low Enriched Uranium (HALUE), characterized by an enrichment level between 5% and 20%. This choice allows the design to be compliant with proliferation policies that prevent the use of uranium with an enrichment level higher than 20%. Furthermore, the proposed system has to meet safety requirements for launch approval and be optimized in terms of mass, which is of most importance for reducing launch costs.

The design of the fission power system is carried out employing Kilopower reactor concept proposed by NASA as a reference, which is the only space reactor that has been recently tested with success through the experimental demonstration of the Kilopower Reactor Using Stirling TechnologY (KRUSTY) performed at the Los Alamos National Laboratory (LANL).

Serpent particle transport Monte Carlo code has been employed for the neutronic analysis. As first step, a model of KRUSTY is developed in Serpent to demonstrate the capability of the code to simulate nuclear reactors for space applications. The results are compared against both numerical simulation performed by LANL with a different neutronics code and with the experimental data collected from KRUSTY testing. Afterward, three possible design paths for HALEU reactor concept are investigated: i) a fast reactor just like KRUSTY, with the exception of using HALEU instead of HEU; ii) a homogeneously moderated thermal reactor, whose core is a homogeneous mixture of moderator and fuel; iii) a heterogeneously moderated thermal reactor, whose core is composed of separate layers of fuel and moderator. Each reactor concept is accompanied by a mass optimization analysis and safety analysis. The HALEU fast reactor is also supported by a study on

how the system approaches criticality and estimations of power density distributions. The analysis performed on homogeneously moderated reactors is treated as an intermediate step to demonstrate the beneficial effect of adding moderator inside fuel, which turns into an improvement in neutron economy. Finally, the effect of heterogeneity is investigated to prove the existence of an optimal fuel cell pitch that permits to maximize reactor performance in terms of neutron economy.

Keywords: Space nuclear reactor, KRUSTY, Monte Carlo, Low Enriched Uranium.

Abstract in lingua italiana

Una delle lacune tecnologiche più rilevanti che necessita di essere colmata al fine di supportare l'esplorazione di altri pianeti riguarda sistemi di generazione di potenza in grado di fornire per diversi anni una fonte di energia superiore a 1 kWe agli insediamenti planetari. Tra tutti i possibili sistemi di alimentazione, i reattori nucleari a fissione rappresentano la soluzione più interessante grazie alla loro elevata potenza specifica e alla capacità di produrre energia indipendentemente dalla posizione o dalle condizioni dell' ambiente esterno. Questo lavoro di tesi mira ad analizzare - dal punto di vista neutronico - diverse possibili configurazioni di reattore spaziale a base uranio a basso arricchimento (HALUE), caratterizzato da un contenuto di U-235 compreso tra il 5% e il 20%. Questa scelta consente al progetto di essere conforme alle politiche di anti-proliferazione che impediscono l'uso di uranio con un livello di arricchimento superiore a 20%. I Il sistema proposto deve soddisfare i requisiti di sicurezza per l'approvazione del lancio ed essere ottimizzato in termini di massa, il che rappresenta un aspetto fondamentale al fine di ridurre i costi di lancio.

La progettazione del reattore viene svolta prendendo come riferimento il design Kilopower proposto dalla NASA, unico reattore per applicazioni spaziali che negli utlimi 40 anni è stato testato con successo attraverso la dimostrazione sperimentale del Kilopower Reactor Using Stirling TechnologY (KRUSTY) eseguito al Los Alamos National Laboratory (LANL).

Il codice Monte Carlo Serpent di simulazione del trasporto di particelle è stato impiegato per svolgere l'analisi neutronica. Come primo passo, in Serpent viene sviluppato un modello di KRUSTY al fine dimostrare la capacità del codice di simulare reattori nucleari per applicazioni spaziali. I risultati del modello vengono confrontati sia con le simulazioni numeriche eseguite direttamente da LANL con un diverso codice neutronico, sia con i dati sperimentali raccolti durante la dimostrazione del corretto funzionamento di KRUSTY. Successivamente, sono state proposte tre possibili opzioni di concetti di reattore a base di HALEU: i) un reattore veloce simile KRUSTY, ma che impiega HALEU invece di HEU come combustibile; ii) un reattore termico il cui il materiale moderatore viene omogeneamente mescolato con il combustibile stesso (reattore omogeneoamente moderato); iii)

un reattore termico in cui il combustibile e il materiale moderatore sono forma di dischi alternati (reattore eterogeneamente moderato). Ciascun concetto di reattore è supportato da un'analisi di ottimizzazione della massa e da un'analisi della sicurezza per garantire l'approvazione al lancio. Sul reattore veloce HALEU è stato effettuato uno studio su come il sistema raggiunge le condizioni criticità e una stima delle distribuzioni di densità di potenza. L'analisi svolta sui reattori termici omogeneamente moderati mira a dimostrare l'effetto benefico dell'aggiunta di moderatore all'interno del combustibile sull'economia neutronica del sistema, che si traduce in una riduzione della massa totale del sistema. Infine, viene studiato l'effetto dell'eterogeneità del combustibile, per provare l'esistenza di uno spessore ottimale dei dischi in termini di economia neutronica.
Parole chiave: Reattori nucleari, spazio, KRUSTY, Monte Carlo, Uranio a basso arricchimento.

Contents

1 | Introduction

1.1. High Power Supply in Space

In the last decades, the scientific and engineering community in the aerospace field has focused their attention on solutions for many existing technology gaps, aiming at expanding the available technology base to support space missions involving explorations of other planets. One of the most relevant gap is related to compact power systems (> 1KWe) able to provide a reliable, safe, and durable power source to planetary settlements for several years. To this day, there are three possible ways to attain a proper power supply that can be safely and reliably used in space - chemical, solar and nuclear. Each power source has intrinsic characteristics that determine which source is uniquely the best for a specific mission (Figure 1.1).

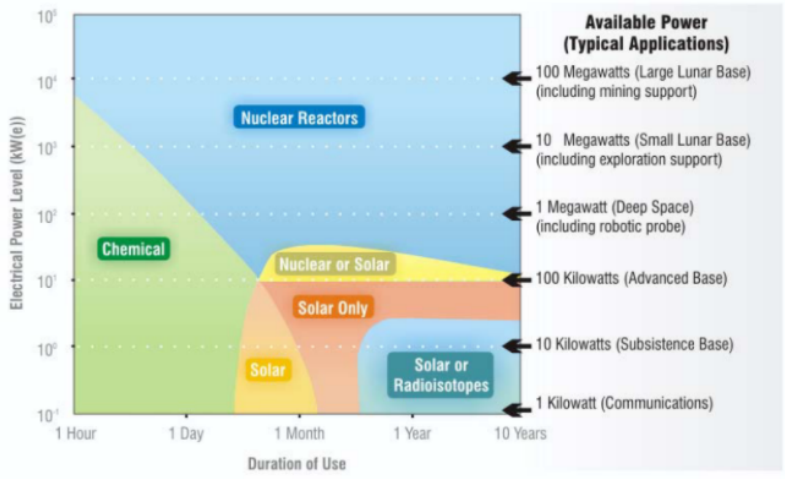

Figure 1.1: Sources of electricity for application in space missions [1].

Chemical combustion can produce a high power level, yet it can be applied only for short periods because of the large masses of fuel required per unit of power produced. Solar and nuclear power devices are thus identified as the only two options potentially able to supply sufficient energy over an extended time period. Solar power systems converts the Sun's energy into electricity, but struggle to gather enough energy in places where the sunlight is

dim or unavailable, such as potentially resource-rich craters on the moon or on the windy, dusty surface of Mars. Furthermore, since the solar energy flux is inversely proportional to the distance from the Sun (Figure 2.6), for deep space mission, a huge array mass would be required to produce the desired power, causing significant problems to structural integrity, deployment in orbit and Sun pointing. Therefore, for interplanetary exploration beyond the Earth's distance from the Sun, solar power reaches its limits, leaving nuclear power sources the only possible solution left for this type of mission.
State-of-the-Art nuclear power sources is based on radioisotope thermoelectric generators (RTGs). RTGs use thermo-couples to convert the heat produced by radioactive decay of Pu-238 into electrical energy, thus being able to provide low power for long duration thanks to the long half-life of the exploited radioisotopes. However, they cannot be used to produce more than 1 kWe, since it wouls take a relatively large amount of fuel, making them a less attractive technology in terms of mass and volume savings.
Above 1 kWe, the most suitable solution are fission power systems, whose working principle is similar to terrestrial reactors yet employing different design options in terms of core structure, neutron moderation, cooling process, and control systems. The most evident advantage of fission power systems is that their performance is independent of the location or the external environment. Furthermore, they are able to supply high power for decades without intervention or re-batching. On the other hand, the safety of these systems still remains a major topic of discussion - e.g., as for shielding from radiation. The inclusion of physical safety systems, eventually redundant ones, necessarily implies an increase of weight that poses a further challenge to this technical solution. However, even considering the additional weight increase due to the presence of safety system and the eventual challenge of sending massive power systems to space, nuclear reactors can still provide a much higher power density that solar arrays and can be reliably used in outer space - whereas the high-mass issue becomes eventually manageable or even non-relevant [2].

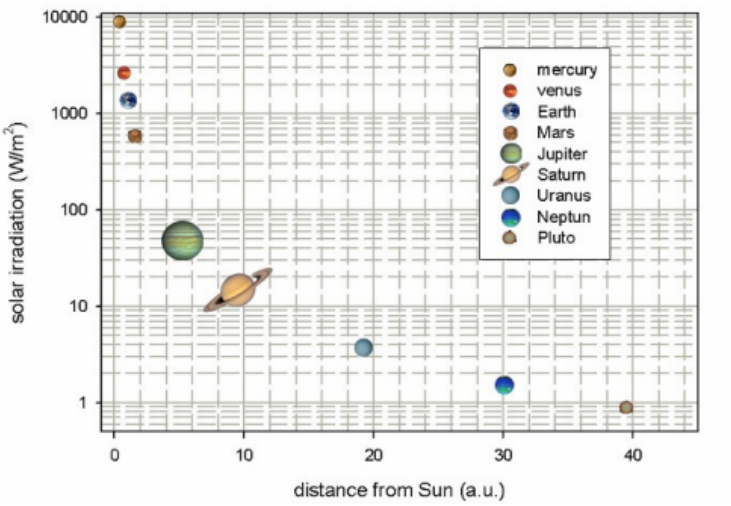

Figure 1.2: Semi-logarithmic graph showing the decrease of solar intensity with the square of the distance to the sun, resulting in a 60% decrease at Mars Obrit and more than 95% decrease at Jupiter orbit compared to its intensity at Earth distance [3].

1.2. Nuclear Power in Space: Past Programs

The US began developing nuclear power technology for space applications in 1955 with the opening of the SNAP program. As part of this program, several spacecrafts powered by RTGs were launched in space during the 1960s. Six nuclear fission powered reactors with thermal outputs ranging from 50 kW to 1 MW were built and operated and one, the SNAP-10A, was launched in 1965 aboard of a satellite to demonstrate the capability of producing higher power than RTGs (up to 500 W), but electrical issues caused it to fail after only 43 days. The SNAP program was shelved in 1973 since at that time, there was no mission that required the performance of a space nuclear reactor, and it was not revived until ten tears later with the start of SP-100 program. SP-100 space nuclear reactor was designed to be used as an orbital power supply, lunar or martian power station, or power supply for electric propulsion, with a scaleable power ranging from 10's kWe to 100's kWe. Unfortunately, after approximately 1 billion dollars invested in design and development, less extravagant missions became more palatable, and the SP-100 program was stopped.

While the US have focused most of their effort on radioisotope power sources, the Soviet space nuclear program has given more priority to the development of space fission reactors, launching in the last 40 years 30 fission power systems abroad low Earth orbit satellites. Unfortunately, some of these satellites suffered of failure, causing the system to eventually

re-enter in atmosphere with subsequent release of radioactive materials contained inside the reactor core [4].

1.3. Nuclear Power in Space: Present Programs

In the last 40+ years many reactor concepts have been proposed, but without any single system completed and not even a single nuclear-powered test. All the programs were moving away from potentially real, achievable reactor concepts. Indeed, the increasing tendency in the US has been to design high-performing "academic" reactors that were not founded on real reactor experience and with complex and uncertain integrated performance. This uncertainty results from the inter-dependencies between various thermal-structural-nuclear interactions/phenomena within the reactor system, causing numerous design constraints, smaller margins and greater potential for unknowns [5].
The development of fission powered systems was resumed only in the recent years, still with the aim of extending the capability to explore space by orders of magnitude, but also to reduce the consumption of Pu-238, that is the most common used RTGs fuel. Indeed, the US Pu-238 stockpiles are extremely low and foreign-supplied Pu-238 has become prohibitively expensive and difficult to obtain. The introduction of a fission reactor as power supply could reduce the dependence on the limited Pu-238 fuel supply, permitting its continued use at lower levels for smaller space missions [6].
The first step that marked the beginning of fission power systems development was taken in 2010, when the Decadal Survey Giant Panel (GPP) requested a short study to evaluate the feasibility of such systems for future unspecified National Aeronautics and Space Administration (NASA) science missions. A joint of NASA and Department of Energy (DOE) study team was formed. This team defined a set of requirements to cover a broad range of potential Giant Planet mission, that included an electrical output of 1 kW, a lifetime of 15 years and a 2020 launch availability. Also, the system should have been safe for launch and operations, which was possible by guaranteeing the reactor to remain sub-critical until commanded to start. While no mass or volume was set, minimizing these parameters would have made the system more attractive to potential mission, but a major priority was given to low cost and risk, both developmental and operational. Another key goal was the upward power scalability for potential mission extensibility. After reviewing many options, the study team selected a reference concept of reactor for further study and analysis.
The team successfully developed a viable, low-risk fission power system concept that could be delivered for launch by 2020. The space reactor concept consists of a UMo-fueled, heat

pipe-cooled reactor with distributed thermo-electric converters. The basic concept can be readily scaled to several kilowatts with thermo-electric conversion or up to 10 kWe using Stirling power conversion with minimal changes to the reactor design [7].
Such reactor design was subsequently taken as guideline for the 3-year Kilopower project started in 2015, whose goal was to build and test a full scale flight-prototypic nuclear reactor by the end of 2017.

1.4. Kilopower Project

The Kilopower project aims to develop and demonstrate a scalable fission power system with common technologies, capable of delivering an electric power ranging from 1 kW to 10 kW. Such specific choice in the power level was to allow some design simplifications, such as the use of monolithic fuel and the elimination of pumped liquid metal loops, but also to exploit existing government facilities to perform a nuclear ground test. Higher power levels would have required to build new facilities at a greater cost, which would move away from the goal of performing an affordable and quick experimental demonstration.
The development strategy consists in advancing the reactor design throughout the test program with a near-term goal of a full-scale nuclear ground test named KRUSTY (Kilopower Reactor Using Stirling Technologies).
The Demonstration Using Flattop Fission (DUFF) experiment completed in 2012 at Los Alamos National Laboratory (LANL) represented the first step in the development of Kilopower fission power systems. It was the first nuclear test able to bring the fission power system technology to an advanced state where it could be converted from a technology demonstration into a flight program. The key to success was to use available facilities with the aim of performing an affordable and achievable test. LANL team identified a criticality experiment named "flattop" that had specific characteristics to facilitate a proof-of-concept test. Since the Kilopower reactor concept consisted in a heat-pipe-cooled reactor coupled to either thermo-electric or Stirling power conversion systems, a heat pipe would be inserted inside Flattop's uranium-based fuel to remove heat and send it to the Stirling engines [8]. DUFF test allowed to demonstrate that reactors could be coupled to Stirling power convertors through heat pipes and produce electricity.
KRUSTY demonstration represented the second step towards a successful development of a space reactor. Differently from DUFF, which was not a high fidelity representation of a Kilopower system, KRUSTY was intended to be as flight prototypic as possible. Nevertheless, some choices in the design were influenced by the fact that goal of KRUSTY test was not to demonstrate a space reactor with best performances, but rather a real space

reactor with acceptable performance, staying within the cost and time-table constraints of a 3-year and $<$ 20 millions program.

1.5. Objectives of the Thesis Work

The objective of the thesis is to perform neutronics analysis on different possible configurations for a space nuclear reactor employing High-Assay Low Enriched (HALEU), which is characterized by an U-235 content between 5% and 20%. Such limit in fuel enrichment is for the purpose of safeguarding against nuclear proliferation, as the International Atom Energy Agency considers uranium having a U-235 content higher than 20% (referred to as Highly Enriched Uranium) as a useable nuclear weapon. If terrorists gained access to HEU fuel in civilian research reactors, potentially they could use it to make an improvised nuclear device fuel. The concern would be even more important for the specific case of a nuclear reactor for space applications, since during launch and transportation there is an non negligible risk of re-entry or crash of the core to the ground. The only way to avoid HEU fuel falling into the wrong hands would be to provide a large specialized force in case of retrieval. For all the reasons mentioned above, recently there have been calls for a ban on the use of HEU for non-military applications [9].
Clearly, the employment of HEU fuel is particularly attractive for a nuclear reactor for space applications. Aside of the mass benefits, the consequent reactor compactness would greatly simplify many neutronics and heat transfer issues, and it would also allow the use of smaller components (fuel, reactor, shield, etc.) that are generally easier to manufacture. Also, the nuclear properties of U-235 have been subject of several studies, which reduces nuclear uncertainty. However, despite all these advantages in using HEU fuel, because of the anti-proliferation policies it is convenient from the very beginning to discard the option of a HEU space reactor concept and to dedicate the study to HALEU reactors only.
There are three design paths that can be followed for a HALEU space reactor:

- Consider a fast reactor concept just like KRUSTY, with the exception of using HALEU instead of HEU fuel.
- Use a fuel that combines metallic uranium and moderator into a single material (homogeneously moderated reactor).
- Design a reactor with metallic uranium and moderator as separate elements (heterogeneously moderated reactor).

The first design path is the most attractive, mainly because Kilopower performance and

the development risks are supposed to be largely independent upon the use of HEU or HALEU. On the other side, the addition of neutron moderation has the beneficial effect of improving the system neutron economy but it can add significant risk in development, operation and reliability. In the following work, all reactor concepts are supported by mass optimization analysis and safety analysis to find a geometry that is able to fulfill the goal of reducing the system mass as much as possible while still meeting inadverted criticality safety constraints. Also, the HALEU fast reactor is accompanied by a study on how the system approaches to criticality and an assessment of the power density distributions. The analysis carried out on the homogeneously moderated reactor is treated as an intermediate step to figuring out the dependency of the volumetric moderator fraction inside fuel upon the system neutron economy. Afterward, a study regarding the beneficial effect of heterogeneity is performed on reactors having two different volumetric moderator fractions, aiming to assess an optimal lattice "pitch" yet in terms of neutron economy.

1.6. Methodology

Serpent Monte Carlo particle transport code was used as a fundamental tool to perform neutronic analysis and support the design of HALEU nuclear reactors for space applications. Indeed, due to its inherent capability of modelling complicated three dimensional systems and solve neutron transport problems with high accuracy, Serpent code is particularly useful for core design and safety analysis. Before even starting to propose design concepts, Serpent code required to be benchmarked to demonstrate that it was able to faithfully simulate a fission power system for space applications. The only available simulations of such a system that can exploited for a comparison are those of KRUSTY, directly performed by LANL and already validated through the experimental demonstration concluded in March 2018. For this reason, in this work it was primarily created a Serpent model of KRUSTY to simulate some aspects of the experimental reactor neutronics. The results of the simulations were in part verified through a comparison with LANL simulation results, in part validated through a comparison with available experimental results of KRUSTY demonstration. After that, it was possible to proceed in the design of HALEU reactor concepts.

2 | Kilopower and KRUSTY

2.1. Kilopower Reactor Design

The proposed designs of Kilopower have focused on two power levels: 5 kWt and 50 kWt, to be coupled to 1 kWe 10 kWe power conversion systems, respectively. The system can be divided into 4 further subsystems:

- A **Nuclear Reactor** where heat is generated through fission.
- A **Heat Exchanger** that removes the heat produced inside the reactor and sends it to the engine.
- An **Engine** that moves a piston or a turbine to produce electricity;
- A **Heat Rejection System** that carries excess heat from the engine and liberates it to the external environment (no thermo-electric);

The design of the first two components pertained to LANL, while the latter two pertained to NASA, which are supposed to be integrated into the Nuclear reactor.

2.1.1. Reactor

The Kilopower is one of the most straightforward space power reactor concepts ever proposed, potentially capable of providing a reliable and safe power source to a wide range of space missions for 15 years. It is a compact fast reactor whose essential components are fuel, heat pipes, control rod, reflector, and shielding. The whole reactor is solid-state, with the control rod being the only moving part. Fuel is in the form of a solid cylinder made of UMo alloy suitable for lower power reactors due to the negligible fuel burnup and volume swelling issues that usually involve higher power reactors. The choice for UMo as fuel was for having the most experience and experimental data of metallic fuels, but also due to the existing infrastructure and production capabilities at Y-12 National Security Complex [10]. Furthermore, alloying uranium with molybdenum slows down the rate of phase change as the fuel passes through the phase transition temperature and has the

beneficial effect of increasing both the melting temperature and the material strength.
The fuel assembly would be contained in a can or a liner to prevent material interactions and inhibit fission gas release (which should be negligible due to the low burnup). This envelope is not needed to maintain physical fuel integrity since the monolithic fuel can provide its structural support. The solid fuel block also provides higher reliability with respect to launch and landing loads since it eliminates potential fuel-pin, and grid plate movements [11].
Kilopower reactor has been designed for two different fuel enrichments: 93% and 19.75%. The highly Enriched Uranium (HEU) concept of reactor is supposed to be superior from a performance and technology point of view since it allows a much more compact system. The only reason why the Low Enriched Uranium (LEU) reactor concept should be considered is due to the anti-proliferation policy [11].
Fuel is provided of a central hole for the insertion of the control rod, which is made of boron carbide (B_4C) and used for the reactor control. The control rod contains the required reactivity worth to ensure that the reactor can be started from a cold subcritical condition (when the control rod is completely inserted) and progress to full-temperature critical operation. Beryllium oxide is used as reflector since characterized by optimal moderating properties. Indeed, it has one of the highest moderating ratios (MR) among all commonly used moderating materials. The moderating ratio represents a complete measurement of the moderator's effectiveness since it also considers neutrons' absorption. Specifically, it is defined as:

$$\mathrm{MR} = \frac{\xi \Sigma_\mathrm{s}}{\Sigma_\mathrm{a}} \tag{2.1}$$

ξ is the average logarithmic energy decrement per scattering collision, Σ_a is the macroscopic absorption cross-section and Σ_s is the macroscopic scattering cross-section. Clearly, a high moderating ratio is an index of a high probability of scattering vs. absorption interactions, which is a desirable feature for material used as a reflector. Furthermore, BeO takes part in the improvement of the system neutron economy thanks to the (n, 2n) reaction involving neutrons having energy above the threshold of 1.8 MeV.
Finally, BeO has high thermal conductivity, good shock resistance, high refractoriness and compatibility with fuel. Most importantly, all these properties are conserved even in high-temperature environments [12], such as those it would be exposed to in a space nuclear reactor.
BeO is used instead of pure Be because the first allows a to obtain a more compact system due to the high reactivity worth per unit thickness. Indeed, if BeO is employed, the mass of the space reactor increases due to the higher density with respect to Be, but the size is reduced. Consequently, shielding that is supposed to surround the core will be character-

ized by a smaller size, and since they are generally made of high-density materials, this will cause a significant decrease in the reactor mass [13].

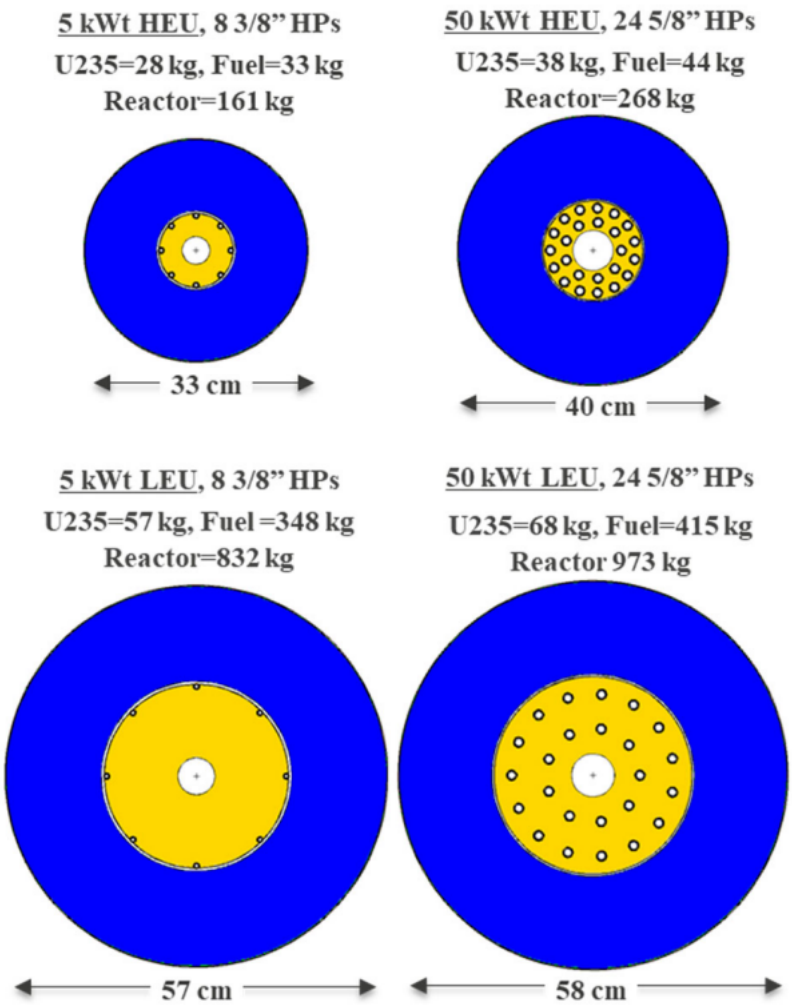

Figure 2.1: Kilopower core cross sectional view [11].

The thermal energy that is produced through fission inside fuel is transported to the power converters via sodium heat pipes. The main advantages of using heat pipes lie in their capability of achieving the working fluid flow through natural circulation, namely capillary forces. The latter feature is particularly attractive for a space reactor since no external pump or moving part would be required, meaning that heat pipes are able to work without any mechanical or electrical input. Ideally, they do not need any maintenance. Heat pipes are intended to be made of Haynes-230, a nickel-chromium-tungsten-molybdenum alloy, due to its good compatibility with sodium and its high creep resistance.
In Figure 2.1 it is shown a cross sectional view of four Kilopower core concepts with

different combinations of fuel enrichments (HEU and LEU) and power levels (5 kWth and 50 kWth). The schematic representation of Kilopower core includes fuel (yellow-colored), reflector (blue-colored), and heat pipes. Heat pipes number, diameter, and spacing are chosen to best accommodate Kilopower specific power level and to make sure fuel temperature remains below 1200 K, to guarantee fuel integrity. When passing from HEU to LEU fuel, fuel mass itself increases due to the reduction in fuel enrichment, while reflector thickness remains the same. When passing from 5 kWth to 50 kWth power level, heat pipes number and diameter increase, but the core mass and dimensions remain almost unchanged.
Kilopower uses lithium hydride canned in stainless steel for neutron shielding and tungsten for gamma shielding. Lithium hydride requires to be enriched in Li-6 due to its high capability of absorbing neutrons, allowing to significantly reduce the emission of gamma rays from neutron capture in tungsten [7].

2.1.2. Power Conversion System

High-efficiency free-piston Stirling converters should be attached to each heat pipe in a 1-for-1 approach. To drive the Stirling Engine, a temperature difference between the heat source (reactor) and the heat sink (radiator) is required. This temperature difference is maintained through the use of another heat pipe operating at a lower temperature with respect to the one directly in contact with fuel and using water as working fluid. The heat pipe connects the engine to the umbrella radiator, which liberates the excess heat to the surrounding environment.

2.1.3. Safety

The reactor is designed to be fully autonomous. Clearly, it is not desired to rely for safety on the control rod insertion only, nore it is convenient to rely on a control system to actuate its insertion and that could eventually malfunction. The most promising approach to obtaining a complete safe operation consists of designing a reactor with inherent safety, in which an increase in temperature would directly result in a prompt reduction of reactivity. Thanks to its intrinsic characteristics, Kilopower has a negative temperature coefficient that allows adjusting the power level on its own. For example, if a heat pipe fails, the consequent temperature rise inside the fuel will cause it to expand.
Unlike RTGs, Kilopower reactors are essentially non-radioactive during launch and transport. Thus, even if a rocket intended to carry Kilopower in space exploded, spreading uranium across land or sea, the radiation hazard would be negligible. Once the reactor is placed in its location, it will start running, and only at that point, it will produce highly

radioactive isotopes.
Kilopower reactor is also intended to not become critical during launch accidents such as explosion, re-entry or crash on the ground or in the ocean. For this reason, fuel design is performed to avoid inadverted criticality in case it ends up surrounded by water, dry sand or wet sand. The only condition that may cause a nuclear hazard is an inadverted movement of the control rod with the radial neutron reflector remaining geometrically intact. This accidental scenario would lead to reactor criticality. However, it is unlikely that any impact strong enough to remove the control rod will not significantly crack or deform the fragile radial reflector made of ceramic material. The only safety requirement is to ensure the control rod remains in its place unless it is commanded to do so, a feature that any nuclear reactor must have by definition.

2.1.4. Potential Space Applications

The Kilopower reactor concept was designed to be employed for a wide range of space explorations and missions, accommodating any possible launch and spacecraft configuration. Specifically, it was intended to be used both as a power supply for propulsion and as a power supply for planetary settlements (Figure 2.2 and Figure 2.3). Differently from the Kilopower concept for propulsion applications, the Kilopower concept for planetary settlements has to deal with landing loads and different environmental conditions, such as the presence of gravity or, in some cases, an atmosphere. However, the intent was to use the same reactor power system in both cases, with the only difference being in the shielding and the radiator configuration.
Indeed, Kilopower for planetary settlements requires omnidirectional shielding due to potential scattering off the planetary surface or the atmosphere. On the other hand, for propulsion applications, everything can be hidden behind a shadow shield.
In Figure 2.4 and Figure 2.5 is shown a mass comparison between Kilopower reactor concepts with different fuel enrichments and different power levels. Both when passing from HEU to LEU fuel and when passing from producing 1 kWe to 10 kWe, it results an increase in the overall system mass. In the first case it is mainly due to the higher fuel mass that would be required in a LEU reactor. In the latter case, it is due to the necessity of bigger power conversion and heat rejection systems and thicker shielding for the higher neutron flux obtained when the reactor is operated at a higher power level. Finally, the mass increase in Kilopower reactor concepts for planetary surfaces is due to the omnidirectional shielding instead of the shadow type.

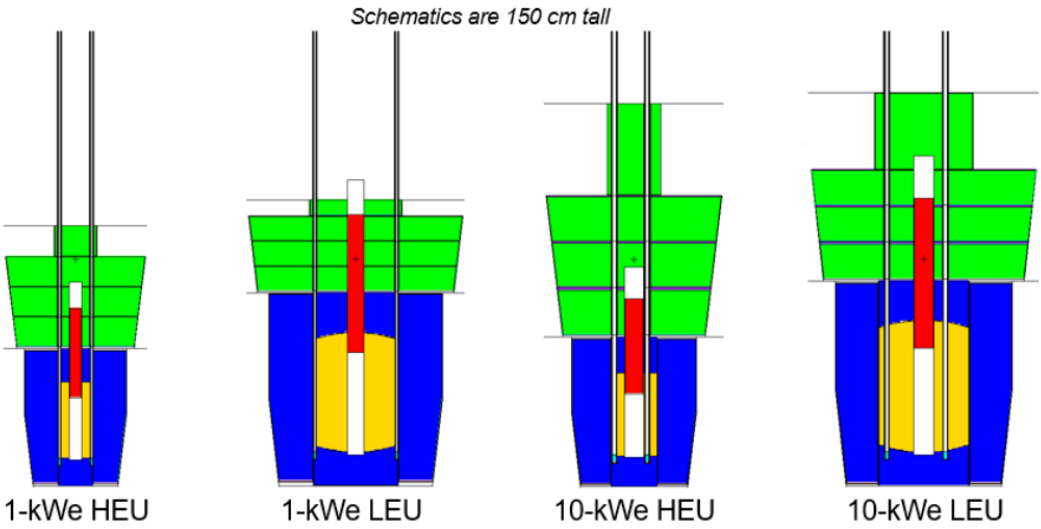

Figure 2.2: Schematic representation of Kilopower reactor concepts for propulsion [14].

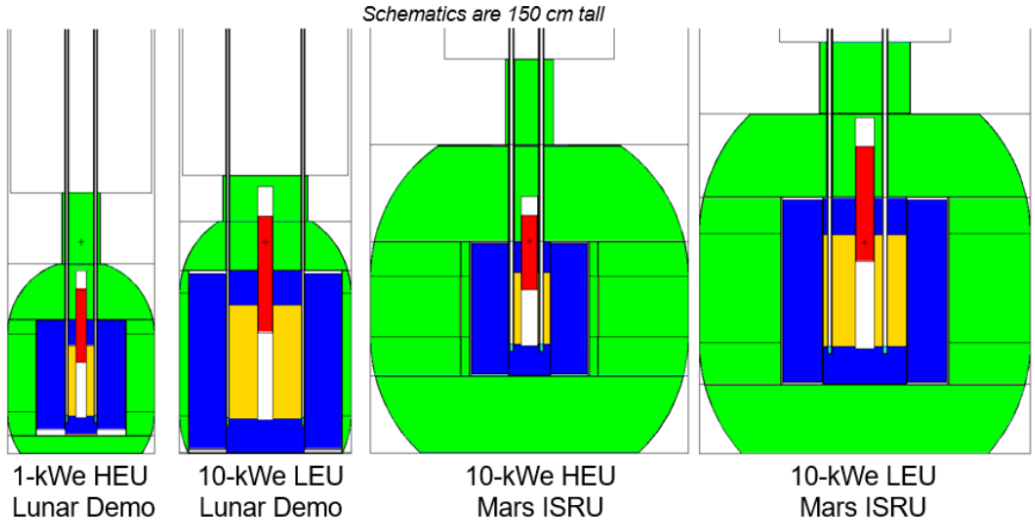

Figure 2.3: Schematic representation of Kilopower reactor concepts for planetary settlements [14].

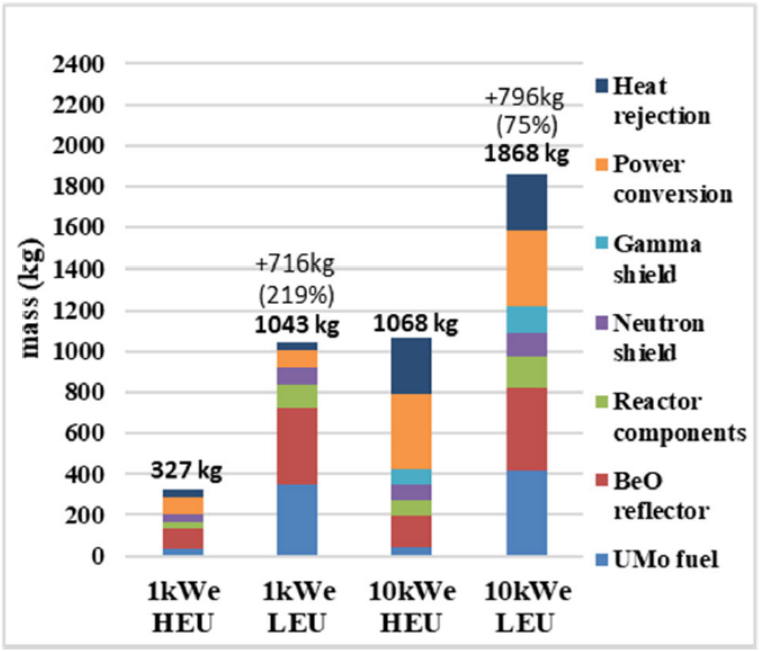

Figure 2.4: Mass comparison of Kilopower reactor concepts for propulsion [11].

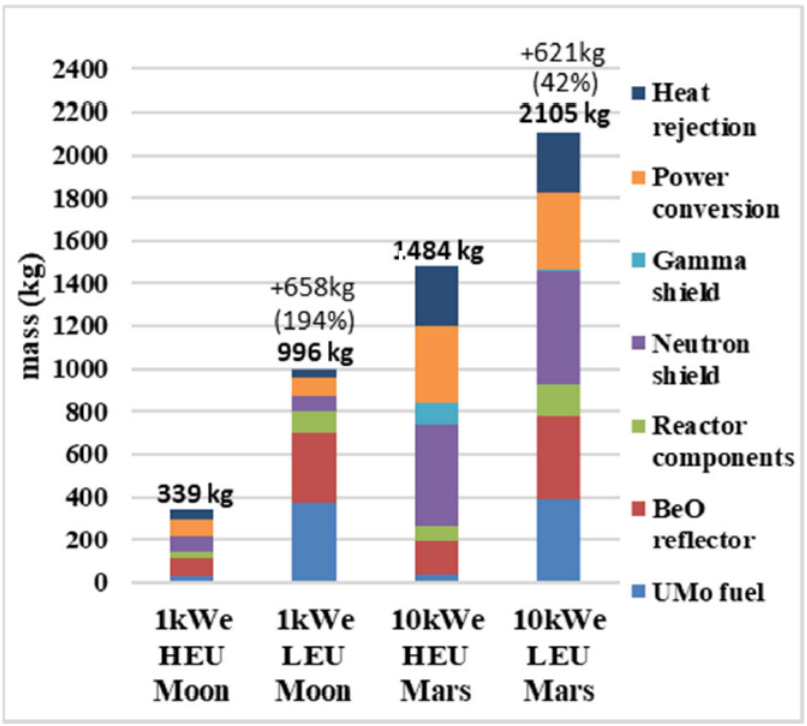

Figure 2.5: Mass comparison of Kilopower reactor concepts for planetary settlements[11].

2.2. KRUSTY Experiment

The main goal of KRUSTY experiment was to demonstrate that a fission power system as close to flight-prototypic as possible could be designed, built, and tested affordably and quickly. The primary key to success consisted of making some convenient choices in terms of materials, components, and facilities that permitted simplifying development and testing. Precisely, the experimental demonstration was accomplished within the time and cost constraints thanks to the following decisions [15] :

1. UMo cast fuel was selected to exploit existing capabilities at Y-12, such that it could be procured affordably and quickly.
2. The experiment was performed in an existing operational facility with an experienced operations, safety and compliance team (National Criticality Research Center).
3. An existing critical assembly machine for dynamic reactivity insertion was selected (COMET machine).
4. A power limit of 5 kWth was selected to provide safety and asset protection risk and remain in line with the previous DUFF test.
5. A 11-cm fuel external diameter was chosen to allow shipping in an existing/approved container.
6. Six Stirling simulators and only two off-the-shelf actual converters were used to reduce cost and schedule.

To certify the success of the experiment, KRUSTY reactor was required to operate in a steady state at the nominal temperature of 1100 K and a nominal power of 4 kWth, within a space vacuum environment.

2.2.1. KRUSTY Design Parameters

The 1 kWe HEU Kilopower reactor concept was taken as the baseline design for KRUSTY. Nevertheless, some changes in the design had to be made with respect to Kilopower reactor concept to allow KRUSTY testing inside a vacuum chamber and to exploit COMET criticality machine. Furthermore, as the assembly of KRUSTY proceeded, other minor variations in the design of components and assemblies had to be performed, meaning that things never went exactly as drawn on paper. However, this manner of working allowed

the experiment accomplishment within a sustainable cost and schedule.

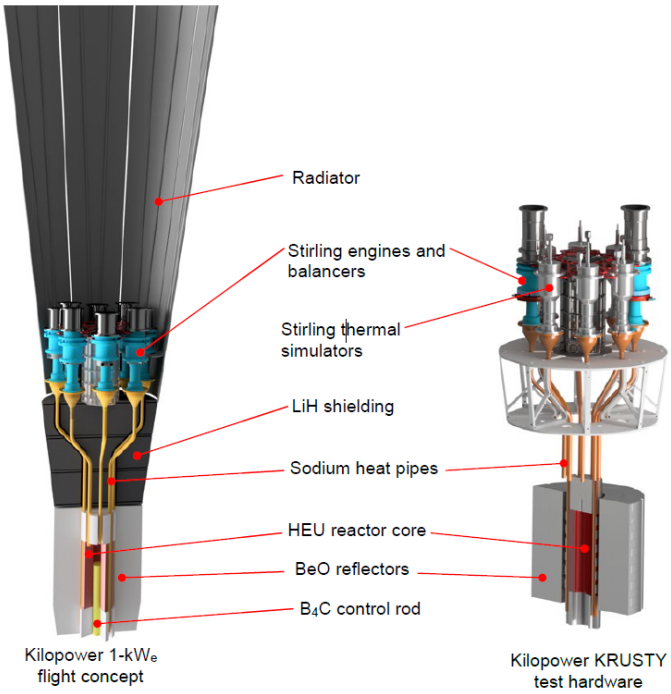

Figure 2.6: Kilopower 1-kWe nuclear power system flight concept comparison with KRUSTY nuclear test hardware [16].

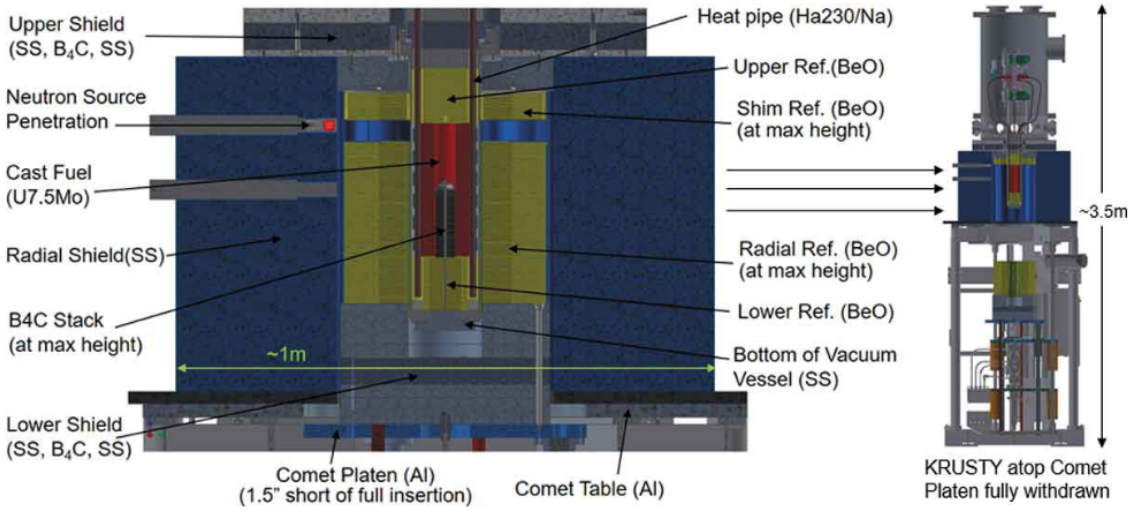

Figure 2.7: KRUSTY reactor schematic representation [17].

KRUSTY was intended to be placed within a stainless steel vacuum vessel to simulate the space heat transfer environment and prevent the oxidation of components. The vacuum vessel contained the reactor, power conversion, and heat rejection systems. Fuel,

heat pipes, axial reflector, and axial shielding were contained inside a "core can" made of SS316, which was an extension of the vacuum vessel. The BeO radial reflector and the lower shielding were not included in the core can, but they were positioned on COMET lift table, which provided the reactor control by raising the reflector to increase the reactivity or vice versa.

All components materials were exactly the same ones of Kilopower reactor to remain as flight-prototypic as possible. The only exception was in the shielding, made of alternating slabs of stainless steel and BC4, as they are both much better materials from a cost and schedule perspective.

KRUSTY fuel was made of HEU (93% enriched in U-235) UMo alloy, with a 7.65 wt% content in molybdenum. It was composed of three cylindrical blocks with an outer diameter of 11 cm and a central hole of 4 cm to allow the insertion of an electrical heater for non-nuclear testing or the boron carbide control rod during nuclear testing.

KRUSTY utilized eight Haynes-230 heat pipes with sodium as working fluid, partially incorporated inside the fuel. The thermal bonding between fuel and heat pipes was achieved through the use of 6 ring clamps made of Haynes-230.

Two different neutron reflector regions were distinguished: the radial reflector and the axial reflector. The axial reflector is further divided into an upper and a lower portion, consisting of two cylinders placed on the fuel's top and bottom, respectively. The radial reflector is further divided into the platen and the shim reflector, either of them composed of several BeO rings. Specifically, the platen radial reflector was the portion of the reflector that had to be raised and lowered by COMET machine and could contain up to 12 BeO rings, while the shim radial reflector was permanently fixed to the upper shield and could hold up to 2 BeO rings. This split of the radial reflector into two portions represents the most significant difference in KRUSTY design with respect to Kilopower. Indeed, the latter was supposed to approach criticality through the control rod withdrawn rather than lifting the platen radial reflector. Nevertheless, this design feature was indispensable in KRUSTY to measure radial reflector and control rod reactivity worths during the experimental demonstration. A thin stainless steel sleeve was placed between the core can and the radial reflector to prevent the reflector rings from getting in mechanical contact with the core can.

The shielding completely surrounded the fuel and reflector. Specifically, the radial shielding was made of type 316 stainless steel (SS316) and was placed on the COMET table. The axial shielding consisted of alternating layers of B4C and type 304 Stainless Steel (SS304) and was strategically placed wherever space was available [17].

KRUSTY was intended to produce 1 kWe for 15 years. The system was designed to have eight independent strings of heat pipes, Stirling converters, and heat rejection radiators.

Therefore, each converter is required to be sized to produce 125 W of electrical power using 375 W of thermal power.

Fuel material	UMo
Total fuel height	25 cm
Fuel inner diameter	4 cm
Fuel outer diameter	11 cm
Heat pipes walls material	Haynes-230
Heat pipes working fluid	Sodium
Amount of working fluid per heat pipe	15 g
Heat pipes outer diameter	1.27 cm
Heat pipes wall thickness	0.089 cm
Ring clamps material	Haynes-230
Ring clamps outer diameter	12.13 cm
Ring clamps thickness	3 cm
Vacuum can material	SS316 %
Vacuum can thickness	0.305 cm
Vacuum can outer diameter	13.3 cm
Vacuum can axial length	52.5 cm
Control rod material	B4C
Control rod diameter	3.5 cm
Reflector material	BeO %
Radial reflector inner diameter	7.25 cm
Radial reflector outer diameter	38.1 cm
Radial reflector disk thickness	2.54 cm
Axial Reflector Height	10.16 cm
Axial reflector diameter	6.325 cm
Radial shielding material	SS316
Radial inner diameter	41 cm
Radial outer diameter	101.9 cm
Radial shielding height	63 cm
Axial shielding material	SS304 and B4C
Axial shielding slabs thickness	2.54 cm

Table 2.1: KRUSTY design parameters [17].

Assuming 1000 W of thermal losses between the core and the power conversion system, the reactor needed to produce at least 4000 W of thermal power at an operating temperature of 1100 K. Such design allowed to operate the system for 15 years with a fuel burnup of 0.1 %, which is essential since fuel burnup must be kept lower than 0.5 % to avoid fission gas release and swelling to represent a potential failure mechanism. However, for the KRUSTY test only two 80 We Stirling converters were used, as there was no time to design the correctly sized units. The remaining converters were replaced by 6 simulators that were able to withdrawn 600 W of thermal power [18]. The actual power KRUSTY reactor was designed for was of 4 kWth, but the Stirling engines acquired for the demonstration could not remove the necessary power, and the Stirling simulators were "limited" as well because they were designed to match the characteristics on the engines for dynamic demonstration reasons. Therefore, the actual nominal test power was of 3 kWth, which still had enough margin to verify that KRUSTY could produce 5 kWth or more [19]. In Figure 2.7 is shown a schematic representation of the KRUSTY three dimensional model that was constructed through MNCP Monte Carlo code by LANL, for the simulation of the system neutronics. In Table 2.1 are listed the main design features of KRUSTY.

2.2.2. Test Procedure

The experimental demonstration of KRUSTY is composed of several phases, that led to the final 28-h nuclear full power test accomplished in March 2018.
Prior to that, material tests had to be performed to study certain material properties that were unavailable or were not considered useful since based on past research data. Such tests consisted in full-scale KRUSTY thermal prototype in which a stainless steel electrically heated core was used instead of a HEU core. Properties as fuel creep, thermal expansion coefficients, diffusion behavior between fuel and heat pipes could be investigated. In parallel with the material testing, NASA performed sub-component tests to verify that the sodium heat pipes where effectively able to transfer heat from the reactor core to the power conversion system.
Afterwards, an electrically heated system test was performed using a Depleted Uranium (DU) core, that was exactly the same material as HEU from the chemical point of view, but depleted in U-235. The use of DU core allowed to investigate the mechanical and material interfaces between metallic UMo fuel and Haynes-230, but it also represented an opportunity for the Kilopower team to perform training exercises regarding reactor refuelling.
Such "non-nuclear" tests were fundamental to reduce risks in performing the actual

KRUSTY experimental demonstration, that was further divided into three tests [20]:

- **Cold Critical testing**, during which several zero power critical test were completed to compare and verify neutronic modelling parameters, providing fundamental information that will be used to re-asses model results before performing experiments at full power. The main goal of the test was to assess the radial reflector and the control rod reactivity worth.
- **Low Temperature Testing**, during which several tests were run at low temperature prior to the testing at full power. Such runs were performed imposing an excess reactivity in the system lower than 0.80$, so that the reactor could work in a regime where it was controlled by delayed neutrons, limiting the system temperature.
- **Full Power, High Temperature Testing**, which consisted in a full power run of KRUSTY. Such test required about 1.70$ in excess reactivity to achieve operating temperature. Nevertheless, to compensate for any possible source of uncertainty in the modelling, 2.20$ worth of excess reactivity was loaded onto the machine in the form of more BeO radial reflector rings, 0.50$ more with respect to what it was needed. During this test, KRUSTY approached operating conditions and it experienced several transients, during which power removal was partially cut or completely removed and the reactor was let to automatically adjust to the new power demand. Afterwards, the original power removal was established, allowing KRUSTY to compensate and load follow back to the original power level.

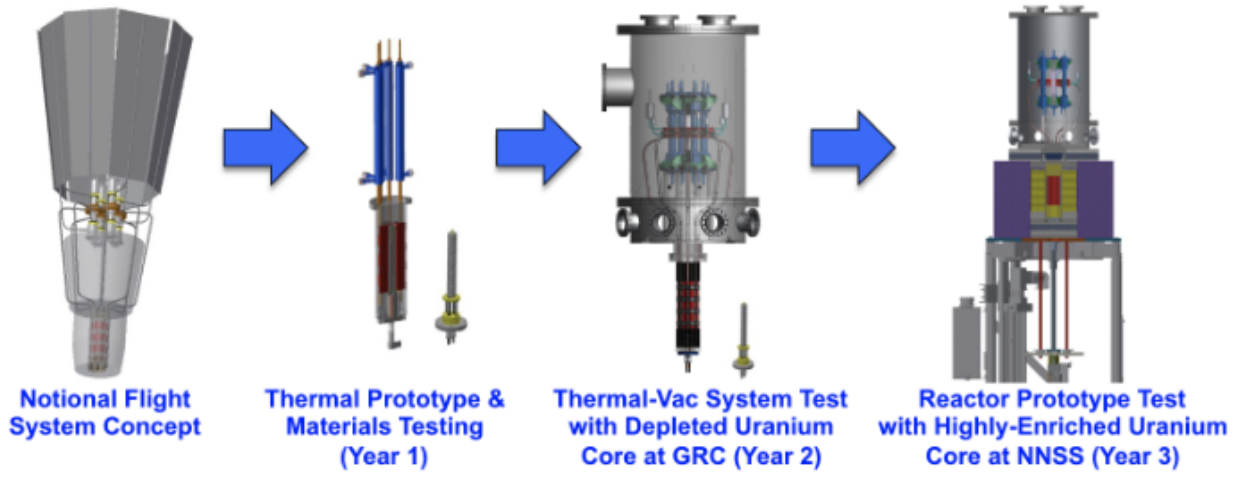

Figure 2.8: Schematic representation of KRUSTY experimental demonstration phases [21]

3 | Modelling of KRUSTY

The serpent model of KRUSTY is created to be as similar as possible to the MNCP model directly performed by LANL, since the results of the latter are intended to be employed for the code verification. Furthermore, LANL simulations accompanied KRUSTY design development, representing the most faithful description of the reactor neutronics. This implies that verification and validation procedures can be carried out on the same model of KRUSTY, without any changes being made. The similarity with the LANL model is attainable thanks to the availability of most design parameters used to create the MNCP input file, particularly to materials, temperature, and dimensions of all the various KRUSTY components.

3.1. Serpent

In this work, Serpent Monte Carlo code developed at VTT Technical Research Centre of Finland is used as a fundamental tool to perform KRUSTY neutronics analysis. The Monte Carlo method is a stochastic computational method of resolution for particle transport problems, whose strength stands in its ability to simulate the transport process without directly solving the transport equation. The working principle consists of simulating each particle's life from its birth to its death, which occurs when the particle is absorbed or escapes from the system. The frequency and outcome of any interaction that the particle may experience are randomly sampled according to interaction probabilities derived from particle physics. If such a procedure is repeated for a large number of particles, the result is a detailed simulation of the transport process that can be exploited to calculate statistical estimates for integral reaction rates. [22].
The process of simulating the movement of every single neutron inside the geometry is referred to as "particle tracking" and is based upon the sampling of the free path length between two points of interaction. In most cases, the geometry consists of several homogeneous material regions, and since the material properties are different in each region, the interaction probabilities change each time the neutron crosses a cell boundary. The delta-tracking method is the conventional particle tracking method used in Serpent, which sam-

ples the next collision point without handling the surface crossings. Such delta-tracking method makes Serpent Monte Carlo code well suited for reactors having a neutron mean free path that is particularly long if compared to the core dimensions [23] (the exact case of a fast space reactor concept, whose main characteristic is its compactness).
All the information regarding particle interaction physics are contained in the so-called "evaluated nuclear data files", which is a collection of nuclear interaction data derived from experimental measurements and supplemented by theoretical nuclear models. Serpent reads neutron interaction data from continuous-energy cross-sections ACE format data libraries based on JEF-2.2, JEFF-3.1, JEFF-3.1.1, ENDF/B-VI.8, and ENDFB/B-VII evaluated data files. The ACE cross-sections library format is shared with MNCP, the Monte Carlo transport particle code developed by LANL that was employed to simulate KRUSTY neutronics. This means that any continuous energy ACE format data library generated from MCNP can be used with Serpent, and the results could be compared to MNCP calculations without additional uncertainties originating from the nuclear data.
To drive KRUSTY design process, LANL used MRPLOW FORTRAN code as a primary tool. MPRLOW input file contained all key parameters that could be used to create a three-dimensional design, calculate steady-state temperatures of various reactor components and generate estimates for mass, nuclear parameters, system efficiency, etc.
The resulting MRPLOW output files were used as input decks for MCNP, that was able to calculate the system multiplication factor, power and reaction rates distributions, and it was used to study basic criticality with various combinations of temperature, rod position or surrounding environment. ENDFB/B-VII cross-sections data library was used for the baseline calculations since it was provided of numerous temperature intervals. If cross-sections were not available in ENDFB/B-VII, LANL used JEF2.2, JEF3.0, JENDL3.2, JENDL3.3 cross-section data libraries. As the reactor design progressed, decks were created by MRPLOW code. Indeed, the latter was able to calculate steady state temperatures through the use of approximated conduction equations, apply shifts in the geometry due to thermal expansion, specify temperature-dependent cross-sections, and create coolant void coefficients [19]. These decks were used to generate reactivity coefficients, control worths, kinetic parameters, ect [17].

3.2. Serpent Input File Description

In Table 2.1 are listed the main geometrical features of KRUSTY that Serpent input file was based on.
Serpent code uses a universe-based geometry, meaning that it is divided into different levels that are nested inside the other. This approach is particularly useful since it en-

ables to model regular lattice geometry structures, such as square, hexagonal lattices or vertical stacks that are commonly present inside nuclear reactors. The model is built from elementary and derived surfaces that are used to form two or three-dimensional regions, denoted as cells [22]. Each cell must be filled with a specific material, whose density, temperature, and isotopic composition must be precisely specified in the input file.
In Table 3.1 are reported the densities at environmental conditions of all materials that were used in Serpent input file.
Except for Uranium inside fuel and Boron inside the control rod, it is assumed that all the other nuclides are present with their natural isotopic abundance inside all the various materials. Indeed, HEU fuel has an U-235 content of 93 %, while the control rod was enriched up to 99 % in B-10, to maximize its neutronic worth.

Material	Density
UMo	17.15
Haynes-230	8.97 g/cm^3
BeO	2.86 g/cm^3 (99.5 %TD)
SS316	7.99 g/cm^3
SS321	8.09 g/cm^3
SS304	8.00 g/cm^3
B4C-enriched	2.15 g/cm^3 (90 %TD)
B4C-natural	1.791 g/cm^3 (75 %TD)
H2O	0.997 g/cm^3
SiO2	2.65 g/cm^3

Table 3.1: KRUSTY input file materials densities.

It is of fundamental importance to use cross section libraries generated at the right temperature to correctly simulate the Doppler broadening of resonance peaks, which causes an increase in parasitic neutron absorption. Indeed, the thermal motion of a target nucleus implies a random variation in the relative velocity between the neutron and the target nucleus itself, which is much more pronounced as the temperature increases. When the neutron energy is close to a high resonance peak, the energy dependence is strong, and the thermal motion of the target atom occasionally shifts the energy closer to the peak value, increasing the nuclear interaction probability [23].
In Serpent input file, when KRUSTY is said to be in "cold conditions", all components

are assumed to be at environmental temperature. When the reactor is said to be in "warm conditions" (to assess the temperature reactivity defect), it is imposed a fuel temperature of 1100 K, while all other components are left at environmental temperature.
It is also essential to use bound atom thermal scattering libraries for moderator nuclides, such as hydrogen inside water, silicon inside SiO2 and beryllium inside BeO. If such libraries are not employed, interactions are treated as they were occurring between neutrons and free target atoms. This is actually a good approximation if the neutron energy is bigger than the atom binding energy inside the lattice or the molecule, which is generally of a few eV. Below this limit, neutron scattering with a bound atom cannot be treated as a collision with a free particle without causing a significant error in the calculations.
The default calculation mode in Serpent is the criticality k-eigenvalue source method, that differently from the external source method does not require the definition of any source distribution inside the geometry. The simulation is run in cycles and the source distribution in each cycle is given by the fission reaction distribution calculated in the previous one. The multiplication factor is defined as:

$$k = \frac{\text{number of source neutrons in cycle n+1}}{\text{number of simulated histories in cycle n}} \tag{3.1}$$

The statistical accuracy of the results depends on the total number of active neutron histories that are run, which is determined by the population size per cycle and the total number of active cycles. This allows to set the desired precision of the model at the only cost of an increased computational time.
The following analysis sets a population size of 100000 neutrons per cycle, with 50 inactive cycles and 100 active cycles, resulting in a relative statistical uncertainty on the multiplication factor ranging from 0.00025 to 0.00035. Inactive cycles are required since in the criticality source method, no source input is set, and the fission source distribution is randomly selected inside the cell where the fissile material is contained. Inactive cycles are run to allow the initial fission source distribution to converge before starting to collect results.
The main source of uncertainty is related to manufacturing tolerances and flaws in the evaluated nuclear data libraries. Deterministic characterization of these uncertainties is a non-trivial task that will not be treated in this work. The only available source of uncertainty is of statistical nature and is directly computed by Serpent [22].
In Figure 3.1 are shown the front and cross-sectional views of the three-dimensional geometry that was constructed through Serpent to simulate KRUSTY neutronics.

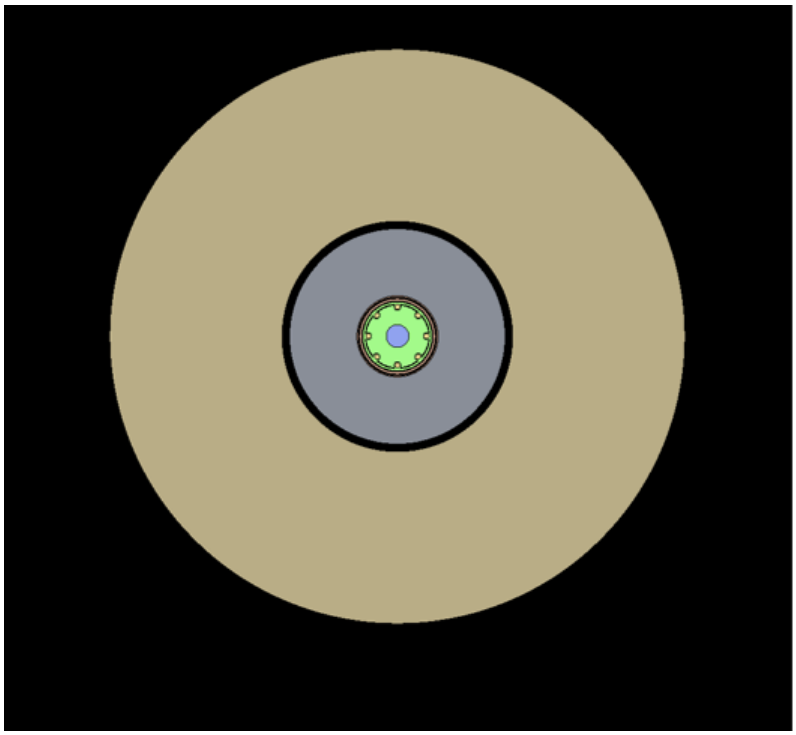

(a) KRUSTY cross sectional view.

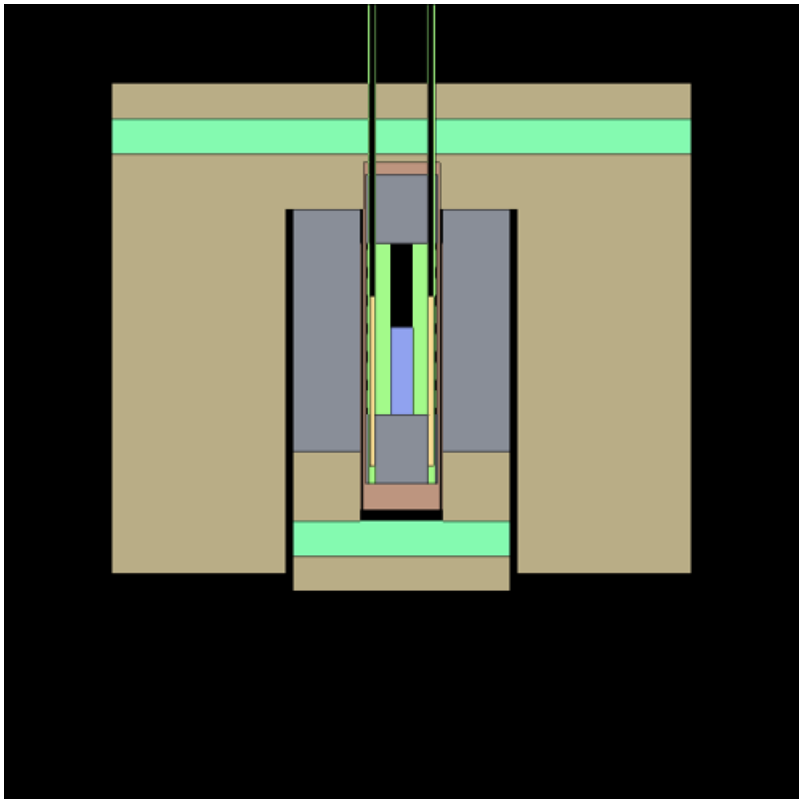

(b) KRUSTY core front view.

Figure 3.1: Frontal and cross sectional view of KRUSTY core.

3.3. Code Verification

The verification of Serpent code is performed by simulating some aspects of KRUSTY neutronics and comparing the results with those of LANL simulations. The main advantage of using LANL simulations is that they had accompanied the design development of KRUSTY, and their results were eventually re-assessed according to the results of the experimental demonstration. Therefore, they represent the most precise modeling of the reactor neutronics. In the following, Serpent code is used to:

- Study how KRUSTY approaches criticality.
- Asses the radial reflector reactivity worth.
- Assess neutron spectra and power density distributions.
- Perform safety analysis to guarantee the system remains largely subcritical in various possible accidental scenarios.

3.3.1. KRUSTY Reactivity Defect

From now on, environmental conditions are referred to as "cold conditions", while operating conditions are referred to as "warm conditions". KRUSTY was specifically designed to insert negative reactivity as it approached warm conditions. Such reactivity defect is composed of two "prompt" contributions:

- Temperature reactivity defect (calculated as 1.63$) due to the rise of various components' temperatures.
- Power reactivity defect (calculated as 0.07$) caused by the phase change of heat pipes working fluid.

Another contribution to the reactivity defect that increases during reactor lifetime is the drift defect due to fissile material consumption. However, for KRUSTY it can practically be neglected due to its short length of operation.
In Figure 3.2, the operating temperature of each single component and the corresponding temperature reactivity defect estimated by LANL are listed, specifically distinguishing the contribution given by thermal expansion and the contribution given by changes in cross-sections due to doppler broadening. Such results refer to a precise KRUSTY configuration with 12 disks in the platen radial reflector stack, 1 disk in the shim radial reflector stack, no control rod inserted and with a 0.5 cm gap left from having the platen radial reflector fully closed.

	Temp(K)	cents	% of defect	% defect expand+xs
expand fuel	1075	-147.7	90.4%	96.7%
warm fuel cross sections	1100	-10.3	6.3%	
expand heatpipes	1051	-1.7	1.1%	2.0%
warm heatpipe cross sections	1100	-1.6	1.0%	
expand bracket	1045	-0.7	0.4%	1.6%
warm bracket cross sections	1000	-1.9	1.1%	
expand axref	413	-0.6	0.4%	0.2%
warm axref cross sections	400	0.3	-0.2%	
expand mfi	806	0.0	0.0%	0.3%
warm mfi cross sections	800	-0.4	0.3%	
expand vacves	374	1.9	-1.1%	-1.1%
warm vacves cross sections	350	-0.1	0.1%	
expand radref	311	-0.9	0.5%	0.5%
warm radref cross sections	300	0.0	0.0%	
platen shielding	309	0.3	-0.2%	-0.2%
Total Temperature Defect		-163.5		
pool up (-4.75cm to 15.25cm)		-7.0		
Total Operating Defect		-170.5		

Figure 3.2: Reactivity defect of all KRUSTY components [19].

The fourth column reports the weight percentage of the single component temperature defect with respect to the total of 163.5 cents. Being KRUSTY a very compact fast spectrum reactor, geometry and density changes are the ones to dominate the temperature feedback, not the change in the cross-sections. Furthermore, the most significant contribution in the temperature defect is the one due to the rise in temperature inside fuel (96.7%), which is why it is the only one considered in the following analysis.
It would be expected that the temperature defect of each single reactor component was dependent on the thermal/geometric state of the balance-of-system. This means that, for example, the fuel temperature defect could depend on the temperature and position of the reflector. An ideal solution would calculate the multiplication factor real-time, along with temperature and geometry changes. Fortunately, these second-order effects are negligible for KRUSTY and each component reactivity defect can be computed separately, assuming all the other densities and geometry remain unchanged. To compensate for it, minor adjustments should be made to individual component reactivity temperature coefficients such that the multiplication factor at nominal operating temperature matches the

all-components warm calculated multiplication factor. The fact that second-order effects are minimal for KRUSTY justifies the choice of taking into account the contribution of fuel only, neglecting the one of all the other components, without making important errors in the calculations.
To understand the reason of such behavior, it is necessary to introduce the analytical definition of the multiplication factor (k) according to the six-factors formula:

$$k = \eta_T * f * p * \varepsilon * P_{NLT} * P_{NLF} \tag{3.2}$$

where:

- the **fast fission factor** ε, defined as the ratio between fast neutrons produced by fissions at all energies to the number of fast neutrons produced in thermal fission;
- the **resonance escape probability** p, defines as the probability that neutrons during the slowing down process will be able to escape the resonance capture;
- the **thermal utilization factor** f, defined as the ratio between thermal neutrons absorbed in fuel and thermal neutrons absorbed in any other reactor component;
- the **reproduction factor** η, defined as the number of fast neutrons produced by thermal fission and the number of thermal neutrons absorbed in fuel;
- the **fast non-leakage probability** P_{NLF}, which is the probability that a fast neutron does not escape from the core;
- the **thermal non leakage probability** P_{NLT}, which is the probability that a thermal neutron does not escape from the core;

Each factor is characterized by a temperature coefficient (α_T), quantifying the differential variation in the system reactivity when the factor is changed due to variations in the system temperature. If a temperature coefficient is positive, an increase in temperature will lead to an increase in the system reactivity, and vice versa if it is negative.
One of the effects of increasing fuel temperature is the Doppler broadening of resonance peaks, which causes an increase in neutron absorption cross-sections. Therefore, the temperature coefficient associated with the resonance escape probability will be negative. Nevertheless, since KRUSTY uses HEU fuel with an extremely low content of U-238, the Doppler broadening effect is expected to be small.
Actually, the dominant contribution in the reactivity defect is related to the reduction in the total non-leakage probability, whose temperature coefficient is analytically defined as

the sum of two contributions:

$$\alpha_T(P_{NL}) = -B^2M^2 * [\frac{1}{M^2}\frac{dM^2}{dT} + \frac{1}{B^2}\frac{dB^2}{dT}] \tag{3.3}$$

Where M is the migration length, whose square is equal to one-sixth of the square of the average distance between the point where the neutron is born (as a fast neutron) and the point where the neutron is absorbed (as thermal neutron). B^2 is the geometrical buckling factor.

Since M is inversely proportional to the fuel density, an increase in the fuel temperature would cause an increase in M^2. On the other side, B^2 is inversely proportional to the square of linear fuel dimensions, meaning that thermal expansion would decrease the geometrical buckling. As a consequence, the first term of Equation 3.3 remains negative and represents the main source of reactivity defect in KRUSTY. The second term turns to be positive, but the first term completely covers its contribution. The resulting $\alpha_T(P_NL)$ is therefore negative.

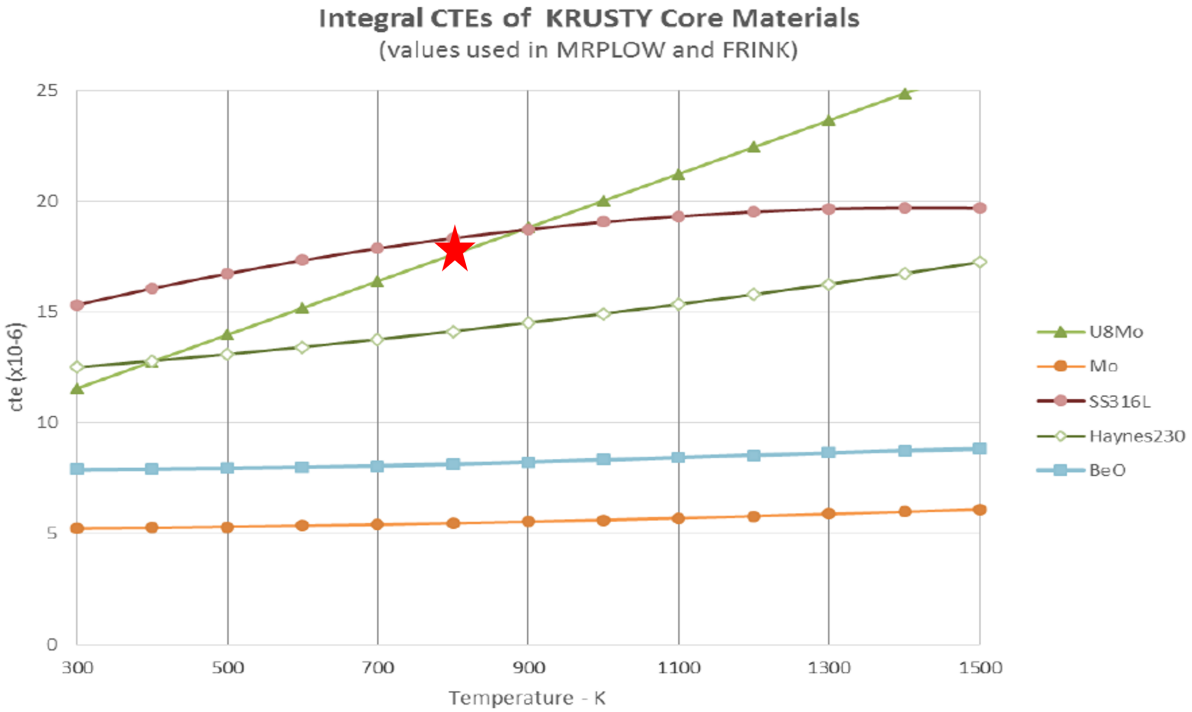

Figure 3.3: Integral linear thermal expansion coefficients of KRUSTY core materials [19].

In this study, thermal fuel expansion was estimated by considering a linear thermal expansion coefficient (CTE) of $1.750 * 10^{-5}$, extrapolated from the graph in Figure 3.3 at

fuel operating temperature of 1075 K. Assuming a temperature jump of 777 K from cold to warm conditions, it would correspond to a 1.36% extension of fuel in all directions.
A correct modeling of KRUSTY neutronics in warm conditions is fundamental for studying how the reactor approaches criticality and for the estimation of the radial reflector reactivity worth.

3.3.2. Approach to Criticality

The study of how the reactor approaches to criticality consists in defining the precise configuration that allows the reactor to become critical at environmental conditions and remain so until it reaches operational conditions. Differently from Kilopower reactor concept, KRUSTY becomes critical through the vertical translation of the platen radial reflector, which is placed on the lifting platen of COMET machine. The shim radial reflector has the only function of adding a proper amount of excess reactivity to the system to guarantee the reactor reaches the desired operating conditions. When there are no disks in the shim stack and no control rod inside the fuel, the reactor is supposed to become critical if the platen radial reflector is completely inserted. Therefore, the effect of BeO disks in the shim stack is to bring the reactor to a supercritical state.
If the platen is sufficiently opened, the reactor is brought into a subcritical state due to neutrons leaking out of the fuel region, which are no longer available to cause fission events. From this subcritical state, by gradually lifting the radial reflector, neutron leakage will be reduced, and at a specific level of insertion, the reactor becomes critical in cold conditions. As the power level increases, the system reactivity gradually decreases with it. The platen radial reflector would require further lifted so that KRUSTY could reach the desired operating conditions.
There are two reasons why excess reactivity is needed:

- to compensate for the operating reactivity defect, which is the reactivity loss when the system moves from cold to warm conditions, and it is composed of three contributions;
- to provide a margin for model bias, which is the difference between simulation results and reality.

Model bias is distinguished in cold and warm bias. Cold bias is the difference between the model and the zero power conditions, and it is expected to be mainly due to uncertainty in BeO cross-sections; warm bias is the difference between the modeled operating defect and the experimental operating defect. If no model bias is left, there is the possibility that KRUSTY is not be able to reach its nominal power even when the reflector is fully

inserted, in a configuration where its performance is maximized and can no more increase the system reactivity. In cold conditions, KRUSTY was loaded with 1.62$ more reactivity than what was needed to cover the operating defect. Ideally, it was desired to reduce this model bias margin to 0.50$, so that the "gap" between the platen and the shim radial reflector will be smaller, resulting in better shielding and power profile.
With two disks in the shim stack and the platen radial reflector completely inserted, the reactor is predicted to be already supercritical in warm conditions. This means that the platen radial reflector must be slightly withdrawn to bring the reactor into a critical state, leaving a gap between the platen radial reflector and the shim radial reflector. To reduce this gap, it is effectively possible to load only one BeO disk in the shim stack instead of two. Indeed, the first case provides an excess reactivity of 0.50$ when the platen is fully closed, while the second case of 1.62$.
Thus, considering only one disk in the shim stack and no control rod inserted inside fuel, LANL evaluated the multiplication factor as a function of platen position in cold and warm conditions (Figure 3.4).

Figure 3.4: LANL simulation: multiplication factor as a function of platen position [19].

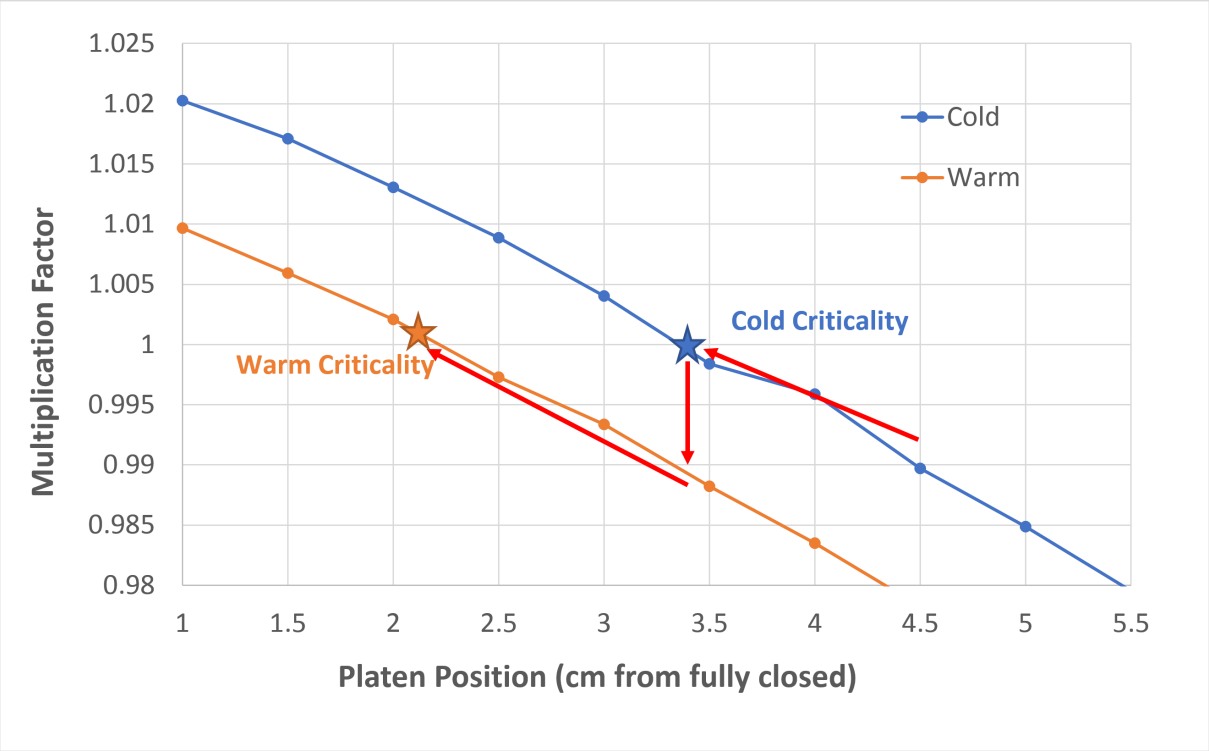

Figure 3.5: Serpent simulation:Multiplication factor as a function of platen position from being fully closed.

According to LANL simulations, the cold reactor would go critical at a platen position of 2.2 cm. As the reactor heats up, the platen would slowly be raised up to 0.5 cm, approaching the steady-state warm operating condition.
Figure 3.5 shows Serpent simulation results, characterized by an average relative statistical uncertainty of 0.00034. Cold criticality is achieved with a 3.4 cm gap between the platen and shim radial reflector, while warm criticality is achieved with a 2.2 cm gap. In LANL simulations, such gaps are a little smaller, but this could be expected since the multiplication factor in Serpent simulations is, on average 1200 pcm greater than what it was obtained in LANL simulations. Furthermore, the radial reflector insertion to pass from cold criticality to warm criticality is of 1.2 cm instead of 1.7 cm, due to the smaller reactivity defect with respect to LANL results. In Table 3.2 is reported a comparison in the multiplication factor evaluated in warm and cold conditions in a reactor configuration where the platen radial reflector is fully closed. The difference in the multiplication factor, quantifying the operating reactivity defect, for Serpent model is 100 cm smaller with respect to LANL model.

	LANL Simulation	Serpent Simulation
Warm Multiplication Factor	1.0147	1.026
Cold Multiplication Factor	1.0027	1.015
Difference	1200 pcm	1100 pcm

Table 3.2: Multiplication factor in cold and warm conditions, with the platen radial reflector fully inserted.

3.3.3. Radial Reflector Reactivity Worth

LANL estimated the radial reflector reactivity worth by assessing the multiplication factor as a function of the radial reflector height (ranging from 0 cm to 35.56 cm) in either environmental and operating conditions (Figure 3.7). Specifically, the radial reflector height was increased in steps of a quarter of an inch, simulating the gradual loading of thin BeO disks onto the platen stack. This procedure was supposed to be performed in the cold critical test for measuring the reflector reactivity worth. In Figure 3.6 is reported the reactivity worth of each single BeO disk, in a range of radial reflector height between 10.75 in. and 14 in..

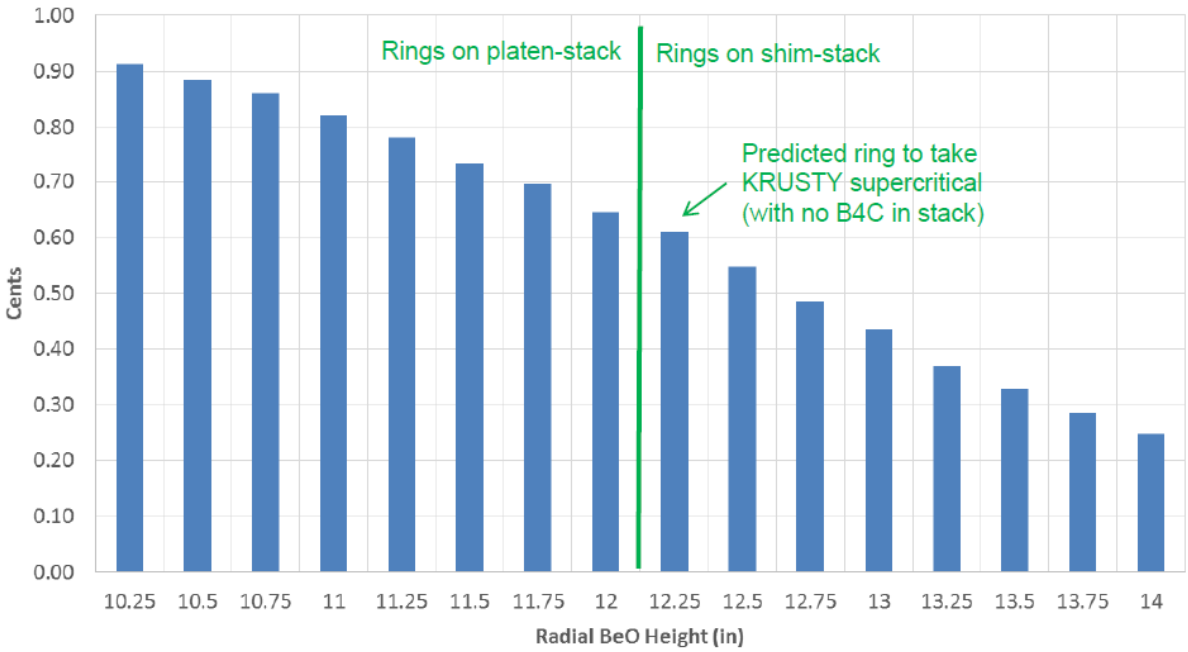

Figure 3.6: LANL simulation: radial reflector BeO disks worth in cold conditions (with and without a 3.8 cm drop in the lifting platen) and warm conditions [19].

As it was previously mentioned, KRUSTY radial reflector is divided into two portions: the platen reflector and the shim reflector. A radial reflector height of 35.56 cm corresponds to the case of having 12 BeO disks in the platen stack and 2 BeO disks in the shim stack, with the platen radial reflector fully closed. Beo disks are in this case, are considered with a reflector thickness of 2.54 cm.
In cold conditions, LANL model predicts criticality at a radial reflector height of 30.48 cm, corresponding to 12 BeO disks. Any BeO disk in the shim stack would make the reactor supercritical. The multiplication factor as a function of radial reflector height was also evaluated in cold conditions with COMET lifting platen dropped of 3.8 cm, to check that KRUSTY would remain subcritical at any radial reflector height. Such configuration, indeed, would allow KRUSTY to be shut down in case of need.

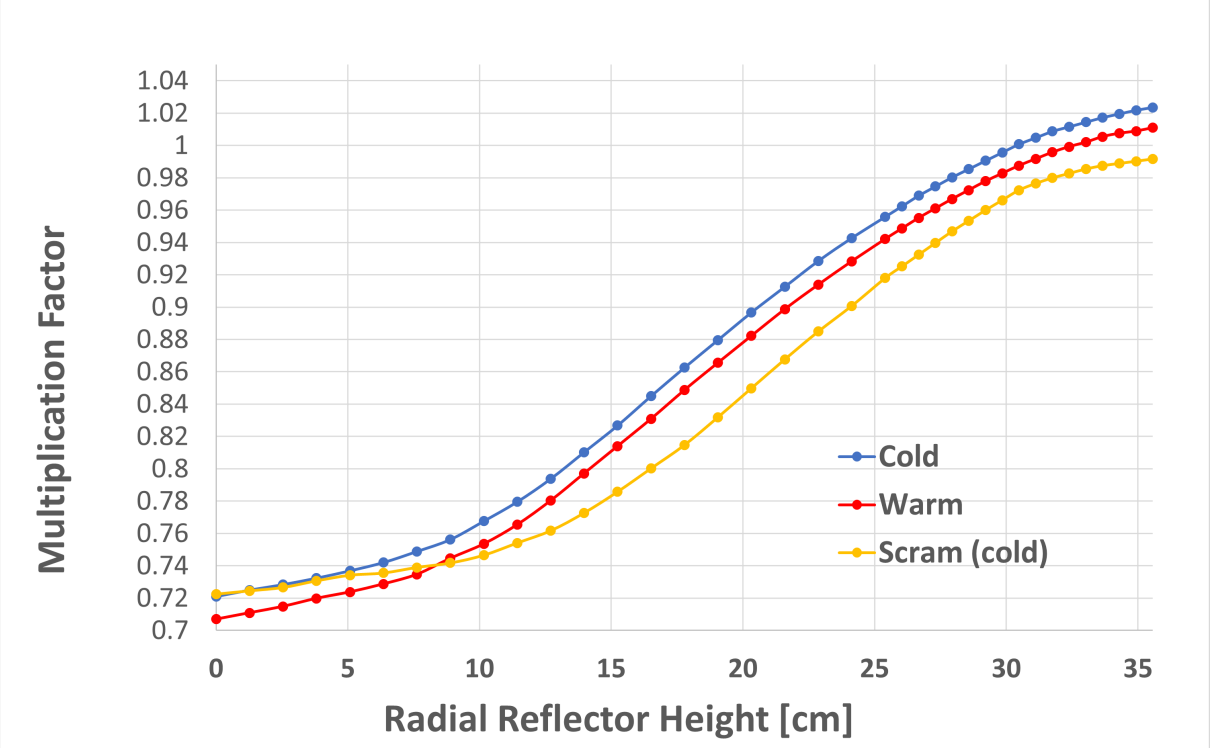

Figure 3.7: LANL simulation: multiplication factor as a function of radial reflector height [19].

In Figure 3.8 the results of Serpent simulations are shown, characterized by an average relative statistical uncertainty of 0.00034. The trend of the multiplication factor as a function of the radial reflector height is in accordance with LANL results. Indeed, the results in terms of radial reflector total reactivity worth are exactly the same (Figure 3.3). Serpent multiplication factors are only characterized by a constant positive error

of 1200 pcm. This suggests the presence of some systematic errors, probably related to small differences in some material densities and KRUSTY three-dimensional geometry built with Serpent with respect to those used in the MCNP code.
Due to the positive error in the multiplication coefficient, in cold conditions, criticality is achieved at a radial reflector height smaller than 30.48 cm. Again in cold conditions, the resulting multiplication factor at a radial reflector height of 35.56 cm is 1.035, 1300 pcm greater than what LANL obtained. Furthermore, in shut down conditions, with a 3.8 cm drop of the lifting platen, KRUSTY results much closer to critical conditions, with a multiplication factor of 0.992.

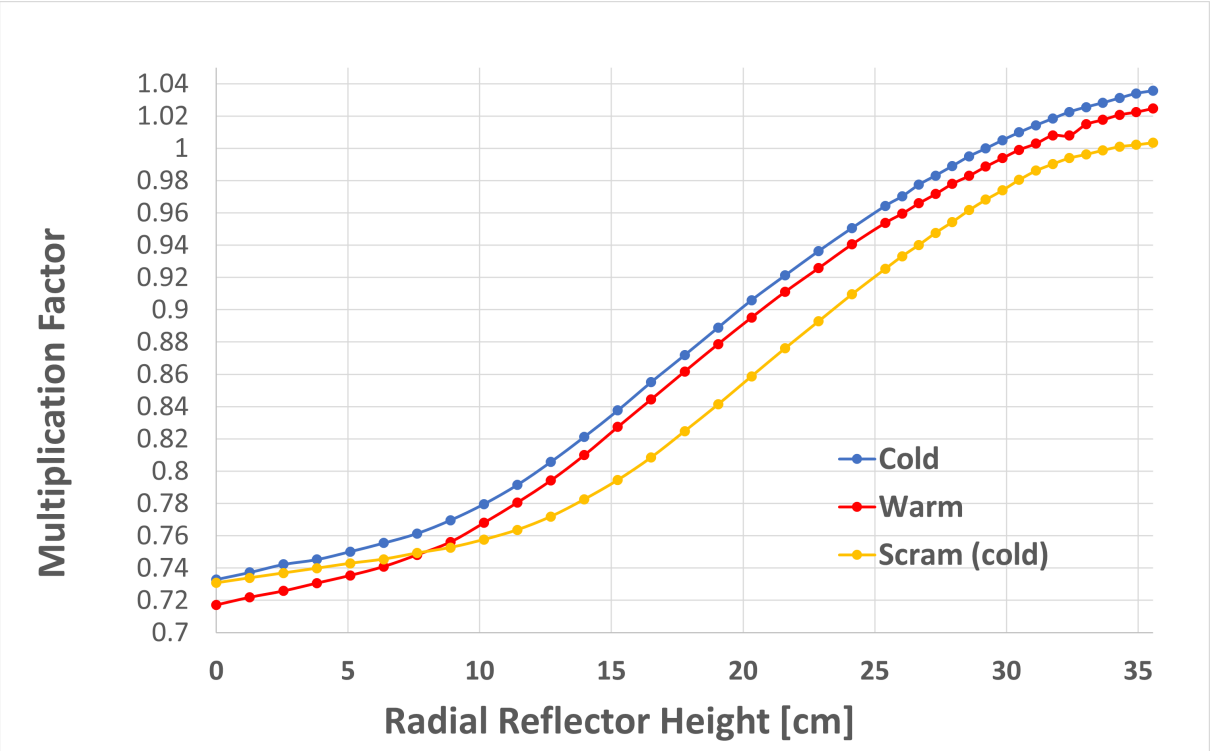

Figure 3.8: Serpent simulation: Multiplication factor as function of radial reflector height in cold conditions (with and without a 3.8 cm drop in the lifting platen) and warm conditions.

	Radial Reflector Worth
Cold Conditions	59$
Warm Conditions	61$
Shut Down Conditions	54$

Table 3.3: Total radial reflector reactivity worth.

3.3.4. Power Density Distribution and Neutron Spectra

KRUSTY was designed to produce 5 kWth, just as Kilopower. Nonetheless, due to limits in the Stirling convertor simulators, the power level had to be reduced to 3 kWth, with a corresponding average power density inside fuel of $1.61 W/cm^3$.
The power density along the axial coordinate is expected to be peaked, but slightly asymmetrical due to the presence of a gap in between the shim and the platen radial reflector. The shape of the power density along the radial coordinate should be flatted in the central region [24]. This typical behavior of fast reactors is due to the relatively long fast neutrons' mean free path, that is of 3 cm for KRUSTY [19]. The neutron mean free path is defined as the mean distance traveled by a neutron between two subsequent interactions. If such distance is comparable to reactor dimensions, power distribution tends to be flat, while if it is bigger than the reactor dimensions, it can result in a local power peaking.
In Figure 3.9 is shown the radial power deposition evaluated by LANL at the core center and at the third clamp elevation. For the reasons aforementioned, such power density distribution is quite uniform in the central region but slightly tilted outward due to thermal neutrons scattered back from the BeO reflector and are therefore characterized by a higher probability of inducing fission. This particular radial power density profile is also beneficial in terms of temperature drop along the radial direction. The core center section is not surrounded by any core clamp, which is the reason why the corresponding radial power density has a more pronounced relative edge peaking. Indeed, the clamp absorbs lower energy neutrons due to the tungsten contained in Haynes-230, causing a spatial depression in the neutron flux. A depression in the neutron flux reduces the number of fission events, consequently leading to a local decrease in the power production.
The third clamp is just below core center, where there is no heat pipes clamp. At such elevation, the radial power density is slightly higher due to the axial peaking caused by the small gap that is left between the shim and the platen radial reflector.
The axial peaking is of 1.1, which is quite small if compared to most reactors. This is due to the neutrons' mean free path of 3 cm, which is smaller enough with respect to fuel height to cause the presence of an axial power peaking but not too big to make such power peaking particularly important.
Furthermore, five relative "peaks" are present between the location of ring clamps, where more moderated neutrons can reach the fuel [19]. Indeed, as aforementioned, the heat pipes clamps presence causes a local neutron absorption and, therefore, a reduction in the power production. In Figure 3.10 is shown the axial power density distribution normalized with respect to the average power density assessed by LANL. It is evident how the bigger is the gap between the platen and shim radial reflector, the higher is the resulting axial

peaking factor since neutron leakage outside the core is much more important.
The average neutron flux is of $9.3 * 10^{11} \mathrm{n/s} * \mathrm{cm}^2$, and the neutron spectrum inside fuel is evidently fast (Figure 3.11).

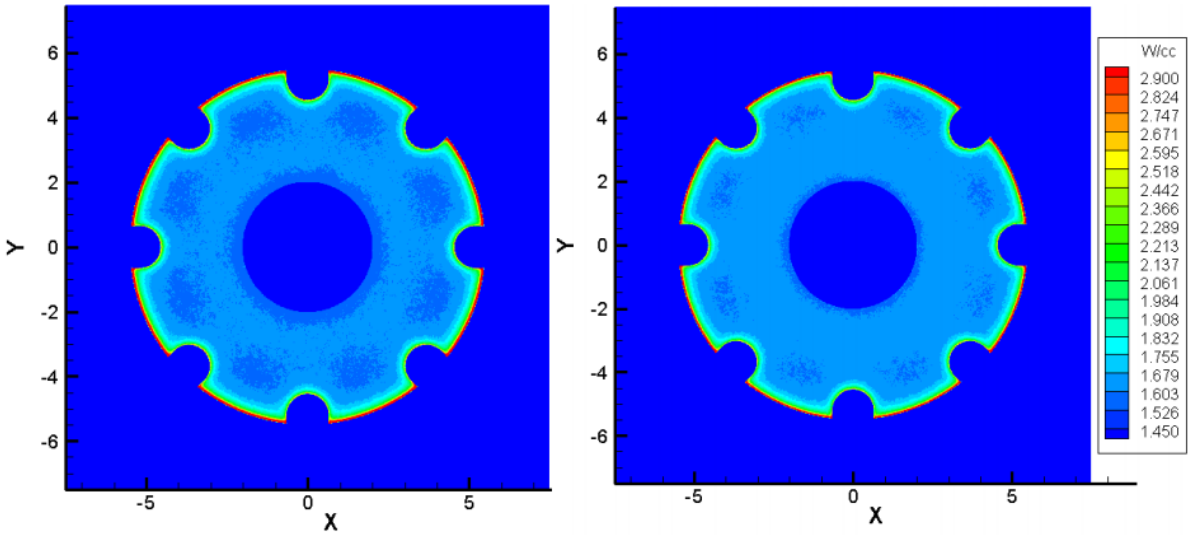

Figure 3.9: LANL simulation: radial core power deposition: axial section at the core centre (on the left) and at the third clamp elevation (on the right) [19]

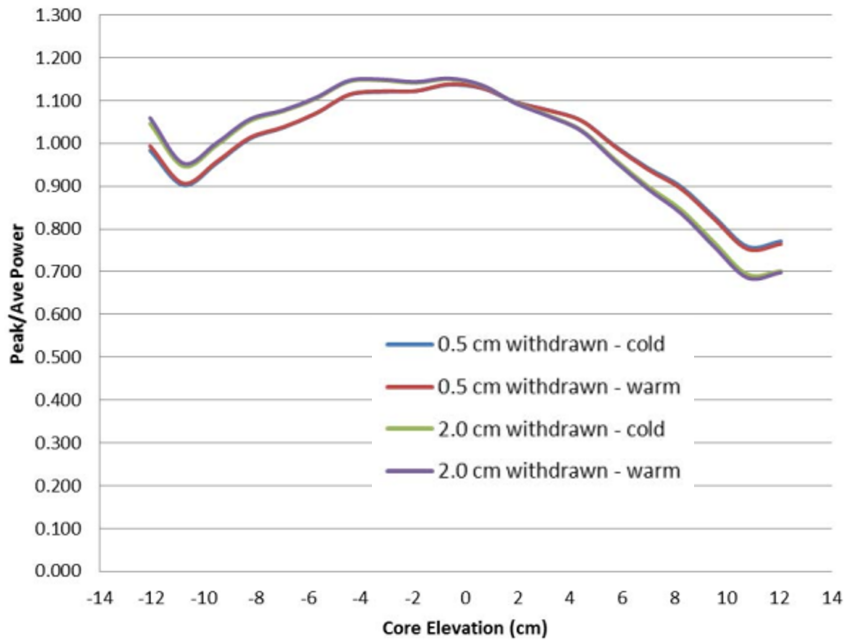

Figure 3.10: LANL simulation: normalized axial power distribution [19]

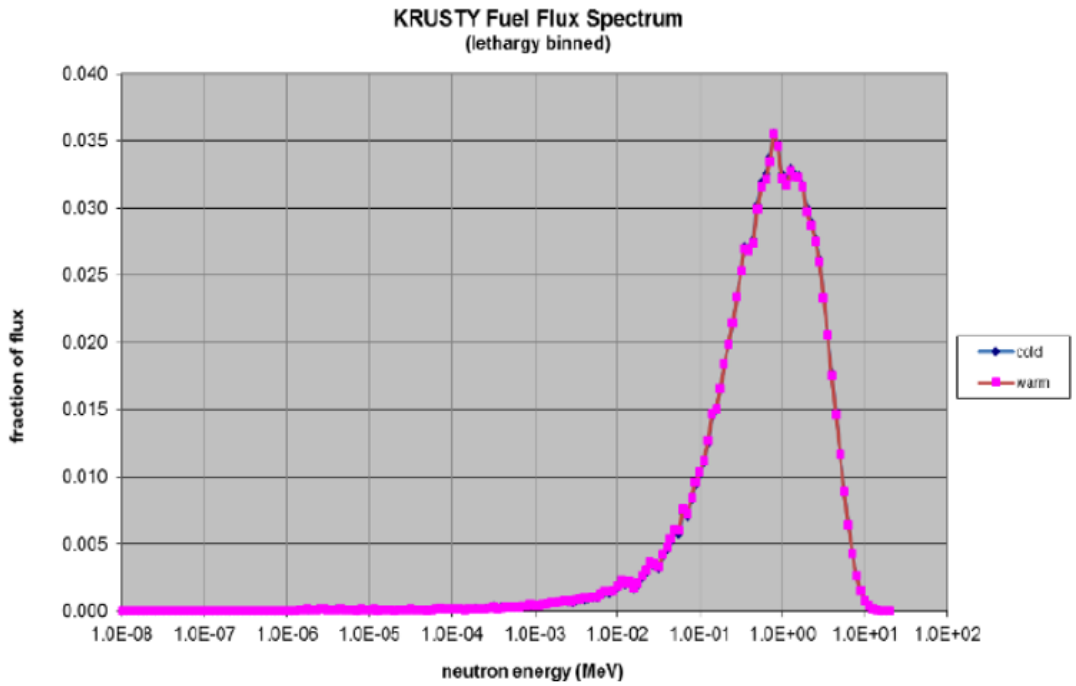

Figure 3.11: LANL simulation: KRUSTY neutron spectra inside fuel, in cold and warm conditions [19].

Serpent is also used to evaluate the axial and radial power density distributions inside KRUSTY fuel. In Figure 3.12 is shown the normalized axial power density distributions resulting from platen radial reflector withdrawal of 3.4 cm and 2.2 cm, respectively, referring to cold critical and warm critical configurations. Normalization has been performed with respect to the average fuel power density. The air gap between the shim and platen radial reflector affects the axial power density profile, which is slightly asymmetrical. The warm critical configuration, characterized by a smaller air gap between platen and shim radial reflector, results in less power peaking, but not by a great amount (1.17 vs 1.15). The five relative peaks due to the neutron absorption from heat pipes ring clamps are also present.
The radial power density distribution is assessed at 45° and 22.5° along the azimuthal coordinate (Figure 3.13), to investigate the influence of heat pipe presence. In (Figure 3.14 and Figure 3.15) are shown the radial power density distributions in cold and warm critical configurations. The profile is uniform in the central fuel region and slightly increases at the fuel surface. The radial peaking edge at 45° is smaller due to heat pipes interposed between fuel and the radial reflector that prevents thermalized neutrons from returning to fuel. Finally, the average power density at operating conditions resulted of 1.55 W/cm^3, evaluated considering the increase in the fuel volume due to thermal ex-

pansion. If thermal expansion was not considered, the average power density would be of $1.61 \mathrm{W/cm}^3$, exactly as the one obtained by LANL simulation.

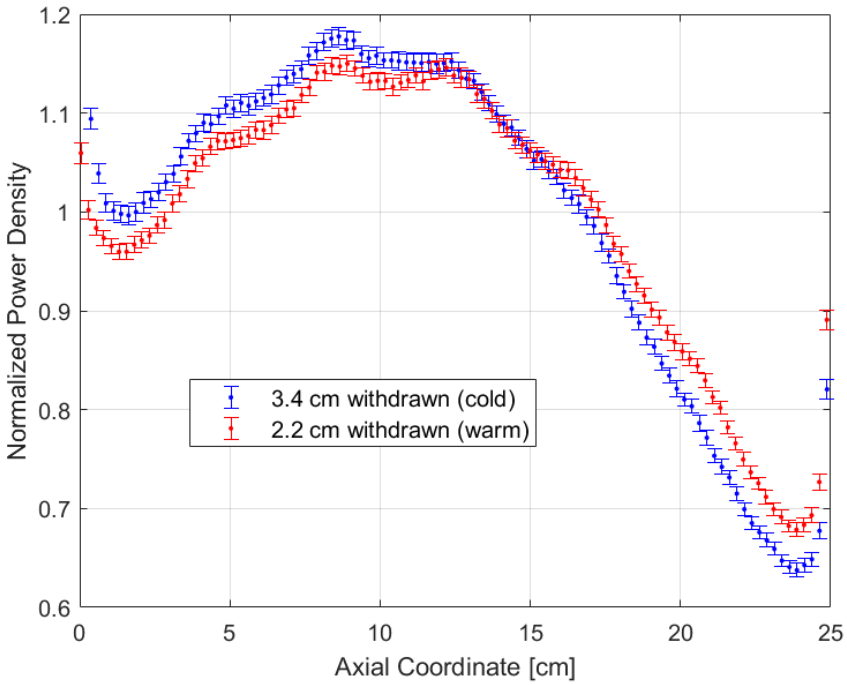

Figure 3.12: Serpent simulation: Normalized Axial power density profile inside fuel, with platen radial reflector 3.4 cm withdrawn (cold critical) and 2.2 cm withdrawn (warm critical).

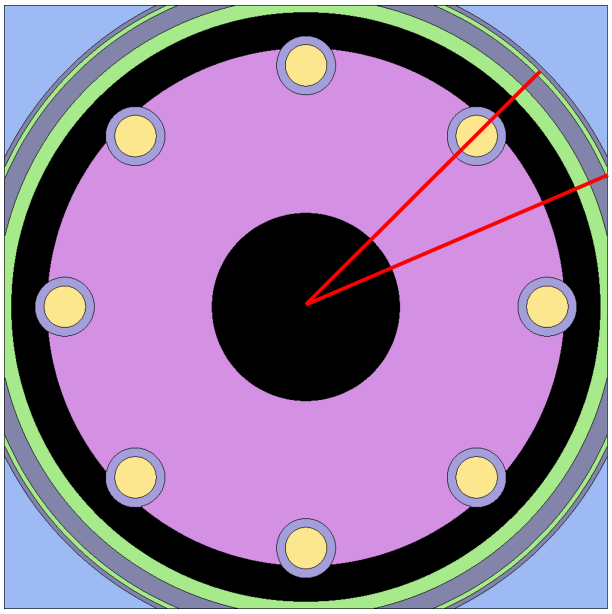

Figure 3.13: KRUSTY core cross sectional view.

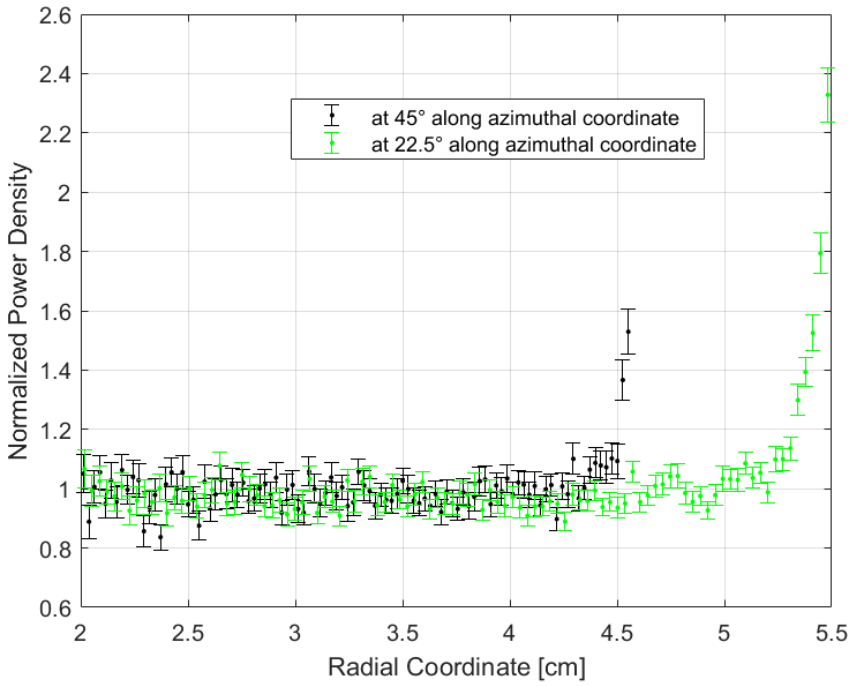

Figure 3.14: Serpent simulation: normalized radial power density profile inside fuel in cold conditions.

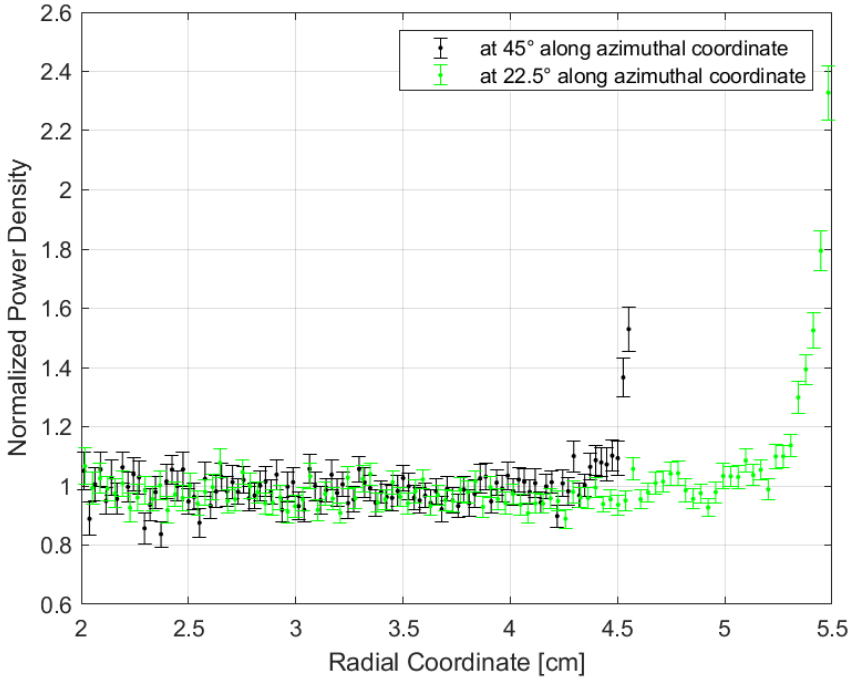

Figure 3.15: Serpent simulation: normalized radial power density profile inside fuel in warm conditions.

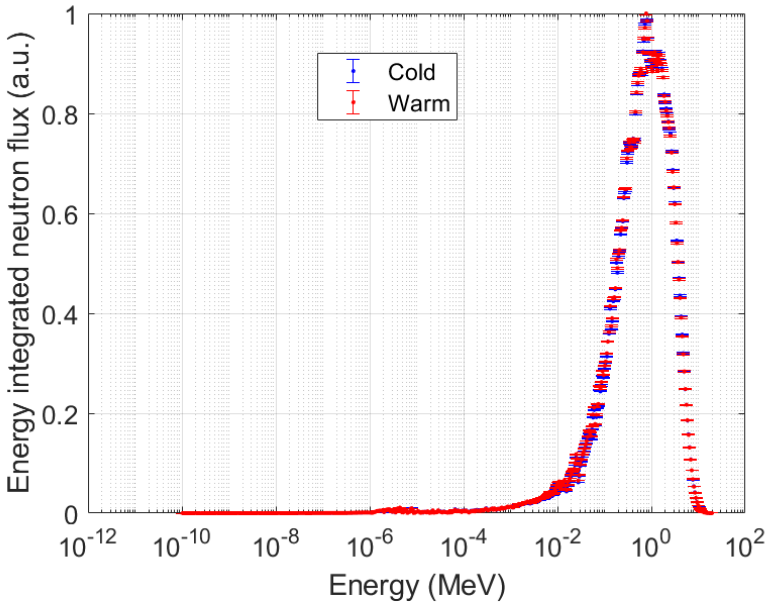

Figure 3.16: Serpent simulation: energy integrated neutron flux in cold conditions.

In Figure 3.16 is shown KRUSTY energy integrated neutron flux evaluated inside fuel and normalized with respect to the maximum value fuel. The average neutron flux in warm conditions was of $8.44 \times 10^{11} \mathrm{n/cm^2 s}$, the same order of magnitude of LANL simulation results.

3.3.5. Safety Analysis

Safety analysis is required to gain launch approval and consists in checking if in the worst accidental scenario the reactor remains largely subcritical. Worst accident scenarios refer to the cases in which KRUSTY fuel lands on the earth's surface and ends up completely surrounded by air, water, sand, or wet sand (with no control rod and reflector). The latter three materials play the role of very effective and almost infinitely thick reflectors and, potentially, they may lead to inadverted criticality. The worst-case scenario is when the control rod is missing without any damage in the reflector. Even if such a situation will inevitably lead to a supercritical reactor, it was not considered in the safety analysis. Indeed, such behavior is typical of any reactor as long as a conventional control rod is adopted as reactivity control system, since the reactor is designed to become supercritical when the control rod is withdrawn if there is no change in other parts of the reactor [25]. Besides, it is expected that a strong impact able to remove the control rod will surely destroy the fragile ceramic reflector.
Since KRUSTY fuel was composed of three cylindrical blocks of equal height and diameter,

LANL considered all the following possible spatial arrangements (Figure 3.18):

- One isolated fuel block.
- Three fuel blocks stacked one on the top of the other one (full length fuel).
- Three fuel blocks in a paint-can stack configuration.
- Three fuel blocks in a triangle pitch configuration.
- KRUSTY assembly outside of core can (including fuel, heat pipes, clamps, upper axial shielding and reflector).

All configurations were completely surrounded and immersed, such that all open voids were filled. Dry and wet sand were assumed to be 64% of silica with 36% of porosity and a homogeneous mixture of 64% silica and 36% water, respectively. According to LANL results, (3.17 there is no material that fuel could be accidentally surrounded by that would make it critical, other than beryllium oxide or more fissile material.
In this analysis, water density is considered to be of 0.97 g/cm^3 and silica density of 2.65 g/cm^3, either of them at environmental conditions. In general, in all cases the multiplication factor is always greater with respect to LANL results (+1000 pcm), coherently with the aforementioned systematic positive error. The only exception regards configurations completely surrounded by wet sand, characterized by a greater error of 3000 pcm. Such deviation may be caused by the different wet sand density that was in LANL simulations, unfortunately not available. Despite this, in all possible accidental scenarios, the system remains largely subcritical. Results of the full-length fuel configuration are the closest to LANL simulations, still with the exception of the case in which wet sand is the surrounding material.

	bare	water	sand	wet-sand
KRUSTY fuel 1 section	0.4577	0.7642	0.6034	0.7127
KRUSTY fuel 3-section column	0.5886	0.9591	0.8310	0.9346
KRUSTY fuel 3-section triangle pitch	0.5776	0.9710	0.8210	0.9368
KRUSTY fuel 3-section paint-can stack	0.5846	0.9806	0.8296	0.9446
KRUSTY assembly outside of vessel/shield	0.6148	0.9155	0.8311	0.9062

Figure 3.17: LANL safety analysis [19].

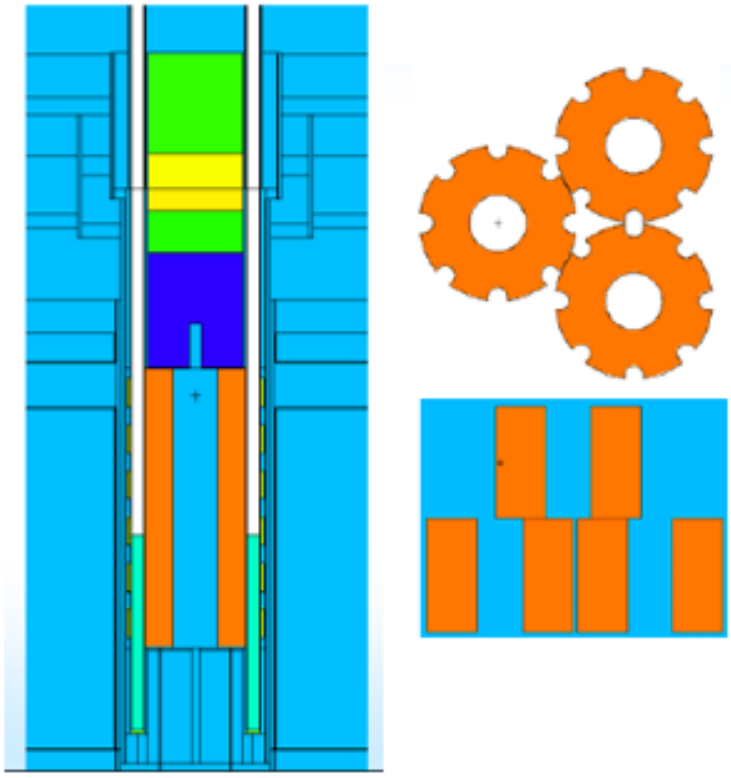

Figure 3.18: KRUSTY assembly, paint can stack and triangle pitch configurations [19].

$K_{effective}$	**Bare**	**Water**	**Dry sand**	**Wet sand**
Fuel 1 section	0.468	0.773	0.613	0.743
Fuel 3 section column	0.599	0.968	0.840	0.966
Fuel 3 section triangle pitch	0.589	0.982	0.831	0.969
Fuel 3 section paint-can stack	0.596	0.990	0.832	0.977
Assembly outside of vessel	0.624	0.925	0.842	0.936

Table 3.4: Serpent Safety Analysis.

Error (pcm)	Bare	Water	Dry sand	Wet sand
Fuel 1 section	+1000	+900	+1000	+3000
Fuel 3 section column	+1000	+900	+900	+3100
Fuel 3 section triangle pitch	+1100	+1100	+1000	+3200
Fuel 3 section paint-can stack	+1100	+900	+900	+3200
Assembly outside of vessel	+900	+900	+1100	+3000

Table 3.5: Relative error of Serpent Safety analysis results.

3.4. Code Validation

The only available experimental results of KRUSTY test that could be potentially exploited for Serpent code validation regard the calibration of the control rod. Such calibration was performed during the cold critical experiment, whose goal was to define the exact reflector and control rod heights in order to obtain the desired 3.00$ of excess reactivity for the hot critical experiment.

The cold critical experiment represented the only reason why in KRUSTY reactor the reflector and control rod were realized in the form of disks stacked one on the top of the other one. Indeed, the experimental procedure consisted in adding a 0.317 cm thick BeO disk on the top of the platen radial reflector stack, such that KRUSTY was placed into a supercritical state in which neutrons population could experience an exponential increase in time. Form this condition, control rod disks of 0.317 thickness were gradually added until the reactor was brought back into a critical state. Each time a B_4C disk was added onto the control rod stack, the exponential rise in the neutron population was measured and recorded. The resulting data were analyzed to determine the reactor period, with whom it was possible to assess the reactivity through the use of the in-hour equation. Such reactivity measurements were performed on 52 different configurations. The first 39 were provided of two 2.54 cm thick BeO disks in the shim pan, the latter 13 of only one disk. The two calibration curves that were obtained (Figure 3.19) shows that the trend remains unchanged when passing from two disks to one disk in the shim pan.

Inhour parameters used for the KRUSTY experiment are listed in Table 3.6 and were originated by Godiva Inhour Parameters, with a beta effective value of 0.0065. The reactivity measurements for each configuration have experimental errors of approximately 1 cent.

In Figure 3.20 and 3.21 results of Serpent control rod calibration modeling are reported and compared with the results of the cold critical experiment. Reactivity has been eval-

uated assuming $\beta = 0.0068$, with an absolute statistical error of 0.000148. The overall statistical error is of approximately 50 cents, justifying the deviation from the experimental data, which could be also due to the presence of systematic errors. The experimental curve always lies within the simulation results error bars.

Group Index (i)	Decay Constant s^{-1}	Relative Abundance $\frac{\beta}{\beta_i}$
1	0.01273	0.037
2	0.03175	0.211
3	0.116	0.187
4	0.3118	0.407
5	1.399	0.131
6	3.876	0.027

Table 3.6: Inhour parameters used to calculate the reactivity form the reactor period [26].

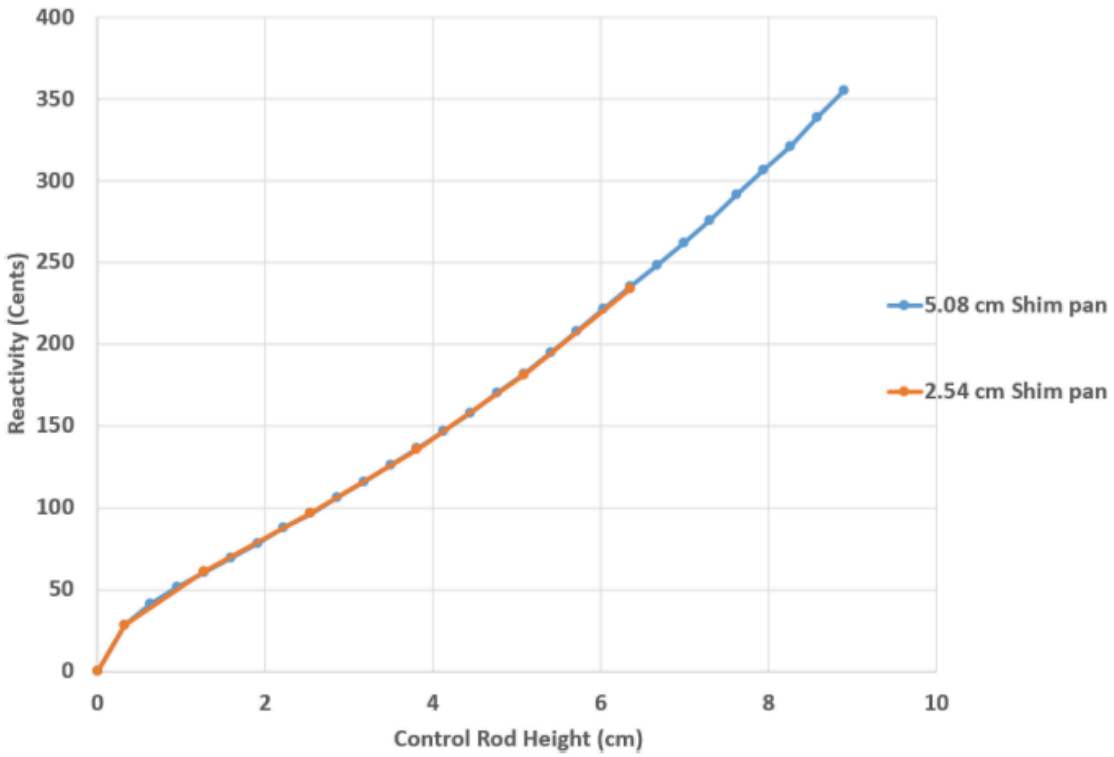

Figure 3.19: Control rod calibration measurements data [26].

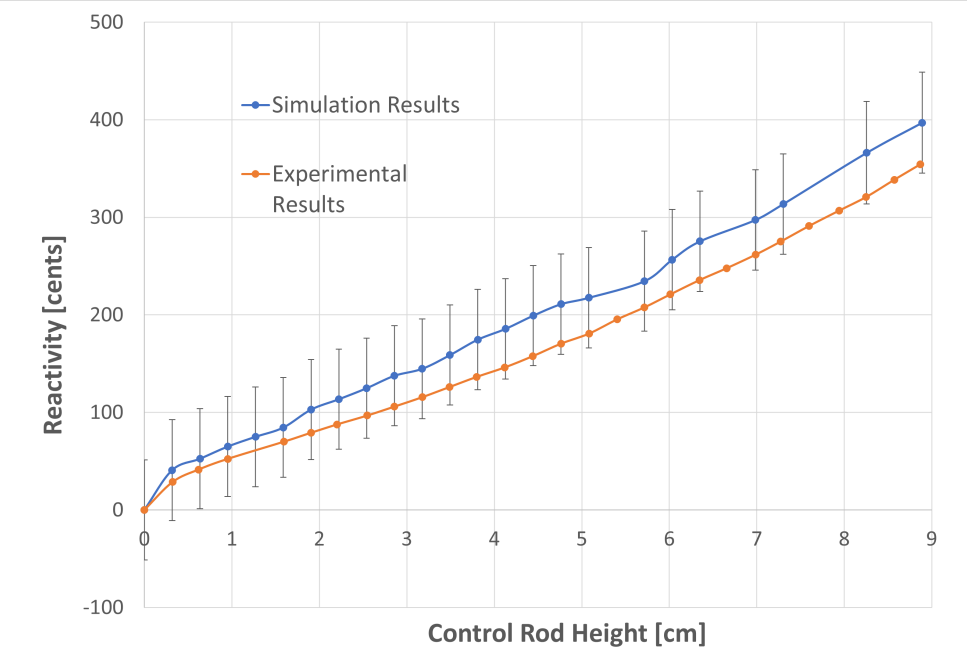

Figure 3.20: Comparison between experimental and simulation results of KRUSTY configuration having 2 disks in the shim pan.

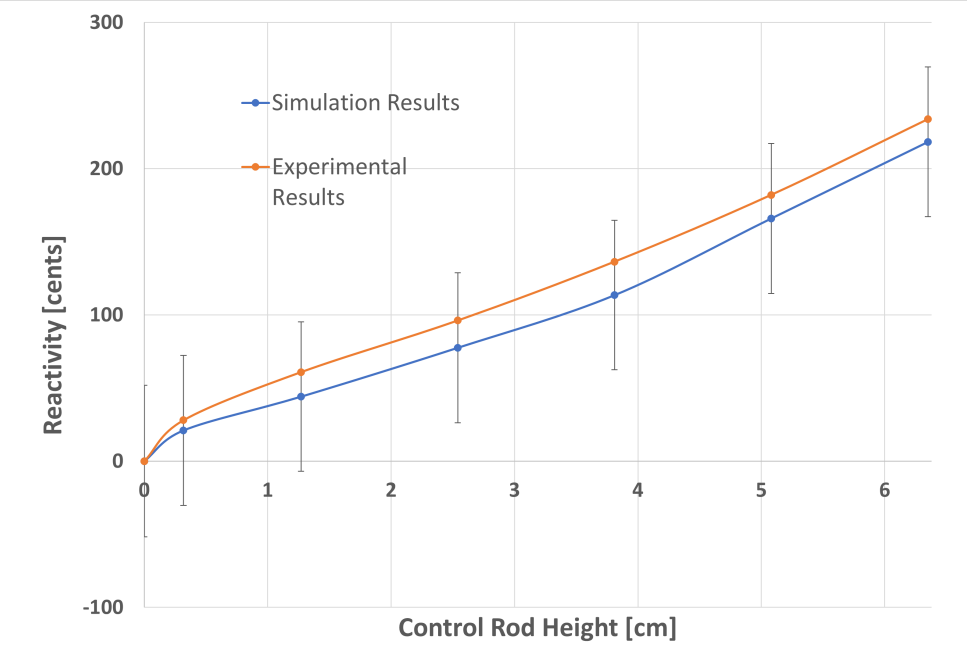

Figure 3.21: Comparison between experimental and simulation results of KRUSTY configuration having 1 disk in the shim pan.

4 | Reactor Design

The code verification was quite successful: the results of Serpent model were similar to those of LANL, only presenting a constant positive error due to some systematic sources of uncertainty related to possible differences in material densities and geometrical features with respect to LANL model. In the code validation, as Serpent model presented important deviations from the experimental data, either due to statistical uncertainty either due to systematic sources of error.
At this point, it is possible to proceed in performing the neutronic analysis of reactor configurations that employ HALEU as fuel. The idea is to start from a simplified reactor geometry similar to KRUSTY reactor, consisting of a cylindrical fuel with a central hole to host the boron carbide control rod and a beryllium oxide reflector. Between fuel and the reflector a 1.75 cm gap is left to allow heat pipes integration, some of which could be located at the fuel surface, partially incorporated inside it (Figure 4.1). Densities and compositions are assumed to be equal to those used in Serpent input file for KRUSTY modeling. The resulting multiplication factor of such simplified KRUSTY-like reactor concept is equal to 1.044 at environmental temperature. As it is reported in Table 4.1, masses and dimensions of such reactor are very similar to those of HEU Kilopower reactor concept proposed by NASA.
The aim of the analysis is to investigate the variation in the total mass of such simplified reactor concept in order to maintain a multiplication factor of 1.044 and to satisfy the non-proliferation requirement (i.e., not employing when HEU fuel). The following design changes are considered:

- Fuel enrichment is reduced from 93% to 19.75%.
- Fuel height-to-diameter ratio ($\frac{H}{D}$) is reduced from 2.27 to 1.81,
- Moderator is integrated inside the core, converting the reactor from fast to thermal.

The resulting reactors will be supported by a mass optimization analysis and safety analysis. Also, the two fast reactor concepts having different $\frac{H}{D}$ ratios are accompanied by a study on how the system approaches to criticality and the assessment of power density distributions and neutron spectra.

For what concerns thermal reactor concepts, a first analysis is performed on homogeneously moderated reactors to demonstrate the beneficial effect of uniformly mixing moderator with UMo fuel. Afterward, the effect of heterogeneity on the neutron economy is investigated.

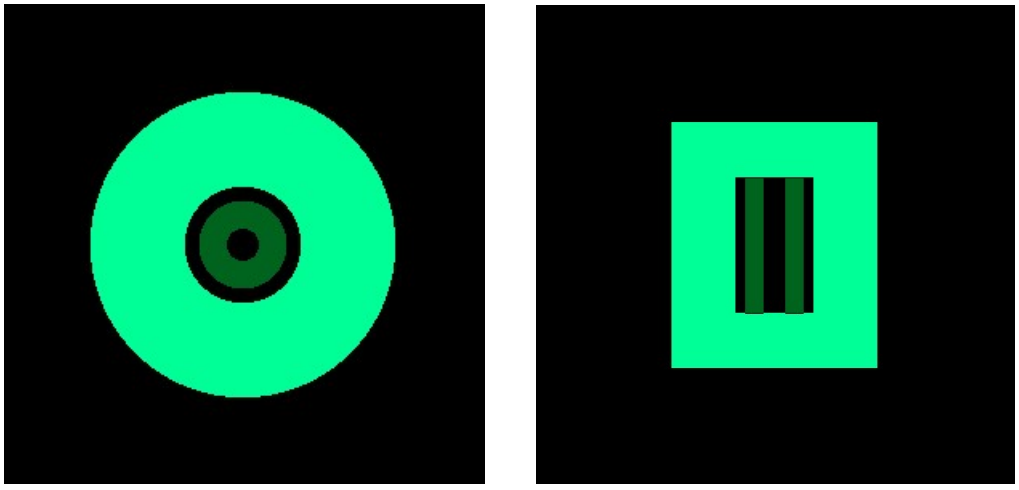

(a) Core cross sectional view. (b) Core fron view.

Figure 4.1: Frontal and cross sectional view of HEU KRUSTY-like core simplified geometry.

	Proposed Design	Kilopower
Fuel Height	25 cm	20 cm
Fuel Outer Diameter	11 cm	11 cm
Fuel Inner Diameter	4 cm	4.4 cm
Reflector Outer Diameter	40 cm	33 cm
Fuel Mass	35 kg	33 kg
Reflector Mass	135 kg	128 kg
System Mass	170 kg	161 kg

Table 4.1: Comparison between the KRUSTY-like reactor concept and Kilopower with HEU as fuel [27].

4.1. Effect of passing from HEU to HALEU fuel

HEU fuel provided significant advantages for KRUSTY, due to its availability and, most importantly, to its compact size that was easier to transport, assemble and test. Further-

more, the use of HEU as fuel seems a natural choice for a space reactor, as it allows to develop a smaller and lighter design. Mass is indeed one of the most essential discriminators in the type of mission that can be performed. Without using HEU, many planetary surfaces and deep space missions will either have reduced science payload or will not even be possible. Indeed, HEU fuel is highly concentrated in U-235 and depleted in U-238. The relative lack of U-238 allows a smaller fraction of neutrons to be absorbed inside fuel and a higher fraction of neutrons to cause fission, meaning that a smaller mass/volume of fuel would be required to guarantee the reactor criticality [14].
Nonetheless, HALEU Kilopower designs are potentially practical for many applications, provided that a 600 kg mass increase is acceptable for the end-user. Moreover, such mass increase is similar regardless of whether the system produces 1 kWe or 30 Kwe [28], meaning that the conversion into a HALEU reactor would not penalize the system in terms of specific power production.
For the aforementioned reasons, a reduction of the fuel enrichment would imply an increase in reactor dimensions to guarantee a specific behavior from the neutronics point of view. Therefore, starting from the KRUSTY-like reactor concept, if the fuel enrichment is set to 19.75%, its dimensions have to be increased until the desired multiplication factor of 1.044 is obtained.
It must be underlined that in Serpent model of KRUSTY, the multiplication factor with the platen radial reflector completely inserted and two reflector disks in the shim stack was of 1.035, which is a little lower than 1.044 of the KRUSTY-like reactor concept. This difference is probably due to the presence of other components in KRUSTY that are not considered in the simplified geometry and could cause further neutron absorption. The excess reactivity of such a system is required to primarily guarantee a complete compensation of the reactivity defect at operational conditions, but it is also necessary to leave some margin for possible errors in the model. Nevertheless, the simplified geometry that is considered in this study makes the necessity of margin for error almost pointless due to the high intrinsic uncertainty of the model. The only reason why it makes sense to start with a configuration whose multiplication factor is greater than KRUSTY is that HALEU core operational reactivity defect is not known a priori, but it can be only assessed once the mass-optimized reactor geometry is defined. If this margin is not left, the reactor may not be able to reach operational conditions.
In this study, since the goal is always to optimize the system in terms of mass, fuel enrichment is chosen to be the highest possible but still within limits to be considered as HALEU. In Table 4.2 is described the specific composition of the HALEU fuel that is employed.

Isotope	Weight Fraction
Natural-Mo	7.65 %
U-235	18.23 %
U-234	0.18 %
U-238	73.92 %

Table 4.2: HALEU UMo fuel isotopic composition.

By reducing fuel enrichment down to 19.75% and maintaining the same KRUSTY-like simplified geometry, the multiplication factor is reduced to 0.55. At this point, it is necessary to increase the reactor dimensions in order to raise the multiplication factor to the desired value of 1.044. The only geometry parameter that will be left unchanged is the inner fuel hole. Two different paths can be followed to improve the system neutron economy:

- Increasing the fuel mass, which implies an increase in the amount of fissile material and consequently an increase in the number of fission events.
- Increasing reflector thickness to reduce neutrons' leakage out of the core.

With the idea of optimizing the system in terms of mass, it is necessary to find the best combination of reflector thickness and fuel dimensions. Indeed, the reflector has two main functions: it allows to reduce the reactor mass, but it also provides sufficient reactivity worth to meet launch accident criticality safety requirements. The greater the reflector thickness, the smaller the fuel mass will be to guarantee the same behavior in terms of neutron economy. Furthermore, as a consequence of the smaller fuel mass, the fuel itself is more easily designed to remain subcritical during forming, handling, transport operations, and in all potential launch accident scenarios [27]. Nonetheless, it is not advisable to increase the reflector thickness as much as possible since this may drive away from the goal of minimizing the system mass.
To demonstrate what it is quoted above, the multiplication factor is assessed as a function of the reflector thickness in a reactor with a fixed fuel geometry equal to the one of the KRUSTY-like reactor concept. From the plot in Figure 4.2, it is evident that the multiplication factor remains unchanged above a reflector thickness of 36 cm, approaching to a value of 0.802. The effect of further increasing the reflector thickness is only to increase the reactor mass, without any important improvement in terms of neutron economy.

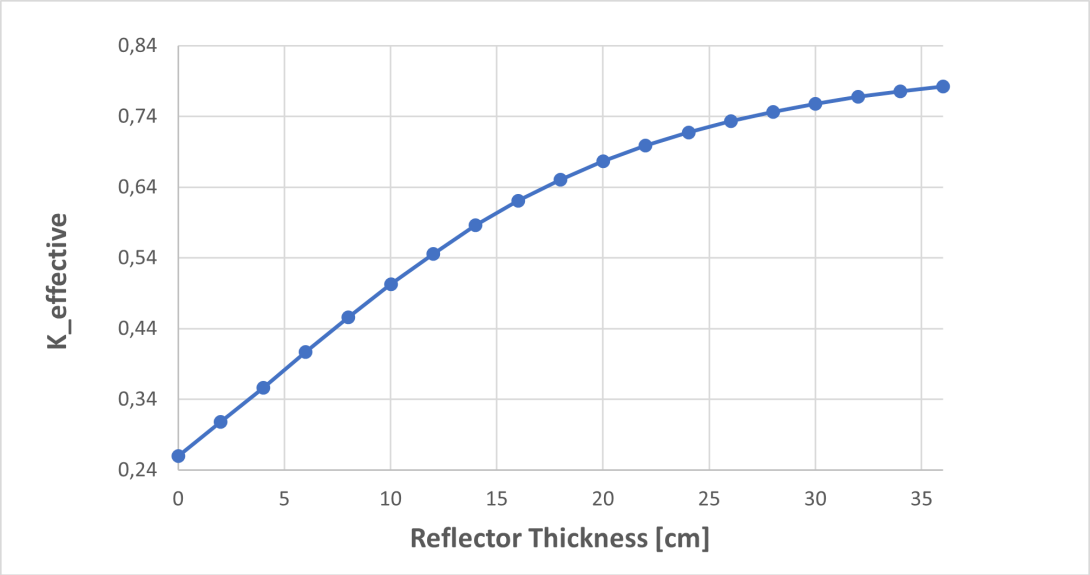

Figure 4.2: Multiplication factor as a function of reflector thickness for a LEU reactor core whose fuel geometry is equal KRUSTY's.

In such geometry, the reactor results to be largely subcritical. To raise the multiplication factor to the desired value, fuel mass must be increased. Assuming a reflector thickness of 36 cm, by gradually increasing fuel dimensions, it is possible to find the geometry that allows a multiplication factor of 1.044. In this procedure, the ratio between fuel height and fuel diameter ($\frac{H}{D}$) is fixed to 2.27, just as it was for KRUSTY.
Actually, in terms of mass minimization, it would be better to have a H/D = 0.9. Indeed, if fuel composition is fixed, there are many combinations of fuel height and diameter that are able to guarantee the same behavior in terms of neutron economy. If $\frac{H}{D}$ was equal to 0.9, fuel will be characterized by the minimum volume possible, and thus the minimum mass [29]. Nonetheless, the constraint on $\frac{H}{D}$ ratio has different reasons. Although in terms of mass minimization, it would be better to have a cylindrical fuel whose diameter is approximately equal to its height, in a fission reactor for space applications, it is preferred to maintain a H/D $>$ 1. This reduces shielding dimensions, increases the heat transfer surface between fuel and heat pipes, and shortens heat conduction paths. A greater $\frac{H}{D}$ also provides more axial separation/shielding from the high flux region of the reactor. Furthermore, the control rod and the radial reflector would have a higher neutronic worth, facilitating criticality safety [27].
In Table 4.3 a mass and dimensions comparison between the HEU KRUSTY-like core and the HALEU core with the most effective reflector thickness is reported. The HALEU core fuel mass is 8 times bigger, while reflector mass is 15 times bigger with respect to the HEU core. Furthermore, the design is far from being similar to HALEU Kilopower

reactor concept proposed by NASA, underlining that this approach of using the most effective reflector thickness is incorrect.
Indeed, the reactor design requires to be accompanied by a mass optimization analysis to figure out a reactor geometry that represents a good compromise between the goal of minimizing the system mass and the requirement of meeting inadverted criticality safety constraints.

Core type	HEU KRUSTY-like	HALEU (36 cm thick reflector)
Reflector Outer Diameter	40 cm	97 cm
Fuel Outer Diameter	11 cm	18 cm
Fuel Height	25 cm	40 cm
Fuel Mass	35 kg	157 kg
U-235 Mass	30 kg	29 kg
Reflector Mass	135 kg	2137 kg
Total Mass	170 kg	2294 kg

Table 4.3: Comparison of HEU KRUSTY-like core and HALEU core with the most effective reflector thickness.

4.1.1. Mass Optimization Analysis

In the previous subsection, the reactor was designed considering the most effective reflector thickness (36 cm). Although the reflector was able to perform at its best, the system ended up to be considerably massive. Clearly, the lowest mass reactor will result from a balance between fuel diameter and reflector thickness, which can be found through a mass optimization analysis. The basic idea would be to consider a range of radial reflector thickness from 0 to 20 cm and performing for each of them an iterative procedure in which the fuel diameter is gradually increased until a geometry that enables a multiplication factor of 1.044 is found, still maintaining $\frac{H}{D} = 2.27$. In Figure 4.3, it is plotted the fuel mass, the reflector mass and the total mass as a function of the reflector thickness of such systems.

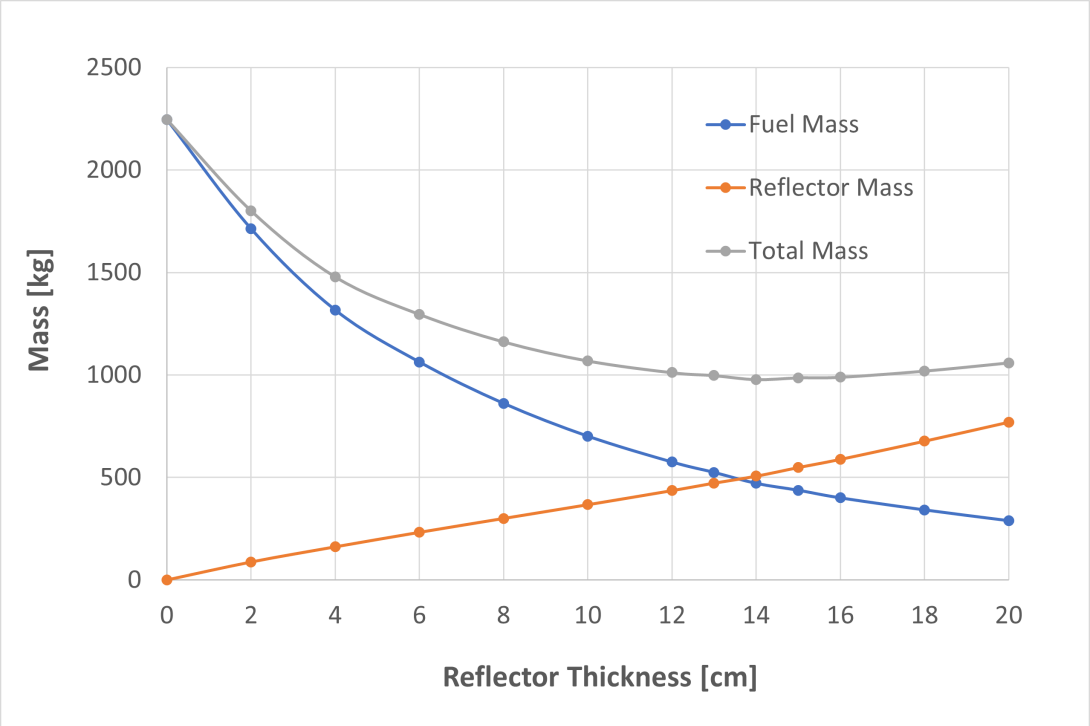

Figure 4.3: Fuel mass, reflector mass and total core mass as a function of reflector thickness.

The minimum reactor mass corresponds to a reflector thickness of 14 cm (less than half of the most effective one). In Table 4.4, HALEU lightest reactor geometry parameters are reported and compared with those of KRUSTY-like HEU reactor concept, the first characterized by a 13 times greater fuel mass and 4 times greater reflector with respect to the latter.

It must be underlined that the analysis is performed without fixing the fissile isotope amount. Each reactor will have a slightly different lifetime according to the amount of fuel and the operating power level, and it will be more or less suitable depending on the duration of the specific space mission is used for. When passing from HEU to HALEU, the U-235 content is more than doubled, which means that potentially the reactor can operate for a longer period of time. Indeed, the reactor lifetime is directly proportional to the initial amount of fissile material inside the core.

Core Type	HEU	HALEU (36 cm thick reflector)	lightest HALEU
Reflector Outer Diameter (cm)	40	97	57
Fuel Outer Diameter (cm)	11	18	25
Fuel Height (cm)	25	40	57
Fuel Mass (kg)	35	157	477
U-235 Mass (kg)	30	29	86
Reflector Mass (kg)	135	2137	509
Total Mass (kg)	170	2294	986

Table 4.4: Comparison of core designs.

4.1.2. Safety Analysis

The resulting reactor is optimized in terms of mass, but it must satisfy safety requirements to avoid the occurrence of inadverted criticality. Therefore, it is necessary to perform a safety analysis such as the one performed for KRUSTY to check if the core remains largely subcritical during launch accidents such as rocket explosion, re-entry or crash on the ground or in the ocean. The safety analysis consists in evaluating the multiplication factor when the fuel is completely surrounded by void, water, dry sand, and wet sand, assuming all its gaps to be filled up with the surrounding material. In KRUSTY, since fuel was composed of three blocks, safety analysis had to be performed considering all their possible spatial arrangements. Conversely, for all reactors proposed in this study, fuel is in the form of a single monolith, and therefore the "full-length fuel" configuration will only be taken into account. Such choice is also convenient since, among all possible KRYSTY fuel configurations that were considered in the safety analysis, the full-length fuel configuration is the one provided of the minimum error if compared to LANL simulation results.

Table 4.5 reports the multiplication factor in all possible accident scenarios, not only for the lightest reactor but also for those reactors that should be provided of a thicker reflector. The thinner reflector in the lightest reactor may turn into a problem since it will have a smaller reactivity worth. Consequently, a higher fuel mass will be required to guarantee the same behavior in terms of neutron economy. For such reactors, inadverted criticality accidents will be more likely to occur. Conversely, reactors with a thicker reflector are supposed be better from the safety point of view, since a smaller fuel size characterizes them. Reactors with a reflector thickness bigger than 14 cm are going to be characterized by a slightly larger mass with respect to the mass-optimized design solution.

K_{eff} of reactor fuel with reflector thickness of	Bare	Water	Dry sand	Wet sand	Total Mass
14 cm	0.683	0.974	0.927	1.001	977 kg
16 cm	0.662	0.986	0.898	0.986	986 kg
18 cm	0.639	0.931	0.857	0.95124	1019 kg
20 cm	0.594	0.913	0.827	0.925	1059 kg

Table 4.5: Results of the safety analysis performed on HALEU cores with $\frac{H}{D} = 2.27$.

The reactors with a reflector thickness ranging from 16 cm to 20 cm are always subcritical, while the lightest reactor is supercritical when completely surrounded by wet sand. Only the reactor concept having 20 cm thickness is able to satisfy safety requirements, having all multiplication factors smaller with respect to those obtained by LANL simulations. The increase in the safest reactor total mass with respect to the lightest reactor is of 82 kg, and is mainly caused by the thicker reflector. The 52 kg mass of fissile material still allows to guarantee the same KRUSTY reactor lifetime. In Table 4.6 is reported a detailed comparison between the lightest HALEU reactor concept and the safest HALEU reactor concept.

	Safest core	Lightest core
Reflector Outer Diameter	60 cm	57 cm
Fuel Outer Diameter	22 cm	25 cm
Fuel Height	49 cm	57 cm
Fuel Mass	289 kg	477 kg
U-235 Mass	52 kg	86 kg
Reflector Mass	770 kg	509 kg
Total Mass	1059 kg	986 kg

Table 4.6: Comparison of HALEU lightest and safest design.

4.1.3. Approach to Criticality

The initial simplified geometry that was proposed for both HEU and LEU core was not provided of a control rod and consequently resulted in a supercritical system. At this point, it is necessary to examine the effect of control rod insertion and study how the reactor approach critical conditions. The following analysis is performed on the KRUSTY-like HEU reactor concept, on the lightest HALEU reactor geometry, and on the safest HALEU reactor geometry. First, it is evaluated the multiplication factor as a function of the control rod length at environmental conditions (Figures 4.5, 4.6 and 4.7). The reason why for such reactors, the multiplication factor is smaller than 1.044 when the control rod height is null is due to the presence of an additional hole that was included at the reflector top to permit the control rod vertical translation (Figure 4.4).

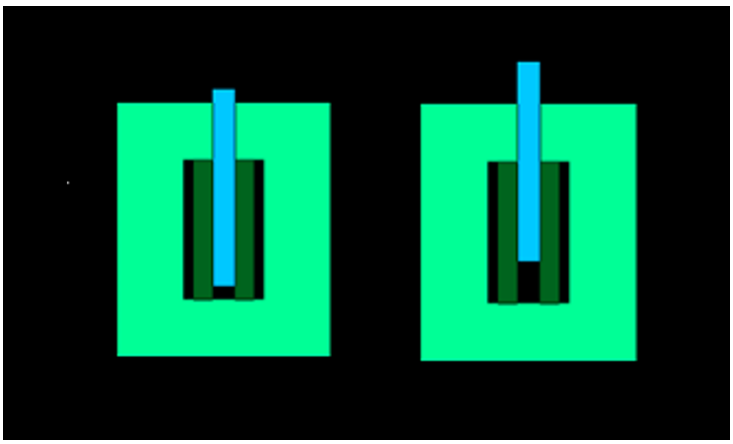

Figure 4.4: Schematic representation of the reactor during the control rod withdrawal.

When the control rod is completely inserted, the reactor must be largely subcritical (shut down conditions). In Table 4.7 is reported the control rod worth and the multiplication factor when the control rod is fully inserted inside the core. It is evident that the smaller the fuel dimensions are, the more effective the control rod will be in its function. Indeed, it will correspond a higher the control rod worth, leading to a smaller multiplication factor in shut down conditions.

	KRUSTY-like HEU	lightest HALEU	Safest HALEU
Multiplication Factor	0.962	0.985	0.975
Control Rod Worth	7400 pcm	5600 pcm	6300 pcm

Table 4.7: Comparison of multiplication factors when the control rod is fully inserted and control rod worths.

The approach to criticality will be possible by slowly withdrawing the control rod. To define how much the control rod has to be removed to allow the system to reach operating conditions, it is necessary to assess the multiplication factor as a function of the control rod distance from being fully inserted, in either cold either warm conditions (Figure 4.8, 4.9 and 4.10). In warm conditions, the reactivity defect is predicted by following the same approach employed in KRUSTY model. Such an approach consists in considering the contribution due to fuel temperature increase and neglecting the presence of all the other components. A fuel elongation of 1.36% is assumed in all directions, as well as a 4% reduction of fuel density. Also, an average fuel temperature of 1100 K is assumed, which is going to be guaranteed through a proper design of the heat pipes.

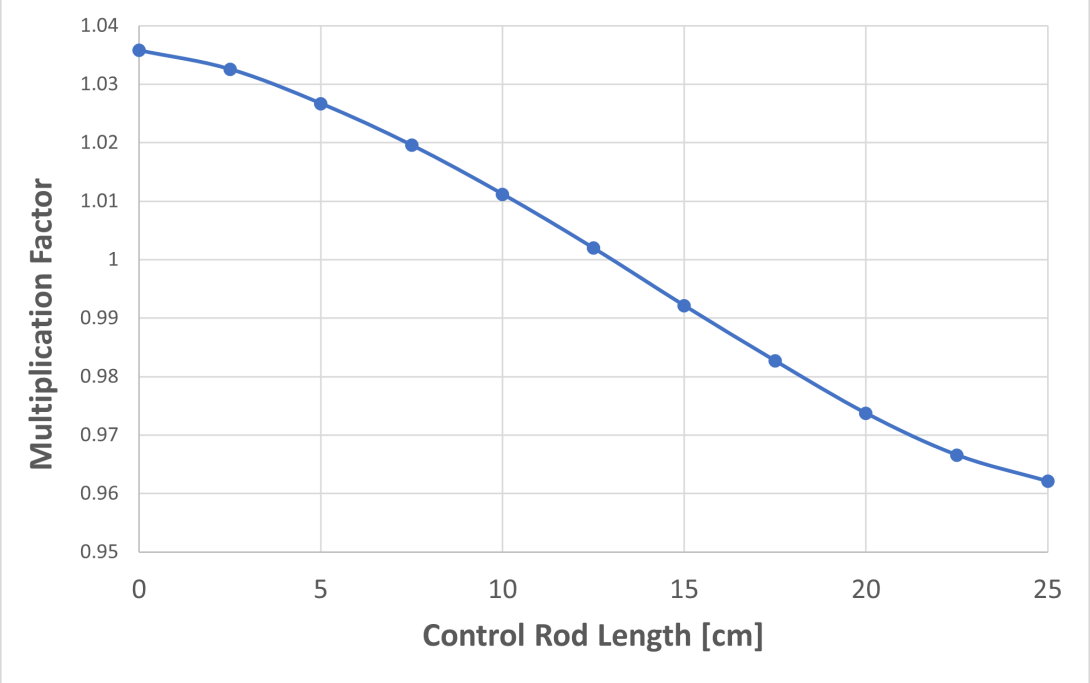

Figure 4.5: Multiplication factor of HEU reactor as a function of control rod length.

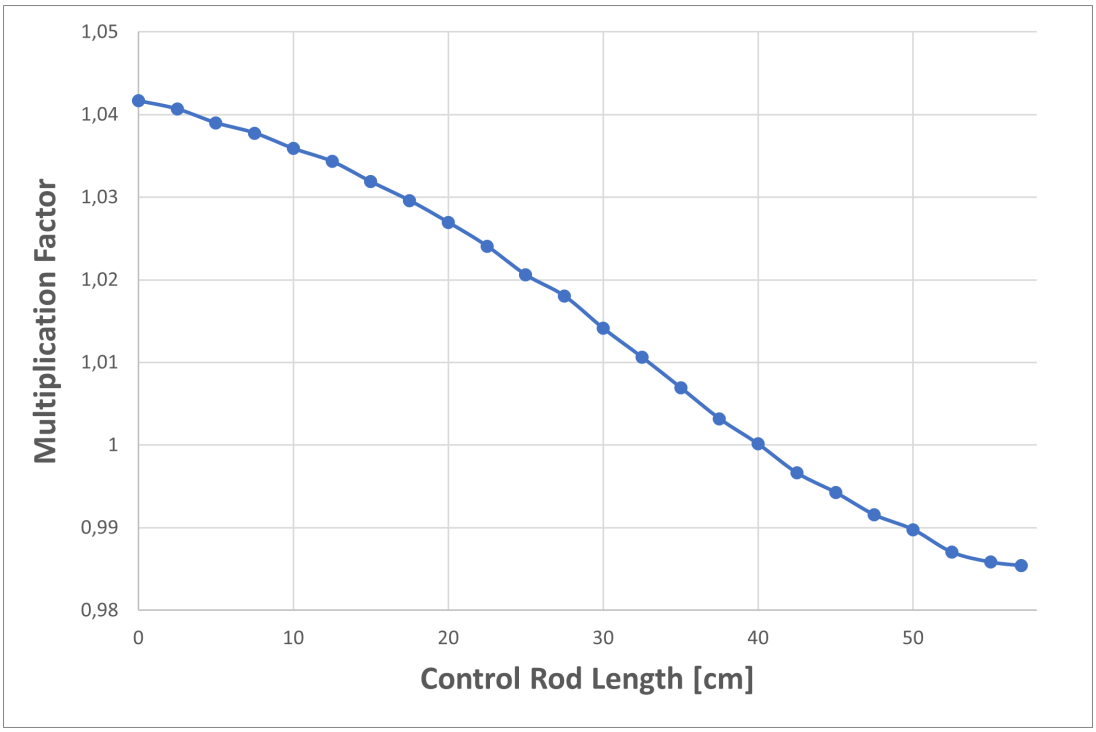

Figure 4.6: Multiplication factor of lightest HALEU reactor as a function of control rod length.

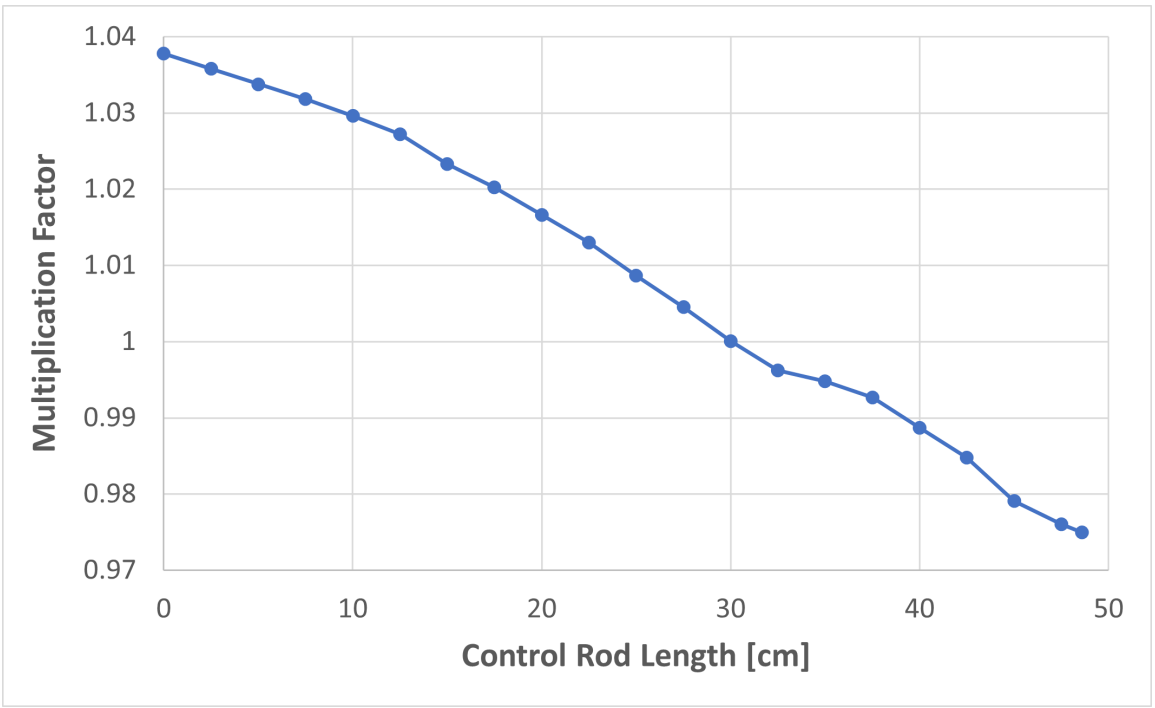

Figure 4.7: Multiplication factor of safest HALEU reactor as a function of control rod length.

In such reactors, the approach to criticality is conceptually similar to that of KRUSTY: starting from cold shut down conditions, the control rod will be removed until the multiplication factor assumes a unitary value. At this point, the reactor power gradually increases to the desired level, causing an increase in fuel temperature that results into a reduction of the system reactivity. For this reason, the reactor approach to the nominal power level has to be accompanied by further removal of the control rod to guarantee the multiplication factor remains unitary.
In Figures 4.11, 4.12 and 4.13 are pointed out the control rod distances from being fully inserted to guarantee the system criticality in either cold and warm conditions. For the HEU KRUSTY-like core, the control rod has to be removed of 2 cm to maintain the system critical from environmental to operating conditions, while for the lightest HALEU reactor core the control rod has to be further removed of 9 cm. This big difference in such value cannot be related to the difference in the reactivity defect, which is exactly the same for all three reactor concepts (Table 4.8), but rather to the difference in the slope of the warm and cold curves. From the approach to criticality point of view, the safest HALEU reactor core has a similar behavior with respect to the lightest HALEU reactor core.

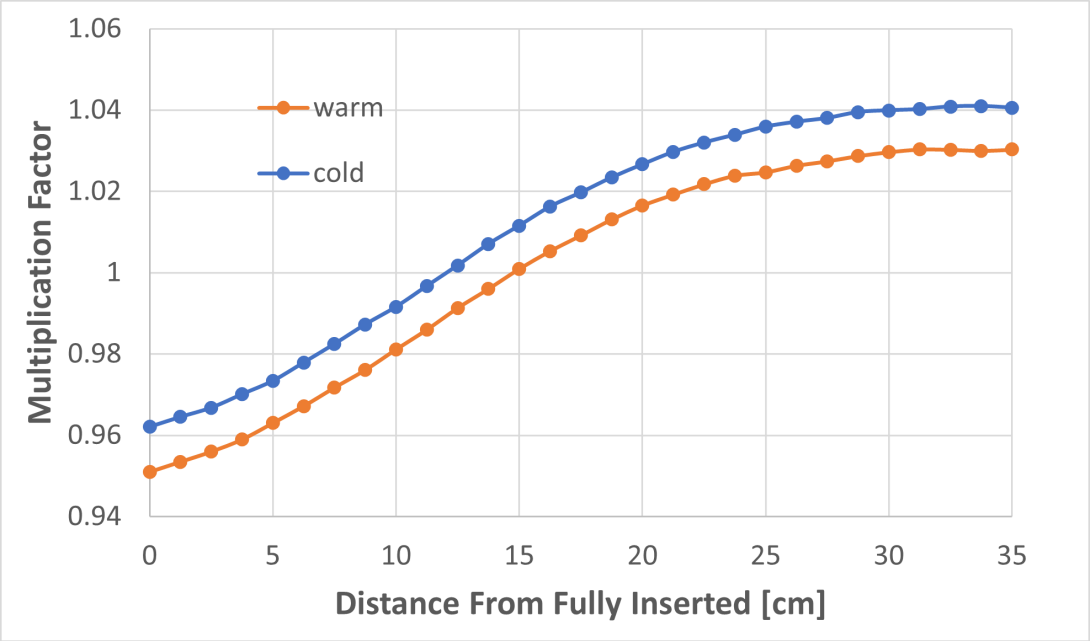

Figure 4.8: Multiplication factor of KRUSTY-like HEU reactor as a function of control rod distance from being fully inserted.

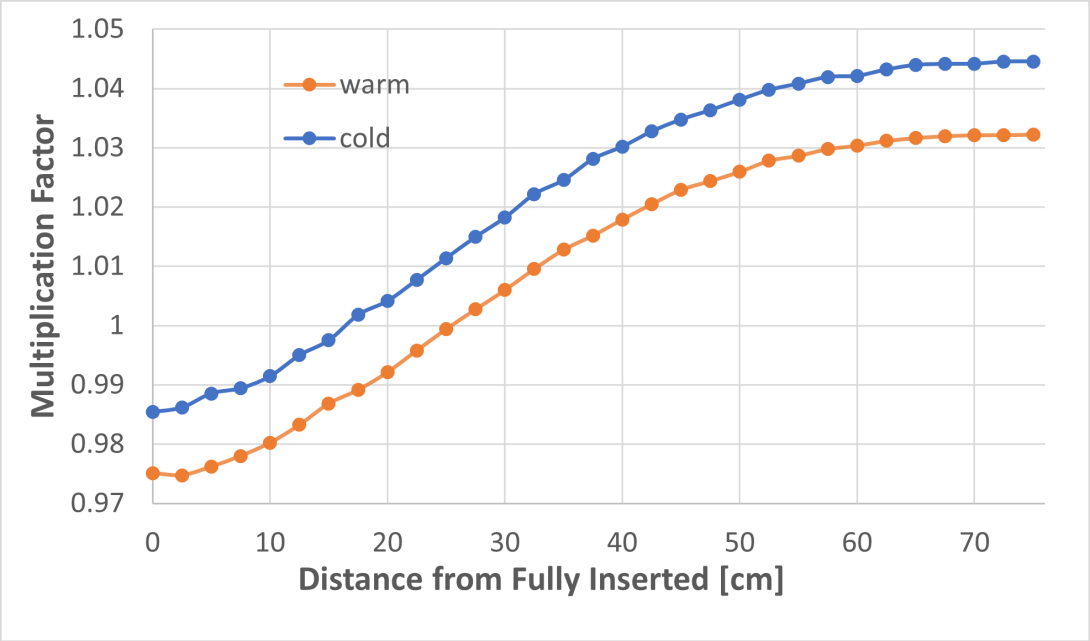

Figure 4.9: Multiplication factor of lightest HALEU reactor as a function of control rod distance from being fully inserted.

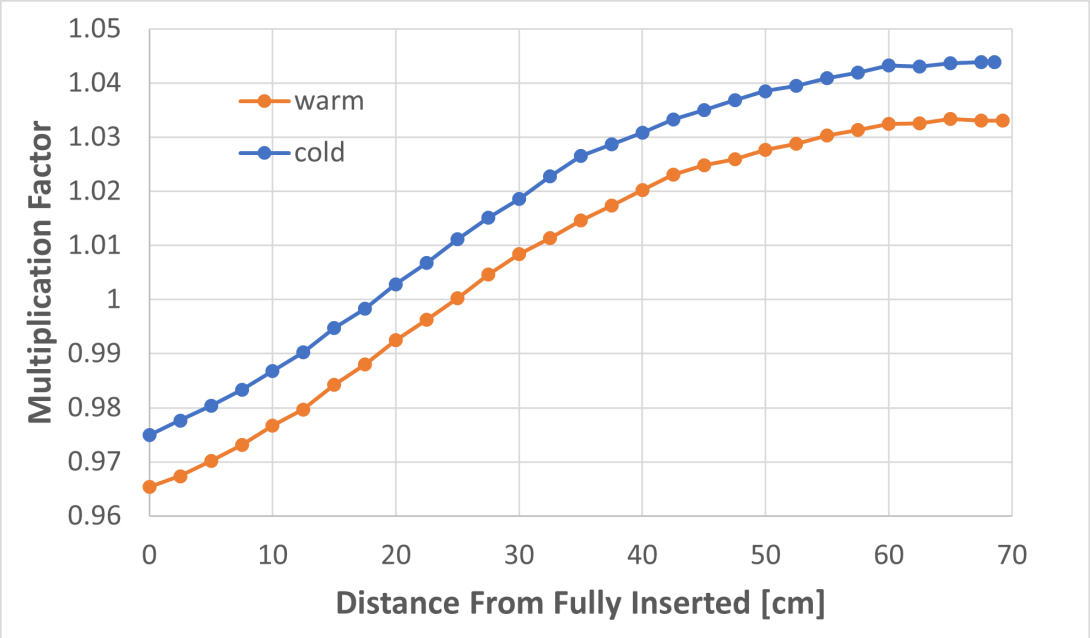

Figure 4.10: Multiplication factor of safest HALEU reactor as a function of control rod distance from being fully inserted.

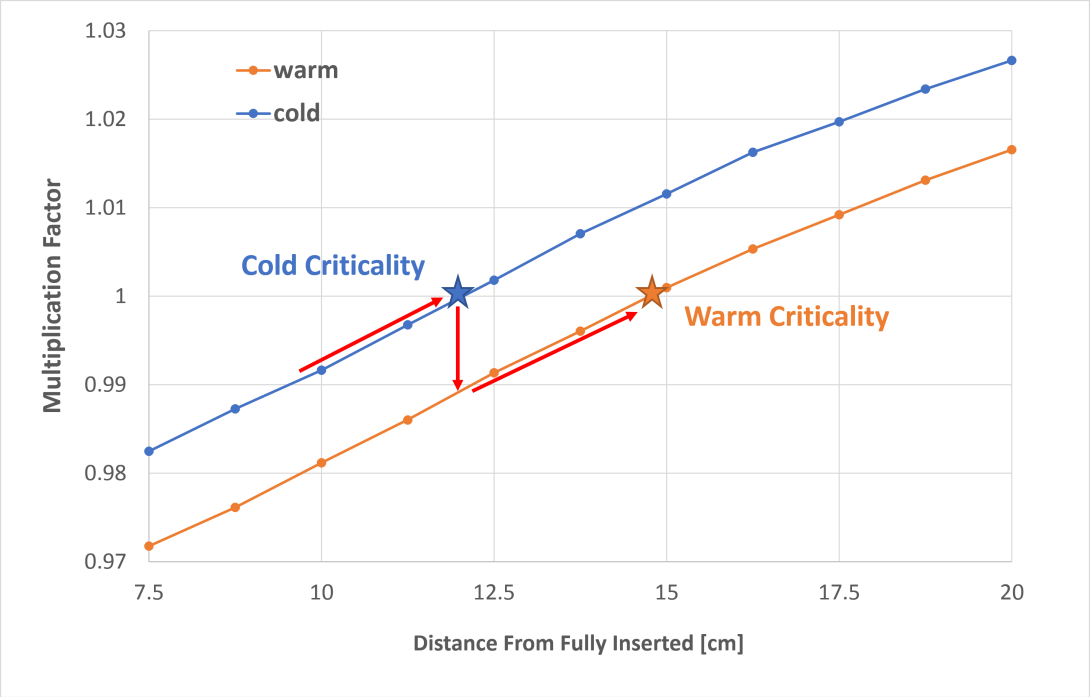

Figure 4.11: Approach to criticality for the KRUSTY-like HEU reactor.

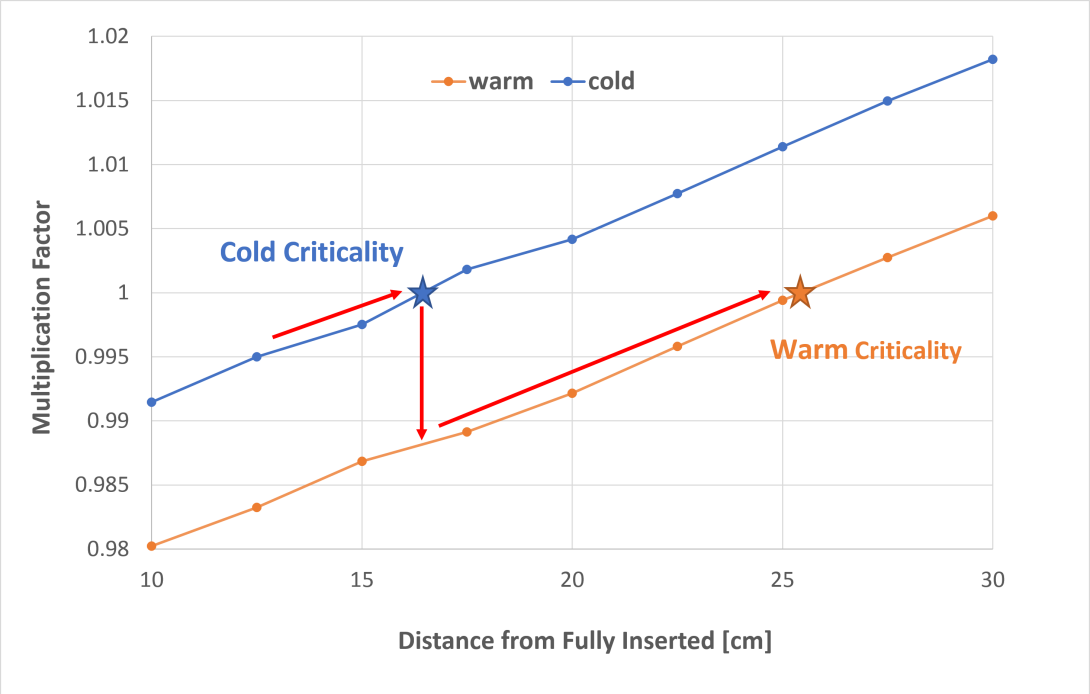

Figure 4.12: Approach to criticality for the lightest HALEU reactor.

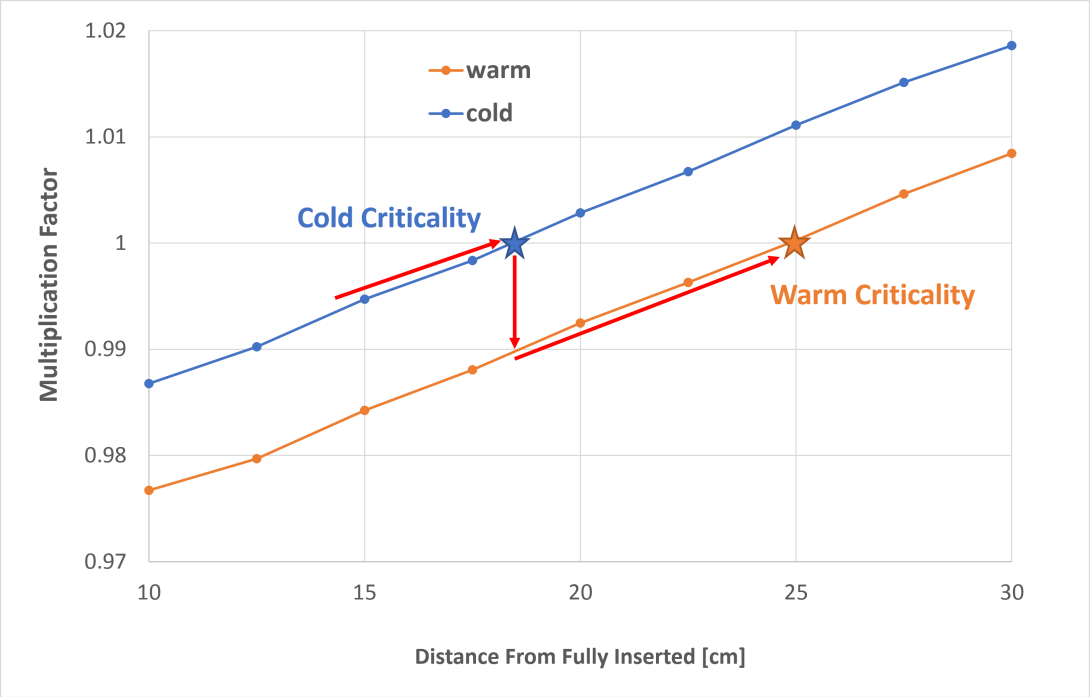

Figure 4.13: Approach to criticality for the safest HALEU reactor.

	KRUSTY-like HEU	lightest HALEU	Safest HALEU
Cold criticality	12.5 cm	17 cm	18 cm
Warm criticality	14.5 cm	26 cm	25 cm
Control rod withdrawal	2 cm	9 cm	7 cm
Temperature defect	-1100 pcm	-1100 pcm	-1100 pcm

Table 4.8: Comparison between control rod distance from being fully inserted to achieve cold and warm criticality, control rod withdrawal and temperature defect.

An evaluation of the separate effects of Doppler resonance broadening and thermal expansion is performed (Table 4.9) both on the HEU KRUSTY-like core and on the lightest HALEU. Such estimation is afflicted by a statistical uncertainty of 50 pcm and it is carried out considering the reactor configuration with the control rod control rod completely inserted. As it could be expected, due to the higher U-238 content inside HALEU fuel, doppler effect is much more important than in HEU fuel. Furthermore, thermal expansion contribution is smaller since fuel dimensions are bigger and the change in the non-leakage probability is reduced.

	KRUSTY-like HEU	Lightest HALEU
Total Temperature Defect	-1100 pcm	-1100 pcm
Fuel Doppler Effect	-100 pcm	-500 pcm
Fuel Thermal Expansion	-1000 pcm	-600 pcm

Table 4.9: Comparison of reactivity defect due to fuel thermal expansion and fuel Doppler effect.

4.1.4. Power Density Distribution and Neutron Spectra

All reactors are assumed to produce 3 kW of thermal power, just as KRUSTY nominal power. Due to the reduction in fuel enrichment, the average power density of the HALEU reactor concept is clearly expected to be smaller. Specifically, it is lowered from 1.397 W/cm^3 to 0.104 W/cm^3 when passing from HEU KRUSTY-like core to HALEU lightest core.
Axial and radial power density distributions have been assessed in cold and warm conditions, corresponding to two different control rod insertion levels. To perform a comparison between the two, they have been normalized with respect to the average power density.
For both HEU and HALEU reactor concepts, the radial power density distribution is quite uniform, except for the superficial region, where it is slightly tilted due to neutron thermalization (Figures 4.15 and 4.18). Axial power density distributions (Figures 4.14 and 4.17) are asymmetrical due to the presence of the control rod that is inserted from the top of the core, whose neutron-absorbing function causes a depression in the neutron flux and consequently a local reduction of power production. Furthermore, since in warm critical conditions the control rod is further removed with respect to cold critical conditions, it is expected an even more asymmetrical axial power density distribution, resulting in a higher peaking factor. HEU KRUSTY-like reactor core shows a smaller peak factor with respect to the HALEU core, as the peaking the power density distribution is generally much more pronounced as fuel dimensions increase.
The neutron spectra is clearly fast (Figures 4.16 and 4.19) and the average neutron flux resulted to be $7.72 * 10^{11} \frac{n}{s*cm^2}$ and $1.94 * 10^{11} \frac{n}{s*cm^2}$ for HEU and HALEU reactor core, respectively.

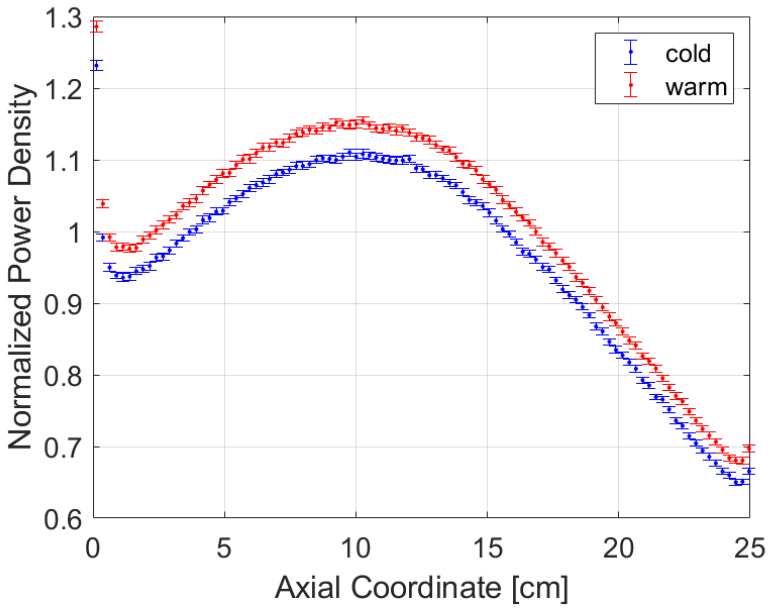

Figure 4.14: Normalized axial power density distribution of KRUSTY-like HEU reactor concept.

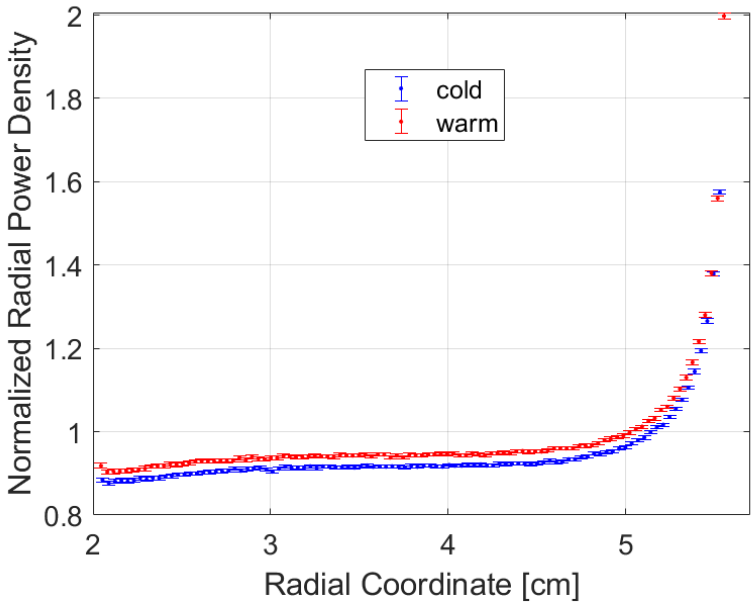

Figure 4.15: Normalized radial power density distribution of KRUSTY-like HEU reactor concept.

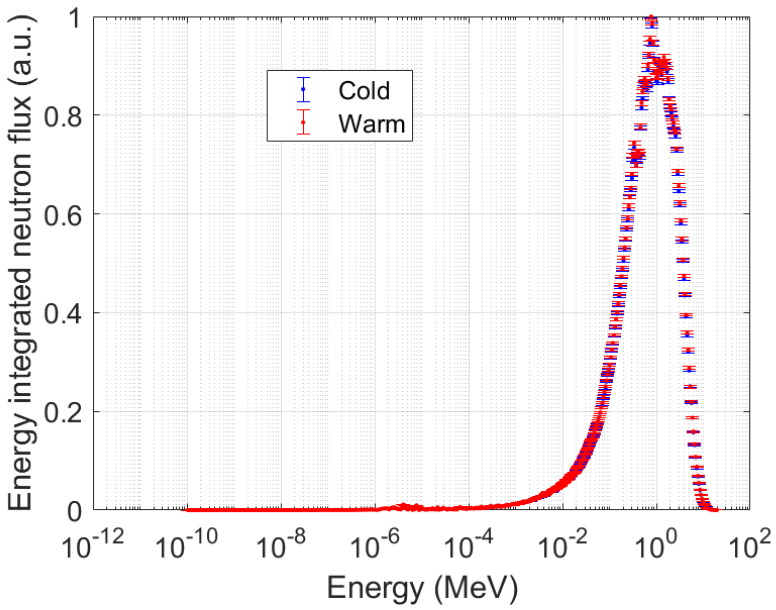

Figure 4.16: Energy integrated neutron flux of KRUSTY-like HEU reactor concept.

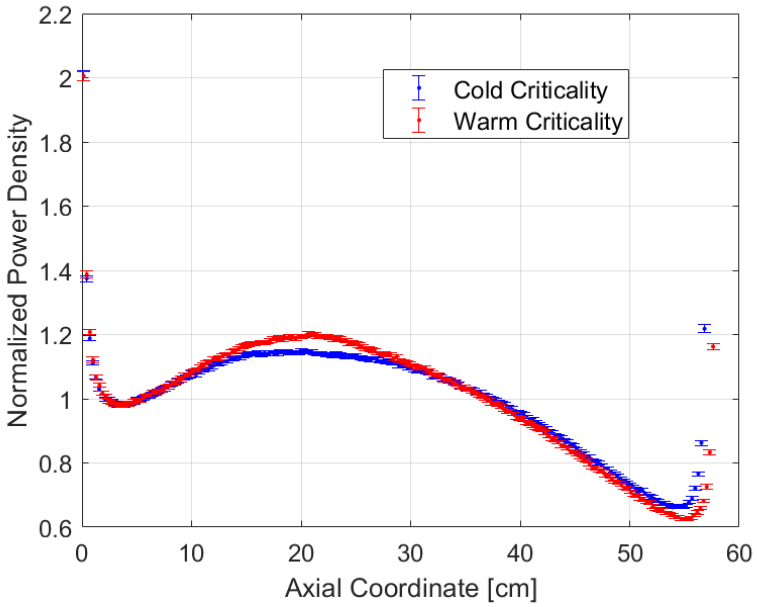

Figure 4.17: Normalized axial power density distribution of lightest HALEU reactor concept.

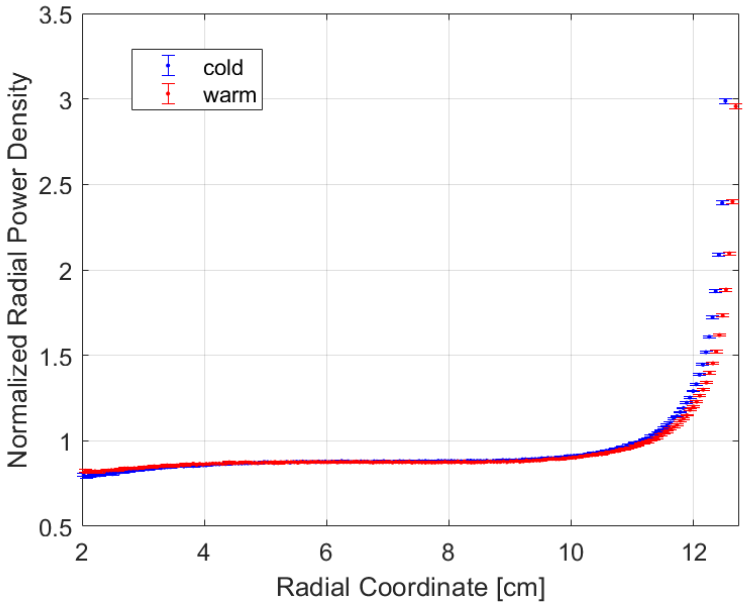

Figure 4.18: Normalized radial power density distribution of lightest HALEU reactor concept.

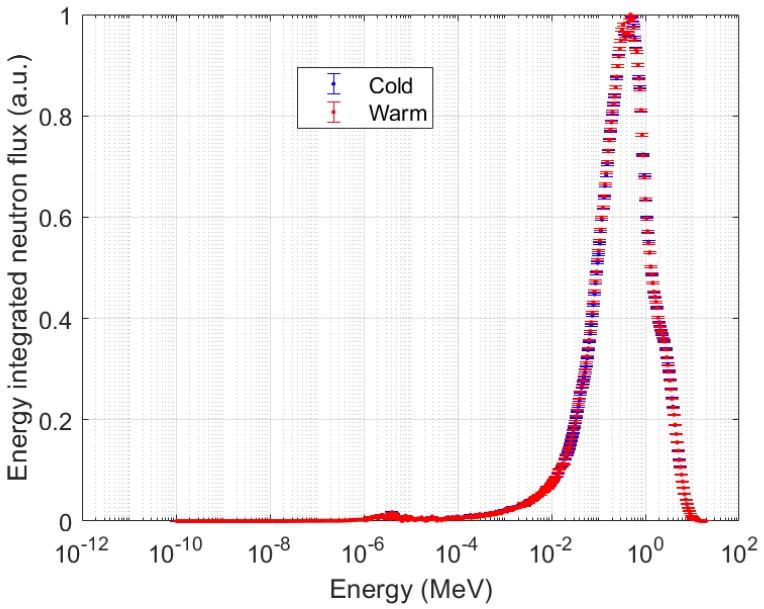

Figure 4.19: Energy integrated neutron flux of lightest HALEU reactor concept.

	KRUSTY-like HEU	lightest HALEU
Average Power Density	1.397 W/cm^3	0.104 W/cm^3
Average Neutron Flux	7.726×10^{11}n/cm^{2}s	1.948×10^{11}n/cm^{2}s
Cold Axial Peak Factor	1.108	1.149
Warm Axial Peak Factor	1.154	1.192

Table 4.10: Comparison of average neutron flux, average power density and axial peak factors.

4.2. Effect of Reducing $\frac{H}{D}$ ratio

During the preparation of KRUSTY experimental test, Kilopower space reactor was taken as guideline, but some of its design features had to be changed to allow realistic cost and schedule. This led to the use of available technologies and components that might be suitable in carrying out their function, but in some cases, they did not represent the best solution. Indeed, LANL decided to use a fuel form that could be produced quickly and affordably. The only viable option was a UMo fuel that could be cast in a similar manner to existing operations at the Y-12. KRUSTY fuel was composed of three blocks for simpler casting and machining, but also to simplify criticality safety approvals. Each block was 8.33 cm high and with an outer diameter of 11 cm to allow the use of an existing shipping container, resulting in a fuel geometry with a $\frac{H}{D} = 2.27$. In the following analysis, it is investigated how the reactor neutron is affected by the reduction of the $\frac{H}{D}$ ratio down to 1.81, as KRUSTY was designed at first [27].

For such a reactor, a mass optimization analysis is performed, and the lightest reactor is obtained at a reflector thickness of 14 cm (figure 4.20), precisely as the lightest reactor having $\frac{H}{D} = 2.27$. The total system mass results 100 kg smaller while fuel is 10 cm longer with respect to the core with $\frac{H}{D} = 2.27$. No relevant change in fuel diameter is observed, as shown in Table 4.15, where reactor geometry parameters are listed.

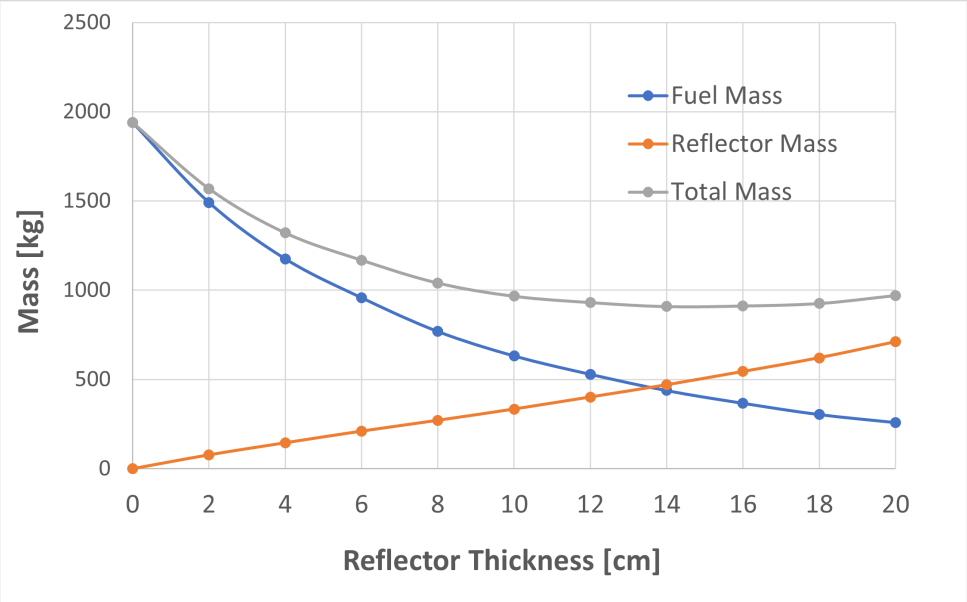

Figure 4.20: Fuel mass, reflector mass and total core mass as a function of reflector thickness.

H/D	2.27	1.81
Fuel Outer Diameter	25 cm	26 cm
Fuel Height	57 cm	47 cm
Fuel Mass	477 kg	438 kg
U-235 Mass	86 kg	80 kg
Reflector Mass [kg]	509 kg	470 kg
Total Mass [kg]	986 kg	908 kg

Table 4.11: Comparison of lightest reactor reactor design parameters for different values of $\frac{H}{D}$.

Furthermore, by fixing fuel mass to 438 kg (corresponding to lightest reactor concept fuel mass) and the reflector thickness to 14 cm, while only changing the $\frac{H}{D}$ ratio, it is proven that the higher $\frac{H}{D}$, the higher the reflector reactivity worth (Table 4.12). Therefore, when reducing $\frac{H}{D}$, two counteracting effects arise: the reduction in the reflector worth and the improvement of fuel neutron economy. The first one is going to cause an increase of the total system mass while the second a decrease of it. Evidently, in terms of mass variation, it is the second effect to dominate due to the higher density of UMo with respect to BeO.

H/D	1.81	2.27
Fuel Outer Diameter	26 cm	24 cm
Fuel Height	47 cm	54 cm
Reflector Reactivity Worth	33800 pcm	37100 pcm

Table 4.12: Reflector reactivity worth comparison between two reactors with same mass of 438 kg and same reflector thickness of 14 cm, but different $\frac{H}{D}$ ratio.

The results of the safety analysis (Table 4.13) still indicates that the minimum mass reactor is not able to satisfy safety requirements. Also, in this case the safest reactor is the one having a reflector thickness of 20 cm, with a total mass 62 kg higher with respect to the lightest reactor.

K_{eff} of reactor fuel with reflector thickness of	Bare	Water	Dry sand	Wet sand	Total Mass
14 cm	0.683	0.974	0.927	1.001	908 kg
16 cm	0.662	0.986	0.898	0.986	911 kg
18 cm	0.639	0.931	0.857	0.951	925 kg
20 cm	0.594	0.913	0.827	0.925	970 Kg

Table 4.13: Results of the safety analysis performed on LEU reactor core with $\frac{H}{D} = 1.81$.

An evaluation of the reactor multiplication factor as a function of the control rod length in cold conditions (Figure 4.21) allowed to demonstrate that the effect of the control rod insertion is not particularly influenced by the $\frac{H}{D}$ reduction. The reactor multiplication factor when the control rod is completely inserted is only 100 pcm higher with respect to the reactor concept with $\frac{H}{D} = 2.27$. In cold conditions, the reactor becomes critical if the control rod is removed of 10 cm. At operating conditions, criticality is maintained by further removing the control rod of 12 cm (Figure 4.22). Finally, No significant difference in the power density distributions and in the neutron spectra is observed with respect to the reactor having $\frac{H}{D} = 2.27$.

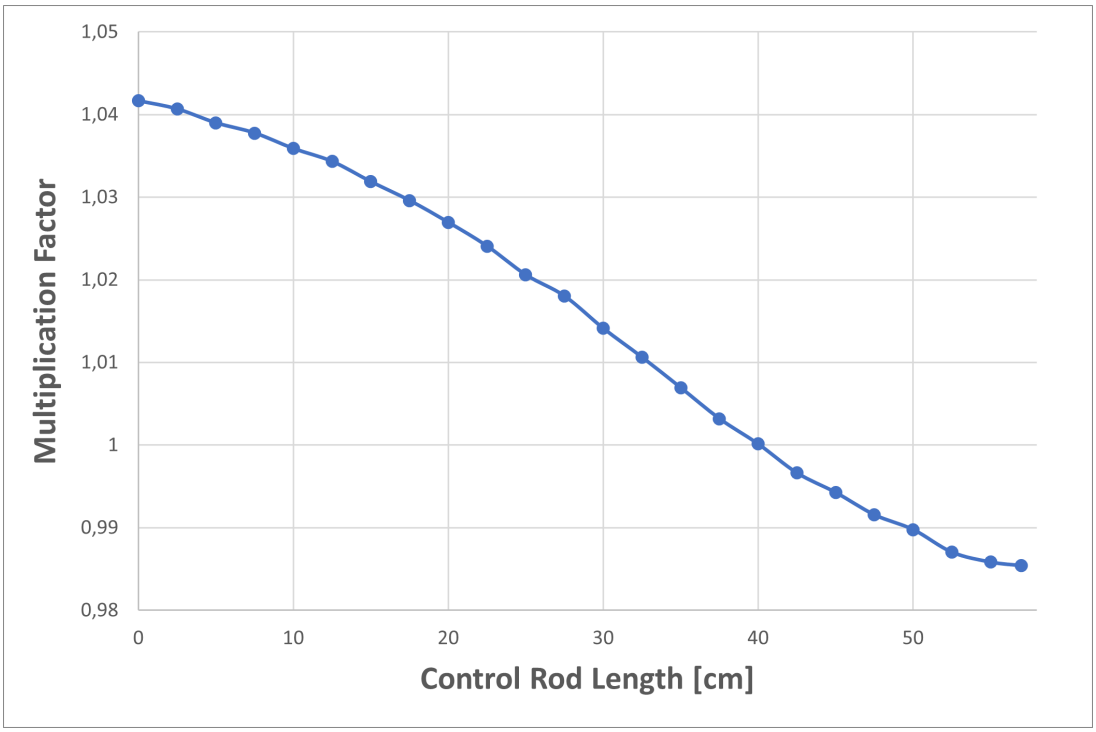

Figure 4.21: Multiplication factor as a function of control rod length for the lightest HALEU reactor having H/D = 1.81.

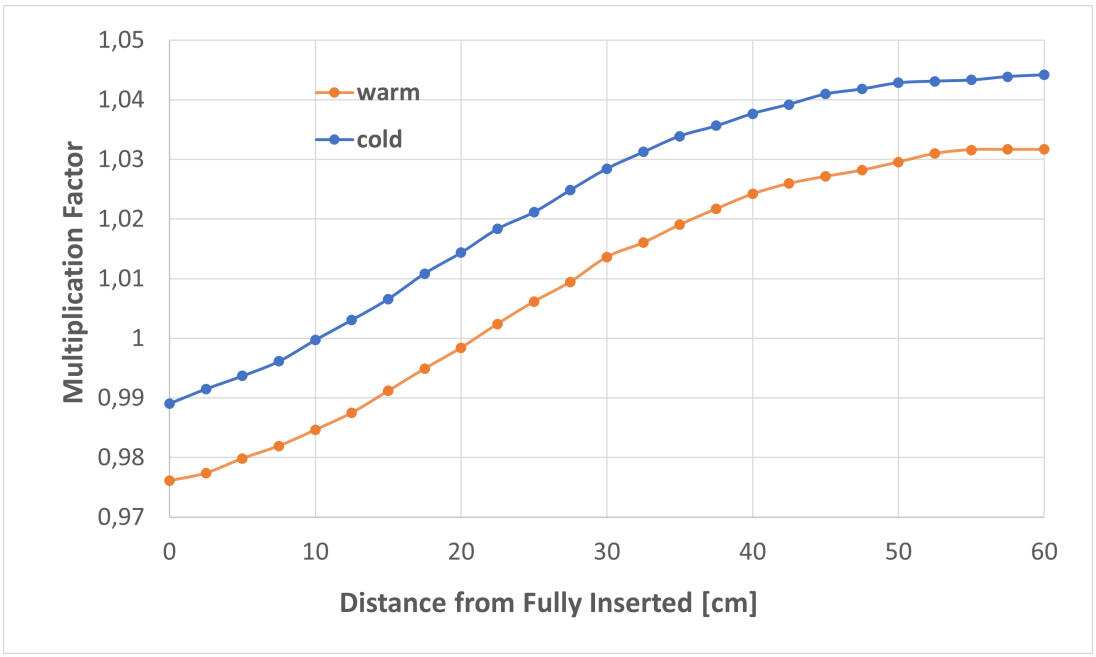

Figure 4.22: Multiplication factor as a function of control rod distance from being fully inserted for the lightest HALEU reactor having H/D = 1.81.

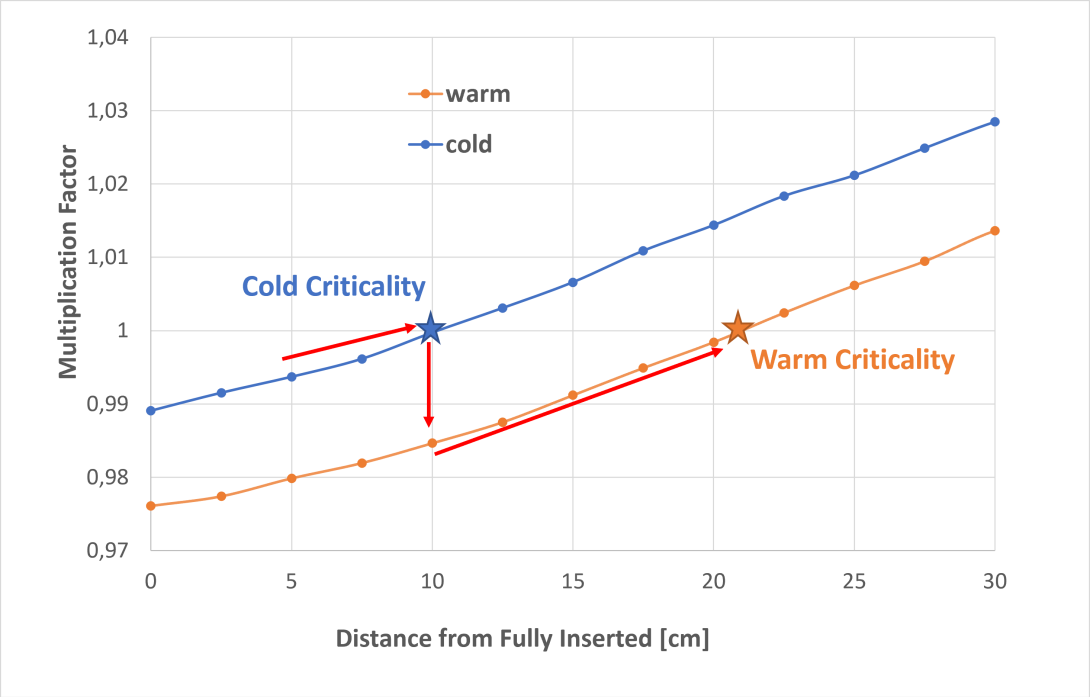

Figure 4.23: Approach to criticality of lightest HALEU reactor having H/D = 1.81.

4.3. Effect of Adding Moderator

The conversion of Kilopower reactor concept into a thermal reactor may result in a further decrease in the system mass [9]. Such conversion involves integrating a proper moderator inside the core, whose effect is to slow down fast neutrons through elastic scattering interactions. Neutrons will first fall in the epithermal energy interval (0.025 eV<E<0.4 eV) and eventually in the thermal energy interval (below 0,025 eV), where the fission cross-section is maximized, resulting 100 times greater with respect to the absorption cross section of U-238 (Figure 4.24). The consequent improvement in the reactor neutron economy permits an overall reduction of the system mass, which makes the solution of adding moderator particularly attractive for the design a compact nuclear reactor [30].

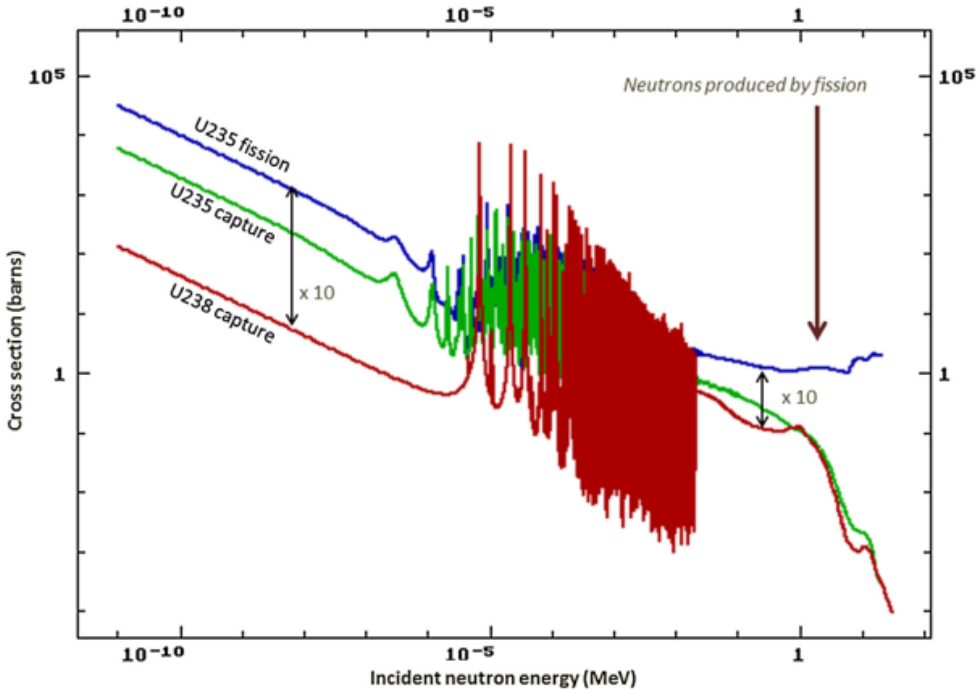

Figure 4.24: Uranium microscopic cross sections [30].

LANL already evaluated the idea of converting Kilopower into a thermal reactor, and proposed two different design paths to integrate moderator inside the core:

- homogeneously mixing moderator and UMo fuel;
- design a reactor core such that the moderator and UMo fuel are separated (e.g. spheres of fuel arranged in a cubic lattice surrounded by the moderator or alternating fuel and moderator disks).

For a space nuclear reactor, metal hydrides are commonly considered to be used as moderators since hydrogen is the best moderator that allows to obtain a compact system. Water and hydrocarbons are not suitable as moderators due to their inability to operate at high temperatures. Water would require an extremely high pressure (700 MPa at 1000 K) to reach a reasonable considerable hydrogen concentration, while hydrocarbons undergo irreversible decomposition if used for a prolonged time at temperatures higher than 800 K [31]. Furthermore, liquid moderators have to be excluded for space reactors that operate at zero gravity and have to withstand launch conditions [13].
Nevertheless, metallic hydrides have some limits regarding the temperature level they can operate. This may be problematic for a space reactor that can only operate at temperatures higher than 1100 K to dissipate a reasonable amount of power through irradiation. Otherwise, the reduced thermal efficiency would make the heat conversion system and

the heat rejection system prohibitively massive [9]. The limit in the maximum operating temperature is because hydrogen decomposition pressure increases with the system temperature. Excessively high temperatures would turn into a high decomposition pressure, leading to hydrogen diffusion out of the solid fuel matrix and causing fuel loss of integrity [32]. In Table 4.1 the maximum operating temperature at atmospheric pressure of various metallic hydrides that can potentially be used as moderators are listed.

Moderator	**Density**	**Maximum Operational Temperature**
LiH	0.78 g/cm^3	1200 K
MgH_2	1.45 g/cm^3	600 K
CaH_2	1.70 g/cm^3	1100 K
$ZrH_{1.5}$	5.60 g/cm^3	1100 K
$YH_{1.5}$	4.20 g/cm^3	1100 K

Table 4.14: Metallic hydrides densities and maximum operating temperatures [25].

Another property to consider when choosing a proper moderator is the neutron absorption capability, which could aggravate the system neutron economy. In Figure 4.25 a comparison of neutron absorption cross-sections of various metals is shown. LiH must be enriched up to 99.9 wt% in Lithium-7, to minimize parasitic neutron absorption from Lithium-6. Magnesium has the lowest neutron absorption cross-section (but the lowest maximum operating temperature), followed by Zirconium, Calcium, and Yttrium. LiH, CaH_2 and MgH_2 lack chemical compatibility with metallic uranium, differently from YH_x and ZrH_x, which are also characterized by a higher thermal conductivity.
In this study, ZrH_x has been chosen as moderator because it was already used in the SNAP-10A space reactor. YH_x would be characterized by a higher moderation efficiency and by a higher hydrogen retention capability with respect to ZrH_x, but the seven times greater neutron absorption cross-section that would lead to a bigger mass system shifts the attention on ZrH_x [13].

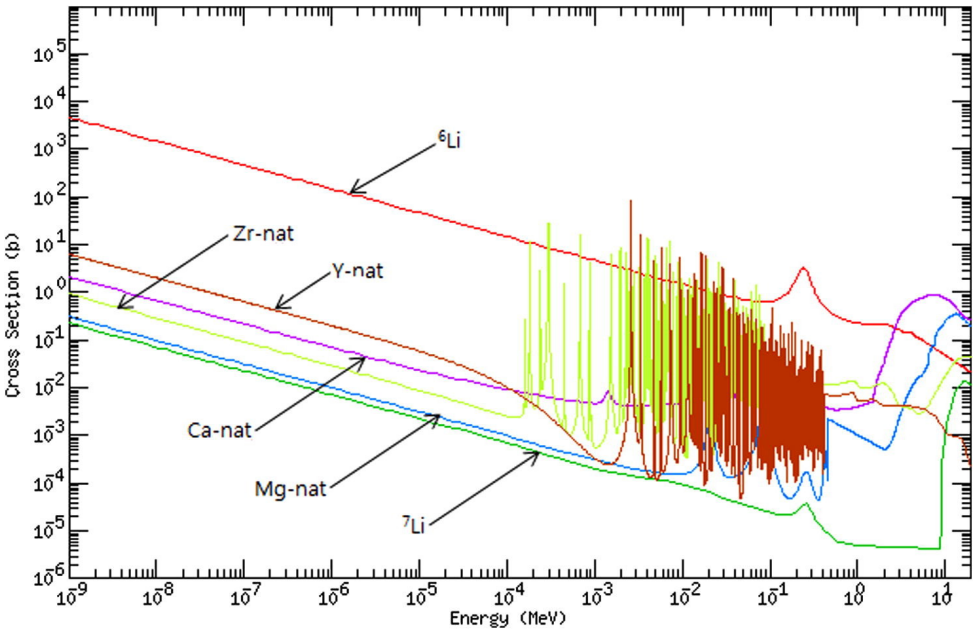

Figure 4.25: Comparison of absorption cross sections of some metal elements [25].

Hydrogen content inside ZrH_x has to be properly chosen. On one side, it is desired to make it as high as possible to obtain the highest moderating efficiency. From the phase diagram of H-Zr in Figure 4.26, it is evident that the hydrogen-to-zirconium weight ratio ($\frac{H}{Zr}$) requires to be higher than 1.5, to avoid any phase transition from environmental temperature up to operating conditions temperature. Nevertheless, there is a $\frac{H}{Zr}$ upper limit because ZrH_x decomposition pressure is also dependent upon it. From the graph in Figure 4.27, it is possible to observe that in order to obtain a $\frac{H}{Zr} > 1.5$ at a reasonable pressure, temperatures lower than 1100 K are required. For $\frac{H}{Zr}$ values approaching 2, in a wide range of temperatures, the corresponding decomposition pressure would make hydrogen diffuse out of the crystalline lattice, which is the reason why hydrating zirconium above 1.5 is of limited interest [32]. Although for the SNAP-10A fuel $1.68 < H/Zr < 1.83$ [33], in the following analysis it was chosen a value of 1.5 to remain conservative.
Serpent input file for the modeling of such reactors includes proper thermal scattering libraries for both zirconium and hydrogen to take into account the influence of chemical binding (especially for hydrogen) upon the probability on neutron scattering.

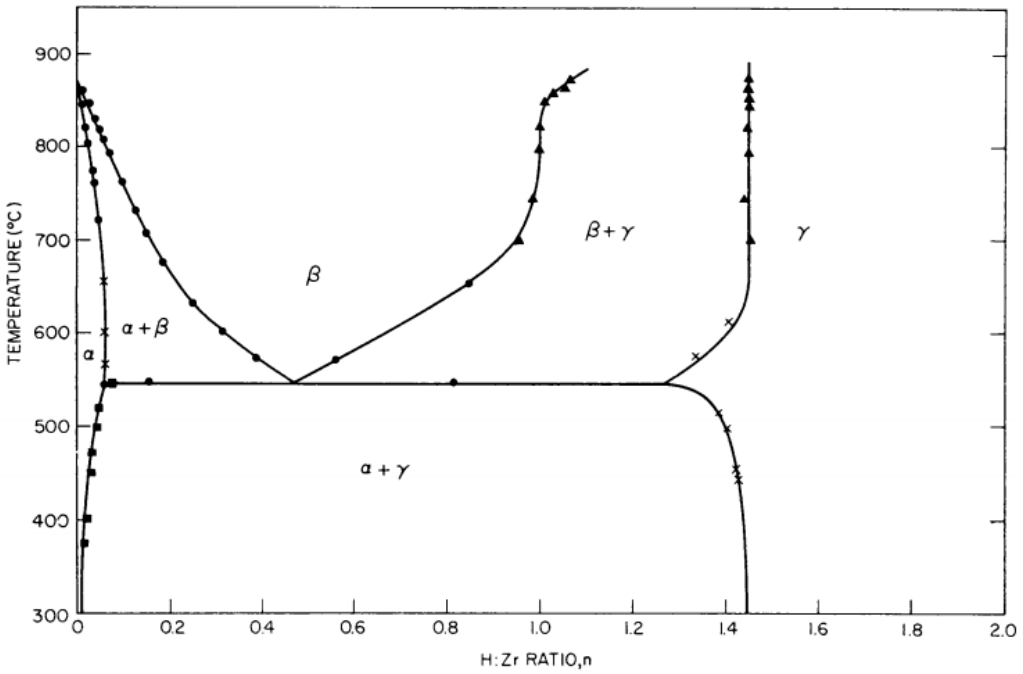

Figure 4.26: Zirconium hydride phase-diagram [32].

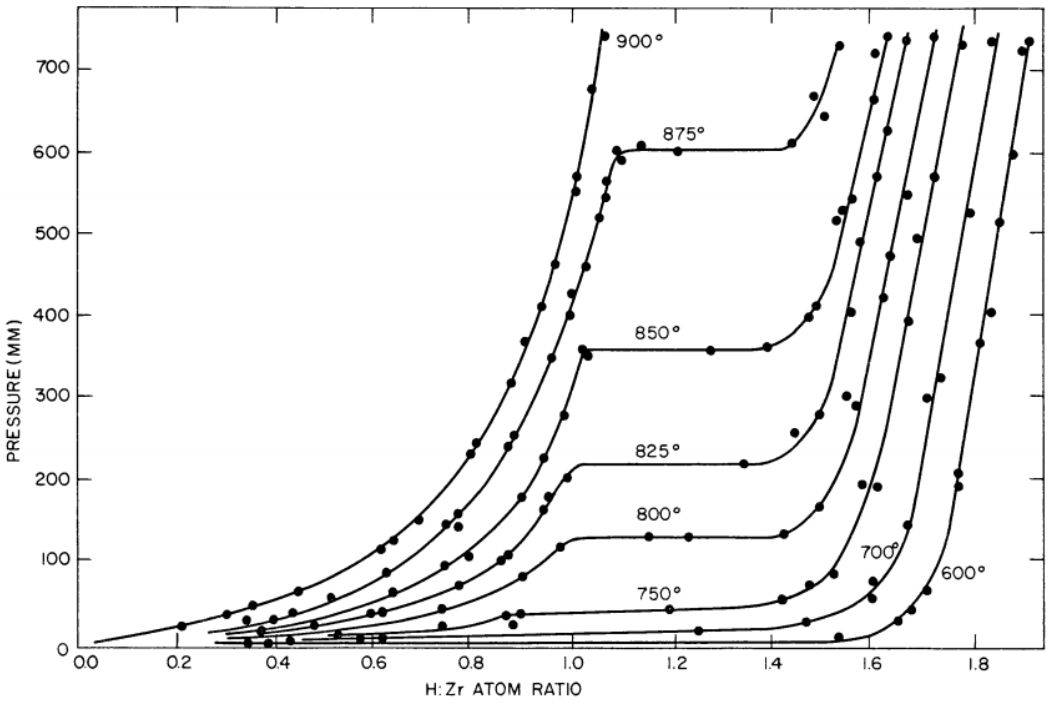

Figure 4.27: Zirconium hydride absorption isotherms [32].

Depending on how the moderator is integrated inside fuel, thermal reactors are distinguished in two classes: homogeneously and heterogeneously moderated reactors. If UZrH is used as fuel, the ability to retain hydrogen would be even more difficult with respect to ZrH and it would also have significant problems due to swelling. Only the separation of fuel from moderator allows to mitigate these issues and would also help to improve the system neutron economy, turning into the possibility of further decreasing the mass [9]. Therefore, for the reasons mentioned above, right from the start, the homogeneously moderated reactor concept should be discarded as a possible solution. Nevertheless, it is still considered in this analysis to investigate the influence of the volumetric moderator fraction ($f_m = \frac{V_{HZr}}{V_{UMo}+V_{ZrH}}$) upon the system neutron economy, to find an optimal value eventually. Only afterward the beneficial effect of separating moderator from fuel, turning the reactor from homogeneously to heterogeneously moderated, will be analyzed.

4.3.1. Homogeneously Moderated HALEU Reactors

In the following analysis, fuel is assumed to have a H/D = 1.81 and to be composed of a homogeneous mixture of HALEU UMo and $ZrH_{1.5}$, the first having the same composition reported in Table 4.2. A mass optimization analysis like the one carried out for the HALEU fast reactor concept is performed for such homogeneously moderated reactors, by varying f_m from 0 % to 90 % (Figure 4.28). The homogeneously moderated fuel density is assessed as a proper combination of UMo and ZrH densities, weighted with respect to their volumetric fraction inside the fuel mixture. The moderator density ($\rho_{ZrH_{1.5}}$) is given by Equation 4.1 [33], valid for $\frac{H}{Zr} < 1.6$:

$$\rho_{HZr_{1.5}} = (0.154 + 0.0145x)^{-1} g/cm^3 \tag{4.1}$$

For this specific type of solid-state reactor, an increase in f_m would always lead to a reduction in the system mass, which is much more pronounced for reactor cores having a smaller reflector thickness. Especially for $0\% < f_m < 40\%$ and a reflector thicknesses ranging from 10 cm to 18, (where the minima are located), curves are practically overlapped. Such reactors have a mere difference in the total system mass, which is practically invariant with respect to the fast reactor concept.
Furthermore, as f_m increases, the location of the minimum shifts towards smaller values of reflector thickness, and curves become flatter and flatter.
In Figure 4.29 is reported the fissile material mass of reactors obtained from the mass optimization analysis. For values of f_m lower than 50 % the amount of U-235 is always greater than KRUSTY in the whole range of reflector thickness, indicating that such re-

actors can still guarantee the same lifetime as KRUSTY.

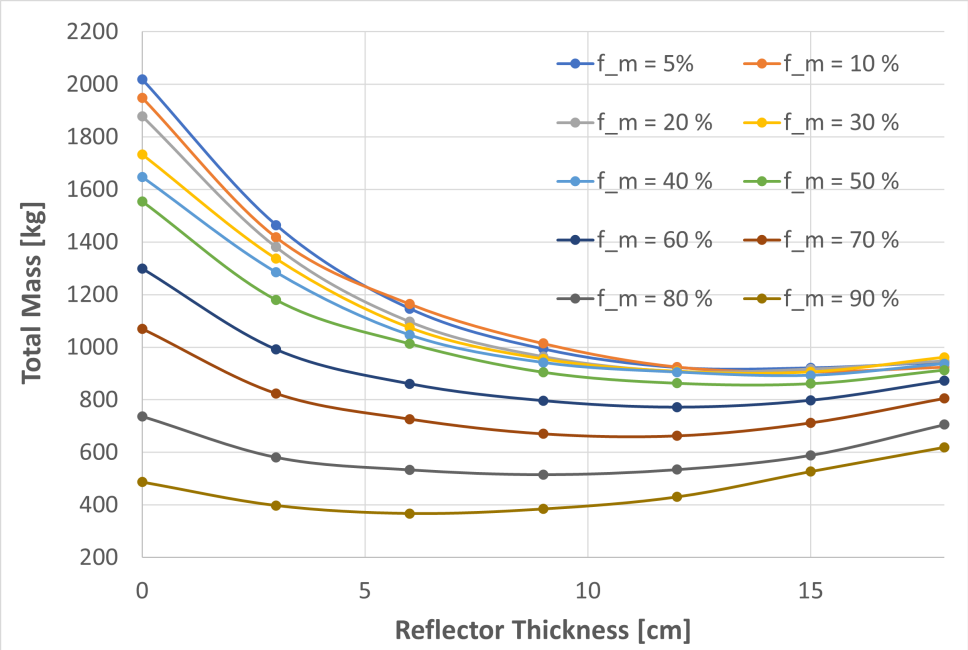

Figure 4.28: Total homogeneously moderated reactor masses with different reflector thickness, different f_m, but the same multiplication factor of 1.044.

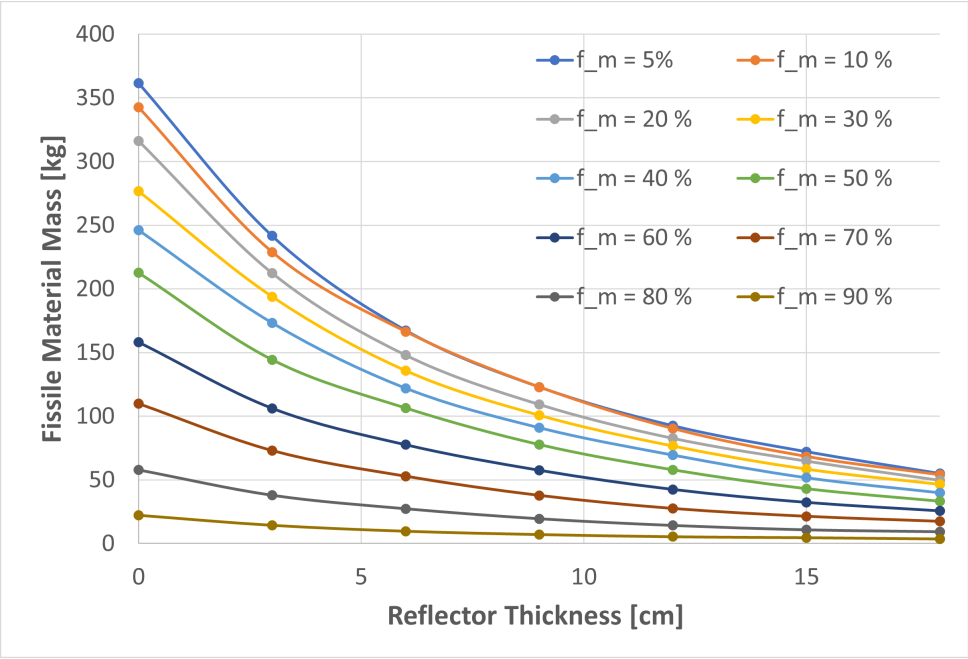

Figure 4.29: U-235 mass contained inside homogeneously moderated reactor cores obtained from the mass optimization analysis.

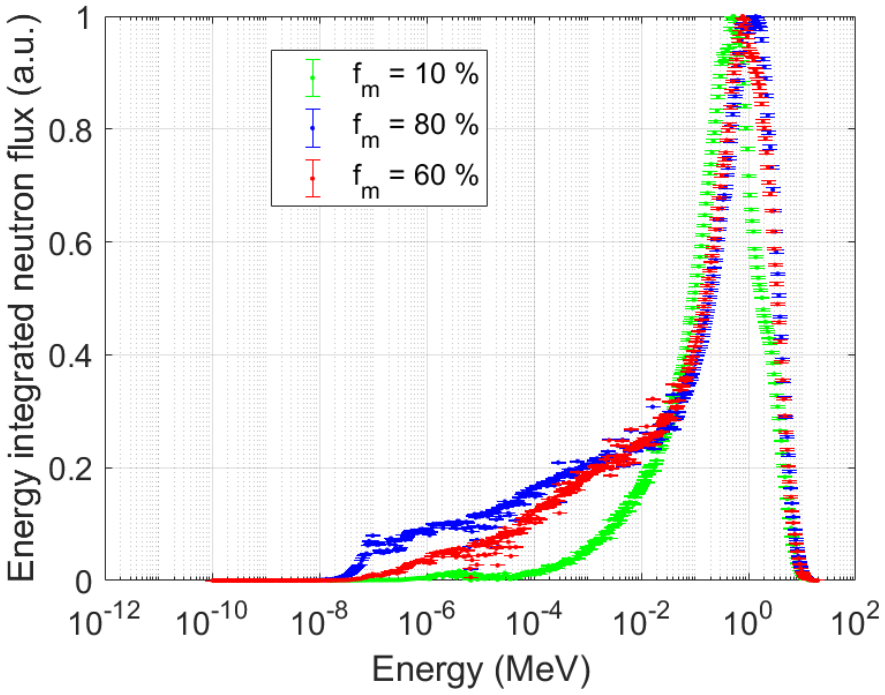

Figure 4.30: Neutron Spectra evaluated inside fuel of lightest homogeneously moderated reactors having different f_m.

f_m	10 %	60 %	80 %
Average Neutron Flux inside Fuel [$n/s * cm^2$]	$2.04204*10^{11}$	$9.76224*10^{10}$	$1.36453*10^{11}$

Table 4.15: Average Neutron flux inside fuel of lightest homogeneously moderated reactors having different f_m.

In Figure 4.30 is shown a comparison of neuron spectra evaluated inside the homogeneously moderated fuel of lightest reactors having different values of f_m. The higher is the volumetric fraction of the moderator, the more important epithermal and thermal components are in the neutron spectrum. Nevertheless, only for $f_m = 80$ % is observed a trace of the typical thermal neutrons Maxwellian distribution.
The absence of an optimal f_m ratio suggests that such reactors are always "under-moderated." To demonstrate so, it is necessary to assess the multiplication factor as a function of the volumetric moderator-to-metallic fuel ratio, by only increasing the amount of moderator while leaving unchanged that of metallic fuel.
The amount of fuel is chosen to be equal to the UMo mass of the lightest reactor having

a $\frac{H}{D} = 1.81$. A reflector thickness of 15 cm was considered. As the amount of moderator is increased, from the total fuel volume and $\frac{H}{D}$ it is possible to determine fuel height and diameter to be used as input in Serpent file. In Figure 4.31 is shown how the multiplication factor increases with increasing moderator-to-UMo volumetric ratio. Such behavior is particularly atypical if compared to that of water-moderated reactors, for which it is expected a maximum multiplication factor at a specific value of optimal moderator-to-fuel ratio. If the reactor is designed to have a moderator-to-fuel ratio lower than this value, it is referred to as "under moderated". In water-moderated reactors, under-moderation is essential to guarantee the system stability since an increase in moderator volume, either due to the presence of voids or due to thermal expansion, would cause a negative reactivity insertion [34].

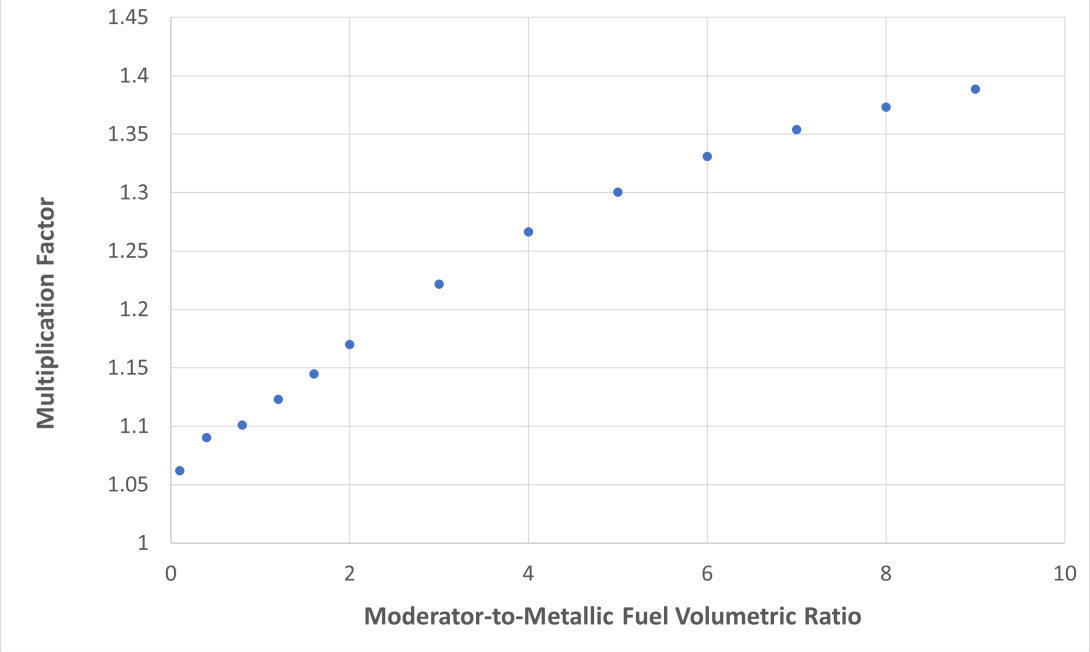

Figure 4.31: Total homogeneously moderated reactor mass as a function of reflector thickness.

In the following, safety analysis will be arbitrarily performed on reactors having a f_m of 60% and 80%. Clearly, due to the different amounts of fissile material contained inside fuel, the two reactor concepts will have different lifetimes if they are operated at the same power level. In Figure 4.32 is reported a comparison of fissile material masses contained inside the same rector cores obtained from previous optimization analysis, having f_m = 60 % and f_m = 80%. It is evident that if two reactors with the same reflector thickness and the same behavior in terms of neutronic are compared, the one having f_m = 60 %

has almost a doubled fissile material mass with respect to one with f_m = 80 %. Such difference is much more pronounced as the reflector thickness is reduced.
Mass optimization analysis are shown in Figure 4.33 and Figure 4.34. Safety analysis is performed for reactors with a reflector thickness ranging from 9 cm to 18 cm. In either case, the reactor geometry having the thicker reflector resulted in being the only one to satisfy launch safety constraints. Multiplication factors for different surrounding moderating materials are listed in 4.16 and 4.17.

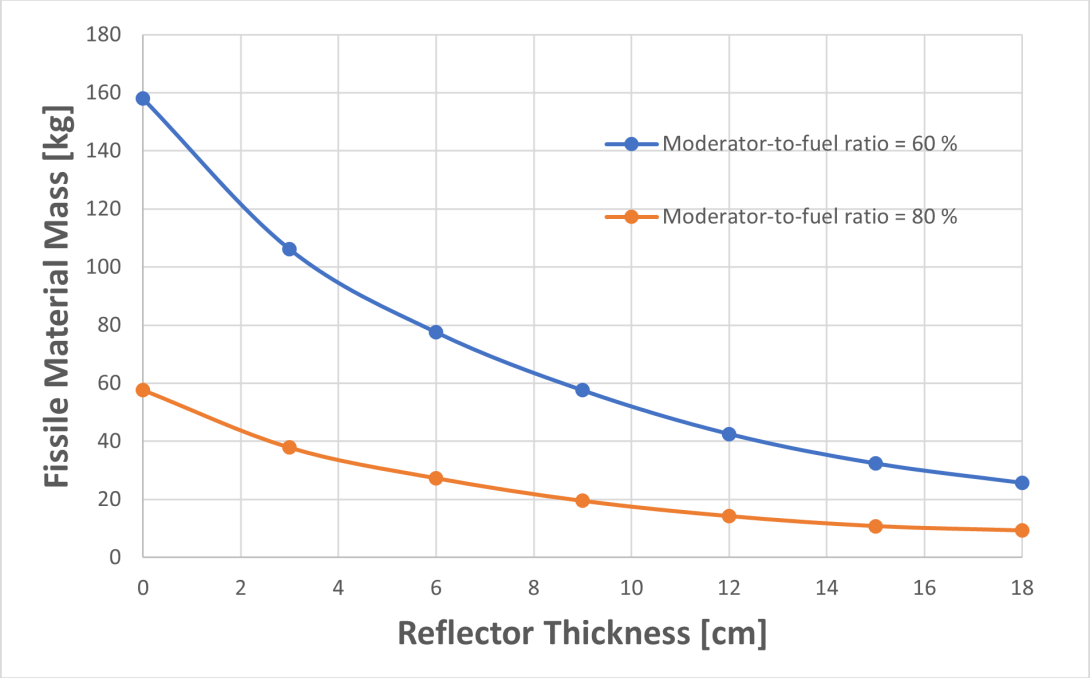

Figure 4.32: Amount of fissile material as a function of reflector thickness for homogeneously moderated reactors with $f_m = 60\%$ and $f_m = 80\%$.

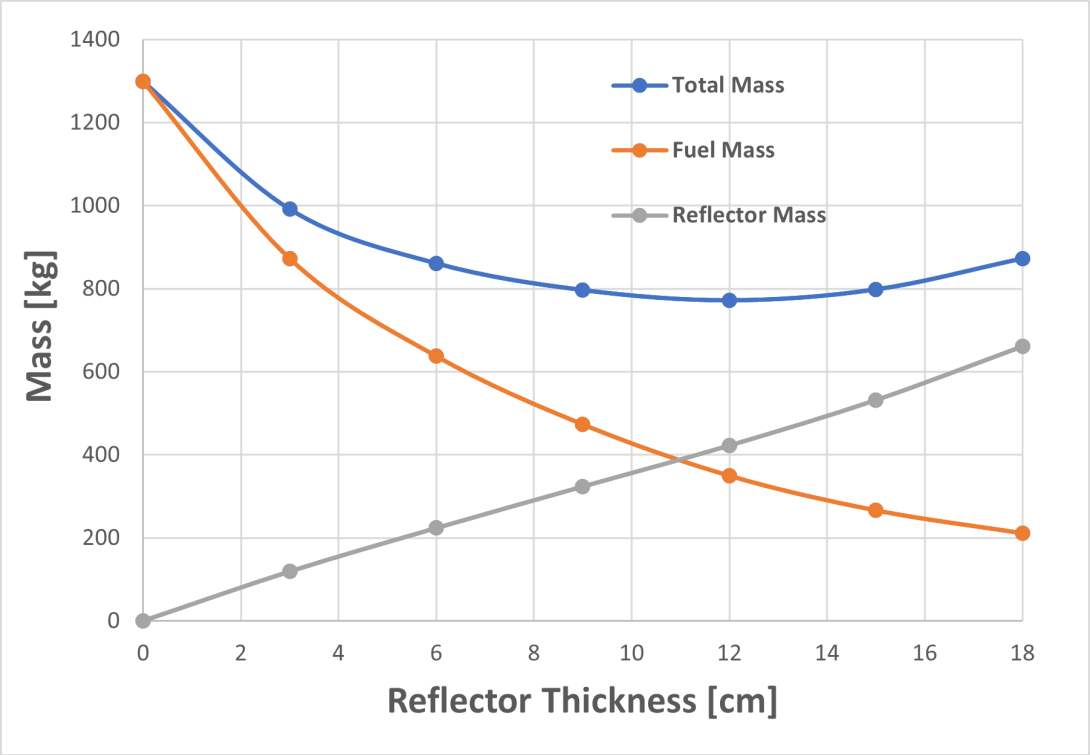

Figure 4.33: Total mass, reflector mass and fuel mass of homogeneously moderated fuel having $f_m = 60$ %.

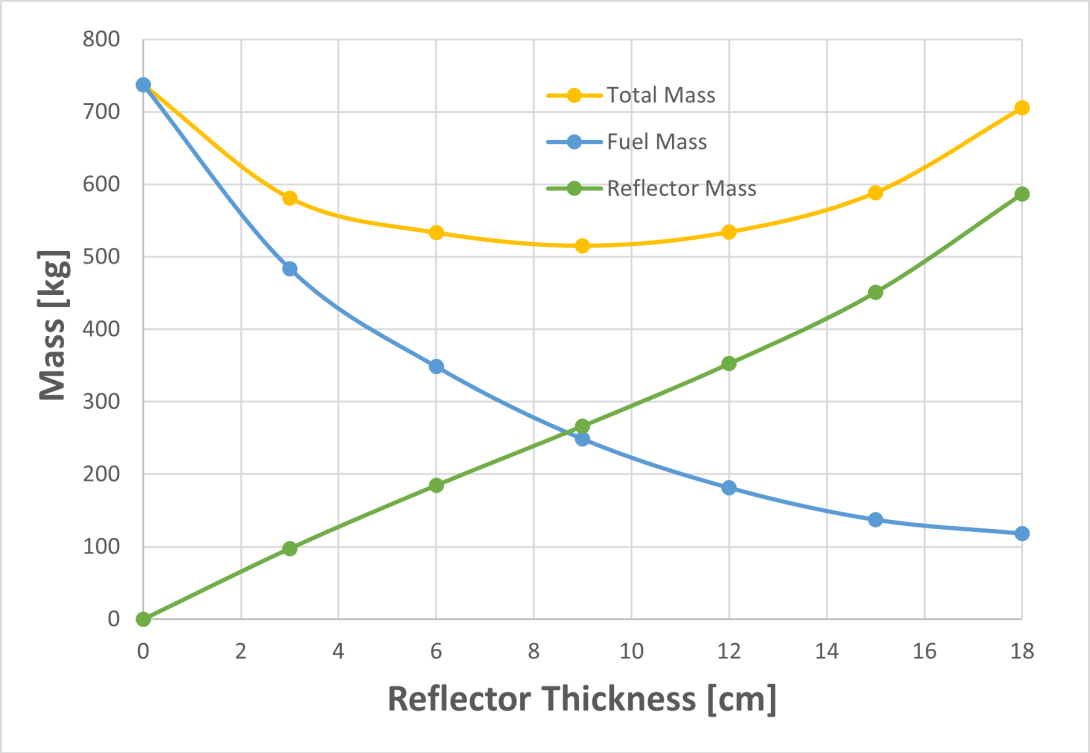

Figure 4.34: Total mass, reflector mass and fuel mass of homogeneously moderated fuel having f_m = 80 %.

K_{eff} of reactor fuel with reflector thickness of	Bare	Water	Dry sand	Wet sand	Total Mass
9 cm	0.849	1.034	1.018	1.055	796 kg
12 cm	0.781	0.997	0.966	1.01698	772 kg
15 cm	0.718	0.962	0.920	0.980	798 kg
18 cm	0.663	0.932	0.875	0.947	872 kg

Table 4.16: Multiplication factor of homogeneously moderated fuel with f_m = 60% when completely surrounded by different moderating materials.

K_{eff} of reactor fuel with reflector thickness of	Bare	Water	Dry sand	Wet sand	Total Mass
9 cm	0.796	1.022	1.001	1.045	515 kg
12 cm	0.714	0.977	0.936	0.996	534 kg
15 cm	0.640	0.935	0.874	0.951	588 kg
18 cm	0.600	0.912	0.840	0.924	705 kg

Table 4.17: Multiplication factor of homogeneously moderated fuel with $f_m = 80\%$ when completely surrounded by different moderating materials.

4.3.2. Effect of Heterogeneity

The study of heterogeneity's effect consists of considering fuel as composed of UMo and ZrH alternating disks stacked orthogonal to the control rod axis and evaluating the multiplication factor of such systems as a function of fuel plate thickness. Indeed, for a fixed value f_m, an increase in plate thickness turns into an increase in fuel heterogeneity. The extreme case of homogeneous fuel is obtained when plates' thickness approaches zero and their number approaches to infinity.

The study of the effect of heterogeneity is performed on the lightest homogeneously moderated reactors having a f_m of 60 % and 80%, whose characteristic design parameters are listed in Table 4.18.

To each value of f_m it corresponds a specific ratio between HZr and UMo plate thickness. Such a ratio is fundamental to directly assessing moderator plate thickness as the UMo plate thickness is varied, guaranteeing that the volumetric moderator fraction is respected. Considering the lightest reactor geometry, it is assessed the multiplication factor as a function of UMo plates thickness (Figure 4.36 and Figure 4.37). For either value of f_m, the best performance in terms of neutron economy is obtained at a specific value of fuel plate thickness.

f_m	**60 %**	**80 %**
Fuel Outer Diameter	29 cm	28 cm
Fuel Height	52.5 cm	51 cm
Reflector Thickness	12 cm	9 cm
Fuel Mass	349 kg	248 kg
U-235 Mass	42 kg	20 kg
Reflector Mass	422 kg	266 kg
Total Mass	772 kg	515 kg

Table 4.18: Comparison of lightest homogeneously moderated core designs.

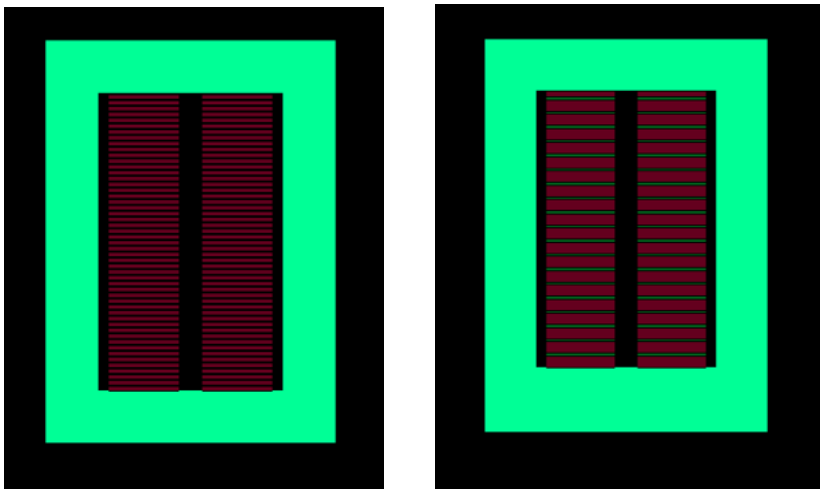

(a) Lower level of heterogeneity fuel view.

(b) Higher level of heterogeneity fuel.

Figure 4.35: Schematic representation of reactor cores with different levels of heterogeneity.

For $f_m = 60\%$, the maximum multiplication factor is obtained at a fuel plate thickness of 1.5 cm and a moderator plate thickness of 2.25 cm, corresponding to 15 fuel plates. The gain in the multiplication factor is 7600 pcm.
For $f_m = 80\%$, such maximum is located at a UMo plate thickness of 0.5 cm and a moderator plate thickness of 2 cm, corresponding to a total of 20 couples of moderator and metallic fuel plates. The multiplication factor gain is 9350 pcm when passing from homogeneously moderated fuel to the heterogeneous fuel provided by the optimal number of fuel plates.

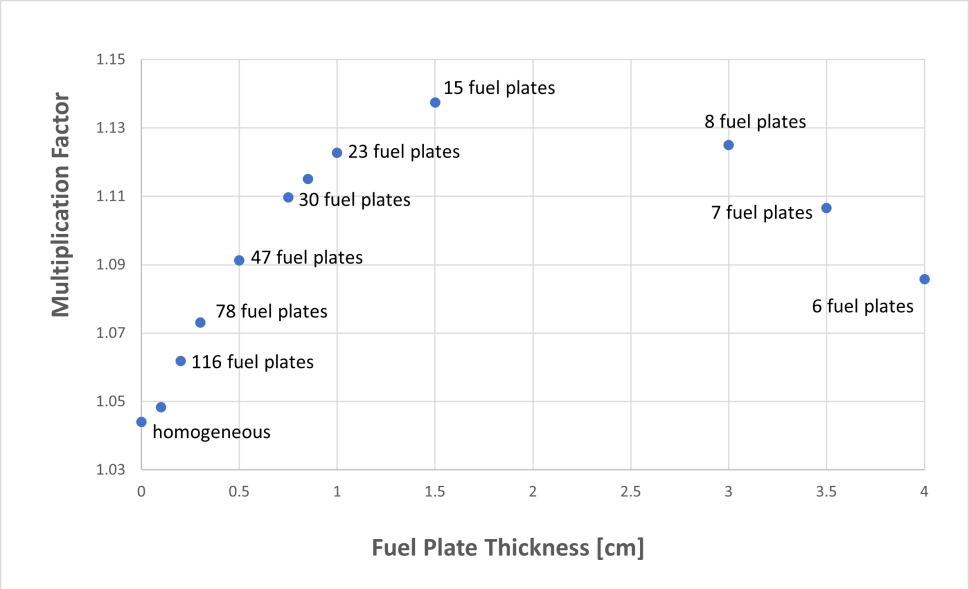

Figure 4.36: Multiplication factor as a function of fuel plate thickness for the lightest reactor core having $f_m = 60\%$.

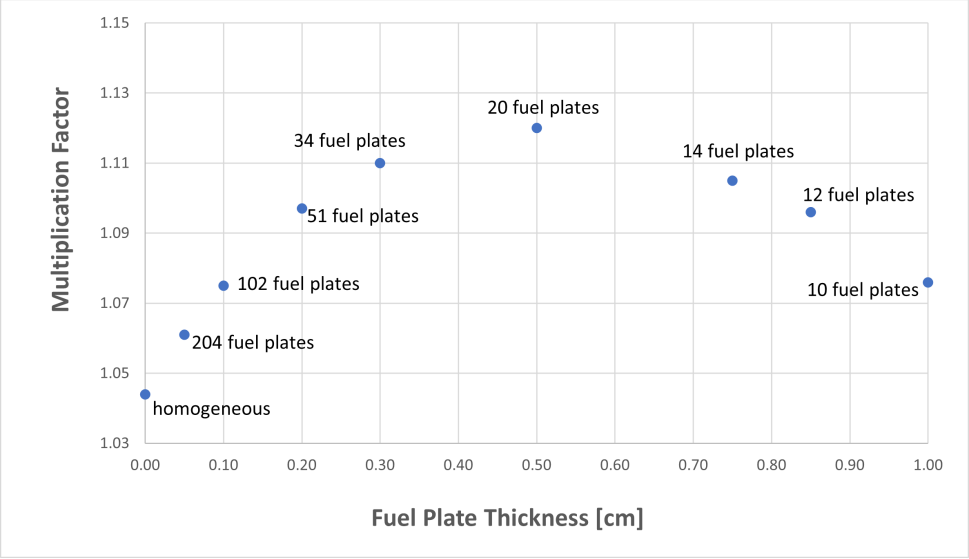

Figure 4.37: Multiplication factor as a function of fuel plate thickness for the lightest reactor core having $f_m = 80\%$.

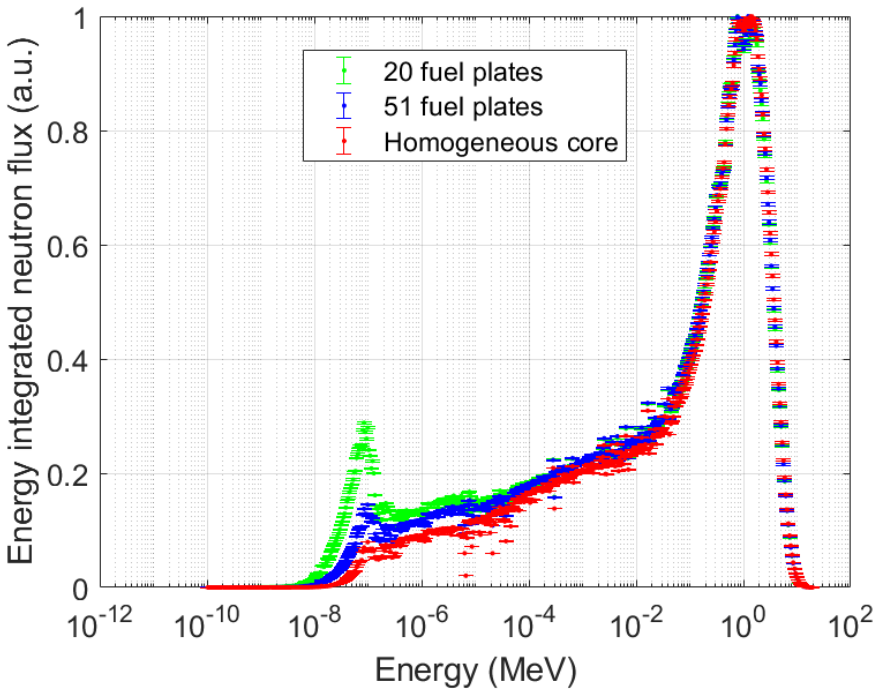

Figure 4.38: Neutrons spectrum inside heterogeneously moderated fuels having $f_m = 80\%$.

A possible explanation of such behavior lies in the definition of the multiplication factor through the six-factors formula (Equation 3.2). The two factors that are mainly influenced by heterogeneity are p and f. Specifically, the resonance escape probability increases as the heterogeneity increases since neutrons have less chance to encounter fuel (a resonance absorber) during their slowing down to thermal energy. In the extreme case of a homogeneously moderated reactor, neutrons are thermalized inside a core composed of a uniform mixture of moderator and resonance absorbers. Clearly, in such conditions, the probability of experiencing resonance absorption is higher. The increase in the resonance escape probability results in an increase in the thermal neutron population, which is reflected in the neutron spectrum. In Figure 4.38 is reported a comparison of neutron spectra evaluated inside fuels characterized by the same geometry (Table 4.18), the same $f_m = 80$ %, but different levels of heterogeneity. Specifically, such spectra refer to homogeneous and two heterogeneous fuels composed of 51 and 20 pairs of UMo and ZrH plates. The higher the number of fuel plates, the more the fuel approaches homogeneity and the softer the thermal neutron Maxwellian distribution becomes.

On the other hand, the thermal utilization factor decreases with the core heterogeneity due to spatial self-shielding [25]. According to this phenomenon, which is typical of heterogeneous reactors only, when thermal and epithermal neutrons that have experienced thermalization inside the moderator return to fuel, they will be more likely to be absorbed

near the fuel surface. Neutrons absorption at superficial fuel layers "shields" the inner layers, leading to a depression in the neutron flux inside the fuel rod [35].
Considering the analytical definition of the utilization factor:

$$f = \frac{\Sigma_{aF} * V_F}{\Sigma_{aF} * V_F * \Phi_F + \Sigma_{aM} * V_M * \frac{\Phi_M}{\Phi_F}} \tag{4.2}$$

Where V_M and V_M are moderator and fuel volumes, Φ_M and Φ_F are the average neutron fluxes inside moderator and fuel, while Σ_{aM} and Σ_{aF} are the respective macroscopic absorption cross-sections. If the average values of the flux in the fuel and moderator were identical, the ratio $\frac{\Phi_M}{\Phi_F}$ would be equal to unity, and the thermal utilization factor would be equal to the equivalent heterogeneous system. Nevertheless, since the thermal flux is depressed within the fuel, $\frac{\Phi_M}{\Phi_F}$ (also called thermal disadvantage factor) always results greater than unity.
Therefore, the characteristic trend observed in Figure 4.36 and Figure 4.37 can be explained as the superimposition of two phenomenon that counteract each other. In the ascending portion before the maximum, it is the increase in the resonance escape probability to prevail, while in the descending portion after the maximum, the decrease in the utilization factor dominates.
In Figure 4.41 and Figure 4.39 it is reported the mass optimization analysis performed on the homogeneously and heterogeneously moderated reactor concepts. In Table 4.19 are reported the lightest heterogeneously moderated reactors geometry parameters. When passing from the homogeneously to the heterogeneously moderated fuel, for $f_m = 80\%$ the lightest reactor total mass is reduced of 141 kg and for $f_m = 60\%$ of 228 kg. For the latter case, the total mass reduction results much more important mainly due to the reduction in the reflector thickness (from 12 cm to 9 cm). In either case fuel mass is only slightly decreased.

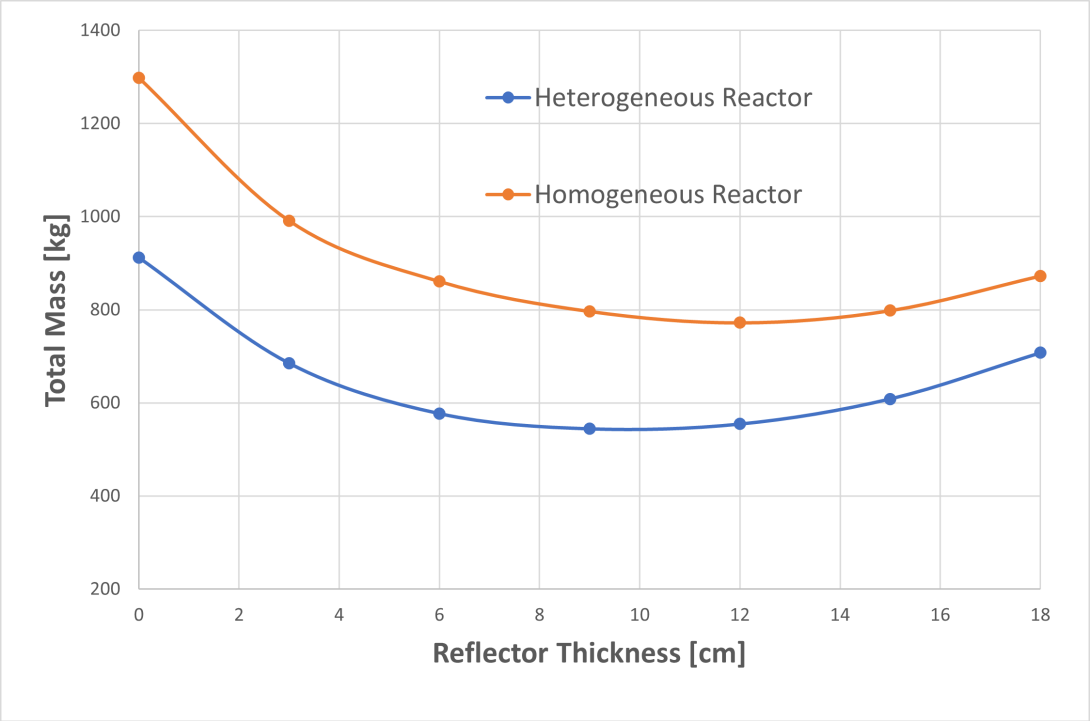

Figure 4.39: Total system mass as a function of reflector thickness for homogeneously and heterogeneously moderated reactor concepts with $f_m = 60\%$.

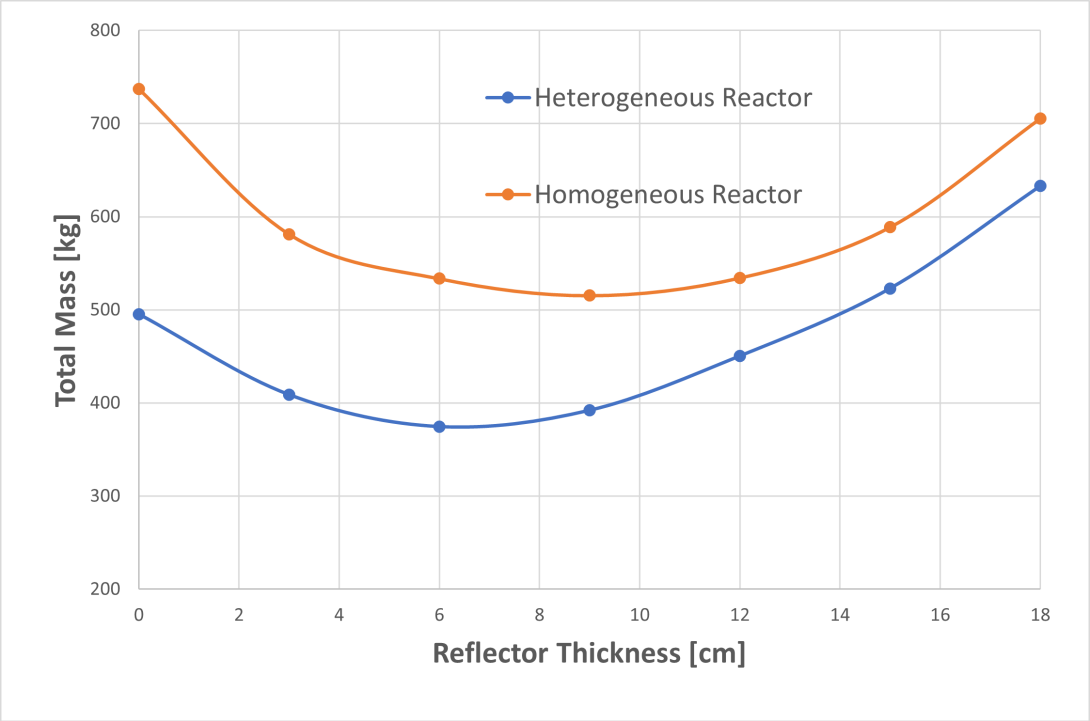

Figure 4.40: Total system mass as a function of reflector thickness for homogeneously and heterogeneously moderated reactor concepts with $f_m = 80\%$.

f_m	Hom-60 %	Het-60 %	Hom-80 %	Het-80 %
Fuel Outer Diameter	29 cm	26 cm	28 cm	27.2 cm
Fuel Height	52.5 cm	52 cm	47	59.5 cm
Reflector Thickness	12 cm	9 cm	9 cm	6 cm
Fuel Mass	349 kg	308 kg	248 kg	227 kg
U-235 Mass	42 kg	37 kg	20 kg	18 kg
Reflector Mass	422 kg	236 kg	266 kg	147 kg
Total Mass	772 kg	544 kg	515 kg	374 kg

Table 4.19: Comparison of lightest heterogeneously moderated core designs.

K_{eff} of reactor fuel with reflector thickness of	Bare	Water	Dry sand	Wet sand	Total Mass
6 cm	0.845	1.062	1.056	1.0941	577 kg
9 cm	0.763	1.009	0.987	1.033	544 kg
12 cm	0.688	0.964	0.924	0.985	554 kg
15 cm	0.627	0.929	0.872	0.947	608 kg
18 cm	0.586	0.903	0.833	0.917	707 kg

Table 4.20: Multiplication factor of heterogeneously moderated fuel with $f_m = 60\%$ when completely surrounded by different moderating materials.

K_{eff} of reactor fuel with reflector thickness of	Bare	Water	Dry sand	Wet sand	Total Mass
6 cm	0.824	1.056	1.049	1.084	374 kg
9 cm	0.743	1.008	0.984	1.035	391 kg
12 cm	0.680	0.965	0.926	0.986	450 kg
15 cm	0.612	0.897	0.858	0.958	522 kg
18 cm	0.593	0.916	0.843	0.927	632 kg

Table 4.21: Multiplication factor of heterogeneously moderated fuel with $f_m = 80\%$ when completely surrounded by different moderating materials.

In Figure 4.41 is reported the amount of fissile material contained inside fuel of heterogeneously moderated reactors obtained from the mass optimization analysis. Reactors having $f_m = 60$ % and a reflector thickness lower than 12 cm would effectively be the only ones with enough U-235 content to have a resulting lifetime at least as long as that of KRUSTY.

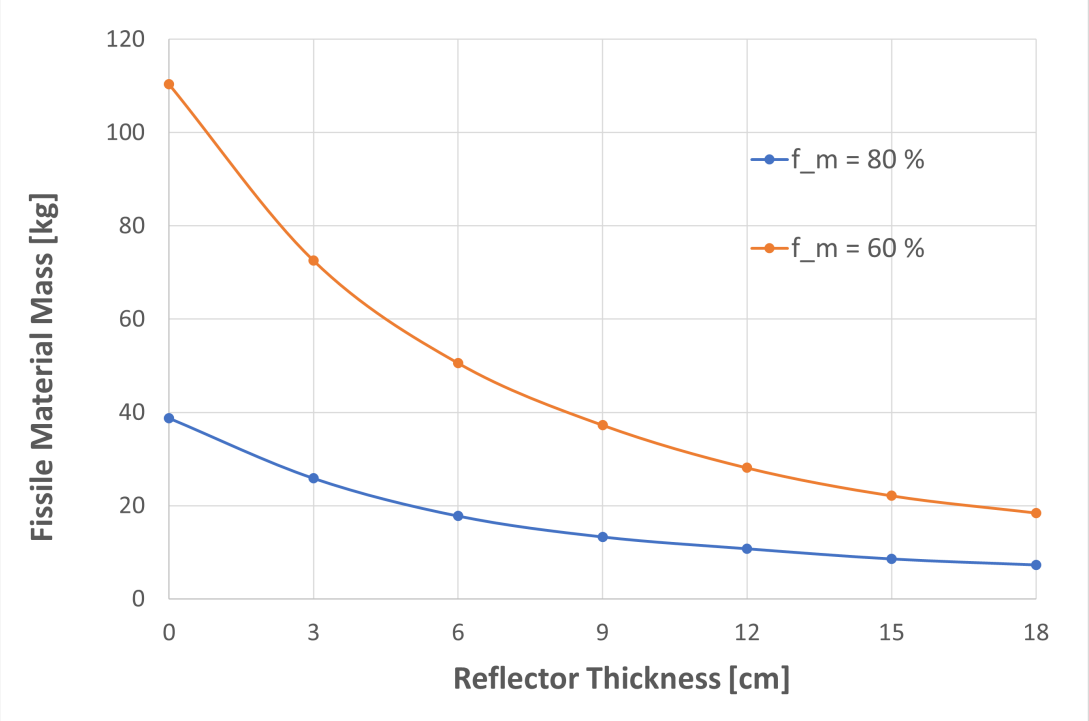

Figure 4.41: Fissile material mass contained inside fuel of heterogeneously moderated reactors obtained from the mass optimization analysis.

4.3.3. Limits in the Development of Thermal Reactors

The results of the analysis evidently demonstrate that the integration of moderator inside fuel always has a beneficial effect on the overall system mass. Therefore, the thermal reactor concept seems an extremely attractive solution for a space nuclear reactor whose design is driven by the goal of mass optimization. Nonetheless, several potential risks can be introduced from the development, operation, and reliability point of view, that are highly dependent on how the moderator is integrated into the reactor system [28]. Some of the complications caused by adding moderation to lower the reactor mass are:

- The smaller neutronic radial reflector worth of a moderated reactor can make launch and transport safety harder to address.
- In most cases, the moderator can withstand a lower temperature than the rest of

the core, which will increase the potential for irrecoverable core damage in case of any malfunction in the heat removal system.

- If the moderator is intended to operate at a lower temperature with respect to fuel, some cooling system is required.
- A moderated reactor is generally much more sensitive to impurities, as well as unknown or uncertain reactivity effects.
- The reactivity of the hydride-moderated system can be susceptible to the hydrogen ratio maintained by the material, with detrimental operational effects if hydrogen deviates a few percent from the design value or hydrogen is lost or redistributed during operation.
- Moderation will almost always substantially increase the magnitude of feedback coefficients, making operation and transient response more uncertain.
- Moderation will almost always move the reactor neutron spectrum into regimes where nuclear data are less uncertain.

Altogether, moderated systems have more complex and uncertain reactivity feedback and reactor dynamics. Furthermore, they are more difficult to engineer to meet launch accident safety requirements, and they usually require a larger excess reactivity, which can complicate safety as well [28]. The added complexity of moderation could make the difference between the success and failure of such a reactor.

5 | Conclusions and Future Developments

In this thesis work the design of a HALEU reactor for space applications was performed through the supplement of Serpent neutron transport Monte Carlo code. Prior to the design, it was ensured that Serpent was able to reliably simulate the neutronics of a space reactor by simply bench-marking the code with the modeling of KRUSTY, which is the only space reactor that has been successfully tested.

In the first phase of the design development, a fast nuclear reactor concept as similar as possible to KRUSTY was considered and it was studied the effect of reducing the fuel enrichment from 93% to 20%. To guarantee the same behavior of KRUSTY in terms of neutron economy, such change in the fuel composition consequently led to a significant increase in the overall system mass.

Afterward, the effect of reducing the H/D ratio from 2.27 down to 1.81 (as KRUSTY fuel was initially designed) was investigated, and it was proven to have a beneficial effect on the reactor neutron economy, allowing a further reduction in the critical fuel mass.

Finally, the effect of converting the reactor from fast to thermal through the integration of ZrH inside the core was investigated. After the homogeneously moderated reactor concept was proven to be under-moderated at any possible f_m, it was studied the effect of heterogeneity in the system neutron economy. The heterogeneously moderated reactor was assumed to have a core composed of alternating disks of ZrH and UMo alloy. It was demonstrated the existence of an optimal lattice pitch that enables the best performance from a neutronic perspective. The analysis was specifically performed on two heterogeneously moderated reactors having a different f_m of 60% and 80%, proving that the optimal lattice pitch is not a constant, but it is dependent on the volumetric moderator fraction.

Each reactor concept proposed in this study was supported by a mass optimization analysis to find the best reactor geometry that addressed the goal of minimizing the system mass. Also, safety analyses were carried out, in which all possible worst accidental scenarios the system could experience were simulated, and the multiplication factor was

assessed to check that the reactor would remain largely subcritical. This analysis allowed to demonstrate that the satisfaction of inadverted criticality safety constraints could be guaranteed at the only cost of an increased mass with respect to the mass-optimized reactor concepts due to the necessity of a thicker reflector.

The whole thesis work demonstrated the feasibility of HALEU fast reactor concepts for space applications able to satisfy launch safety approvals, but at the only cost of a 900 kg increase in the total system mass with respect to the case of using HEU as fuel. A further reduction of 100 kg in the system mass could be achieved by figuring out a solution that eliminates the risk of inadverted criticality. Incorporating a proper amount of spectral shifters absorbers, characterized by a significantly higher absorption cross-section for thermal vs. fast neutrons, can potentially offset the reactivity increase when fuel is surrounded by moderating materials. Indeed, water, sand, and wet sand have the effect of shifting the neutron spectrum towards thermal energies, potentially turning fuel into a supercritical state.

On the other hand, a hypothetical thermal reactor for space applications requires to be heterogeneously moderated. Indeed, it is not possible to consider the use of homogeneously moderated reactors at such high operating temperatures due to hydrogen diffusion and consequent fuel loss of integrity. In a heterogeneously moderated reactor such problem could be offset through the moderator thermal insulation. As an added benefit, heterogeneity was proven to improve the system neutron economy, turning into a further reduction of the system fuel mass with respect to the corresponding homogeneously moderated reactor concept.

The only limit in the entire analysis is related to the fact that the amount of fissile material inside fuel is not a fixed quantity, but it is determined by the reactor geometry that allows to obtain a multiplication factor of 1.044. Fortunately, all proposed reactor geometry were characterized by an amount of fissile material at least equal to the amount contained inside KRUSTY, with the exception of thermal reactors having $f_m = 60\%$. Nevertheless, KRUSTY was designed to have a very low burnup during its 15-years lifetime, suggesting that the small amount of fissile material may not represent a problem. A more detailed analysis involving the estimation of such reactors' burnup would be required to prove it. However, the presence of an optimal lattice pitch at each specific f_m value would allow to design a heterogeneously thermal reactor whose lifetime can be elongated as it is desired by simply adding more pairs of moderator and metallic fuel plates.

Bibliography

[1] Michael Campbell, Jeffery King, Henry Wise, Bruce Handley, and M. David. The role of nuclear power in space exploration and the associated environmental issues: An overview. 01 2009.

[2] Victoria Pidgeon Friedensen. Space nuclear power: Technology, policy, and risk considerations in human missions to mars. *Acta Astronautica*, 42(1):395–409, 1998. 12th IAA of Man in Space Symposium.

[3] Leopold Summerer, Bruno Gardini, and Giacinto Gianfiglio. Esa's approach to nuclear power sources for space applications. In *Proceedings of ICAPP*, volume 13, page 18, 2007.

[4] Steven Aftergood. Background on space nuclear power. *Science Global Security*, 1(1-2):93–107, 1989.

[5] David Poston. The persistent and growing gap between real and paper special - purpose reactors, 2021.

[6] Lee S. Mason, Marc A. Gibson, and David I. Poston. Kilowatt-class fission power systems for science and human precursor missions. 2013.

[7] Ryan Bechtel John Elliott Jean-Pierre Fleurial Mike Houts Rick Kapernick Ron Lipinski Duncan MacPherson Tom Moreno Bill Nesmith Dave Poston Lou Qualls Ross Radel Abraham Weitzberg Jim Werner Lee Mason, Sterling Bailey. Small fission power system feasibility study final report. Technical report, NASA, 2010.

[8] James L. Sanzi-Michael H. Brace Marc A. Gibson, Maxwell H. Briggs. Heat pipe powered stirling conversion for the demonstration using flattop fission (duff) test. 2013.

[9] David Irvin Poston Patrick Ray Mclure. White paper- use of leu for space reactor. Technical report, Los Alamos Nnational Laboratory, 2017.

[10] Cheryl L. Bowman-David I. Poston Patrick McClure John Creasy Chris Robinson

Marc A. Gibson, Lee S. Manson. Development of nasa's small fission power system for science and human exploration. 2015.

[11] Patrick McClure Marc A. Gibson, David I. Poston. Kilopower reactors for potential space exploration missions. 2019.

[12] W.D.Hide Manly. Utilization of beo in reactors. *Journal of Nuclear Materials*, 14, 1964.

[13] Chang Keun Jo-Chan Soo Kim. Sung Hoon Choi, Sung Nam Lee. Conceptual core design and neutronics analysis for a space heat pipe reactor using a low enriched uranium fuel. page 11, 02 2022.

[14] Marc Gibson Mason Lee Steve Oleson Patrick Ray Mclure, Dvid Irvin Poston. White paper- comparison of leu and heu fuel for the kilopower reactor. Technical report, Los Alamos Nnational Laboratory, 2018.

[15] Marc Gibson Patrick Ray Mclure, Dvid Irvin Poston. Design of the krusty reactor. Technical report, Los Alamos Naational Laboratory, 2018.

[16] Patrick McClure Thomas Godfroy James Sanzi Marc A. Gibson, David I. Poston and Maxwell H. Briggs. The kilopower reactor using stirling technology (krusty) nuclear ground test results and lessons learned. 2018.

[17] David I. Poston, Marc A. Gibson, Thomas Godfroy, and Patrick R. McClure. Krusty reactor design. *Nuclear Technology*, 206(sup1):S13–S30, 2020.

[18] Marc A. Gibson, David I. Poston, Patrick R. McClure, James L. Sanzi, Thomas J. Godfroy, Maxwell H. Briggs, Scott D. Wilson, Nicholas A. Schifer, Max F. Chaiken, and Nissim Lugasy. Heat transport and power conversion of the kilopower reactor test. *Nuclear Technology*, 206(sup1):31–42, 2020.

[19] David Irvin Poston. Krusty design and modeling. Technical report, 11 2016.

[20] Marc Gibson Steven R. Oleson Patrick Ray Mclure, David Irvin Poston. Nasa's kilopower reactor development and the path to higher power missions. Technical report, NASA, 2017.

[21] Lee Mason Michael Houts Ross C. Robinson Donald T. Palac, Marc A. Gibson and Patrick McClure. Nuclear systems kilopower overview. Technical report, 2016.

[22] Tuomas Viitanen Ville Valtavirta Toni Kaltiaisenaho Jaakko Leppänen, Maria Pusa. The serpent monte carlo code: Status, development and applications in 2013. *Annals of nuclear energy*, 82(sup1):142–150, 2015.

[23] Jaakko Leppänen. *Development of a new Monte Carlo reactor physiscs code*. PhD thesis, Helsinki University of Technology, June 2007.

[24] MuJid S. Kazimi Neil E. Todreas. *Nuclear Systems Volume I Thermal Hydarulic Fuundamentals*. Taylor Francis Group, 2001.

[25] Hyun Chul Lee, Hong Lim, Tae Han, and Stefan Cerba. A neutronic feasibility study on a small leu fueled reactor for space applications. *Annals of Nuclear Energy*, 77, 11 2014.

[26] Travis Grove, David Hayes, Joetta Goda, George McKenzie, Jesson Hutchinson, Theresa Cutler, John Bounds, Jessie Walker, William Myers, and Rene Sanchez. Kilowatt reactor using stirling technology (krusty) cold critical measurements. *Nuclear Technology*, 206(sup1):S68–S77, 2020.

[27] Jeffrey C. King Leonardo de Holanda Mencarini. Fuel geometry options for a moderated low-enriched uranium kilowatt-class space nuclear reactor. *Nuclear Engineering and Design*, 240:122–132, 2018.

[28] David I. Poston. Technical advantages of heu vs leu for special purpose reactors. Technical report, LANL, 2021.

[29] Anthony Baratta John Lamarsh. *Introduction to Nuclear Reactor Theory*. Addison Wesley, 1996.

[30] Tuomas Viitanen Ville Valtavirta Toni Kaltiaisenaho Jaakko Leppänen, Maria Pusa. Fundamentals of reactor physics with a view to the (possible) futures of nuclear energy. *Comptes Rendus Physique*, 18:372–380, 2017.

[31] Committee of Argonne National Laboratory. Organic nuclear reactors: An evaluation of current development programs. 5 1961.

[32] General Atomic Division. Technical foundations of triga. 1958.

[33] D Olander, Ehud Greenspan, Hans D Garkisch, and Bojan Petrovic. Uranium–zirconium hydride fuel properties. *Nuclear Engineering and Design*, 239(8):1406–1424, 2009.

[34] Louis J. Hamilton James J. Duderstadt. *Nuclear reactor analysis*. Wiley, 1991.

[35] Anthony Baratta John Lamarsh. *Introduction to Nuclear Engineering*. Prentice Hall, 2001.

List of Figures

List of Tables

List of Symbols

Variable	Description	SI unit
$\mathbf{K}$	multiplication factor	-
$\boldsymbol{\eta}_{\mathrm{T}}$	reproduction factor	-
$\mathbf{f}$	utilization factor	-
$\mathbf{p}$	resonance escape probability	-
$\boldsymbol{\varepsilon}$	fast fission factor	-
$\mathbf{P_{NLT}}$	thermal non-leakage probability	-
$\mathbf{P_{NLF}}$	fast non-leakage probability	-
$\boldsymbol{\alpha_T}$	temperature coefficient	1/K
$\mathbf{M}$	migration length	cm
$\mathbf{B}$	buckling factor	1/cm
$\mathbf{V}$	volume	cm^3
$\boldsymbol{\Sigma_a}$	macroscopic absorption cross section	1/cm
$\boldsymbol{\Sigma_s}$	macroscopic scattering cross section	1/cm
$\boldsymbol{\Phi}$	neutron flux	$\mathrm{n/cm^2s}$
$\mathbf{f_m}$	moderator volumetric fraction	-

Acknowledgements

My most sincere thanks go to my supervisor Prof. Stefano Lorenzi and my Co-advisor Prof. Marco Enrico Ricotti for the support, advice, guidance and oversight provided throughout the whole period of work on my thesis.
Also, I would like to thank all members of my family, whose support was essential to finish my studies at Politecnico di Milano. I thank them in particular for reminding me that I have the potential to do what I want, especially in those situations where I was the first to think I wasn't able to.
I thank my closest friends, for cheering me up in the most difficult moments of my university career, for helping me to find a balance between study and fun, which resulted fundamental to me to obtain the best results.
Finally, I also thank myself for all the effort and willpower it took to get to this point.